NONEQUILIBRIUM PROPERTIES OF MESOSCOPIC SUPERCONDUCTING RINGS

BY

MARTIN BRETT TARLIE

B.S., University of Michigan, 1989
B.S., University of Michigan, 1989
M.S., University of Illinois, 1991

THESIS

Submitted in partial fulfillment of the requirements
for the degree of Doctor of Philosophy in Physics
in the Graduate College of the
University of Illinois at Urbana-Champaign, 1995

Urbana, Illinois

UNIVERSITY OF ILLINOIS AT URBANA-CHAMPAIGN

THE GRADUATE COLLEGE

AUGUST 1995

WE HEREBY RECOMMEND THAT THE THESIS BY

MARTIN BRETT TARLIE

ENTITLED NONEQUILIBRIUM PROPERTIES OF MESOSCOPIC SUPERCONDUCTING RINGS

BE ACCEPTED IN PARTIAL FULFILLMENT OF THE REQUIREMENTS FOR

THE DEGREE OF DOCTOR OF PHILOSOPHY

Paul M. Goldbart

Director of Thesis Research

Head of Department

Committee on Final Examination†

Paul M. Goldbart

Chairperson

Kenneth D. Sullivan

† Required for doctor's degree but not for master's.

O-517

Nothing in the world can take the place of persistence. Talent will not; nothing is more common than unsuccessful men with talent. Genius will not; unrewarded genius is almost a proverb. Education will not; the world if full of educated derelicts. Persistence and determination alone are omnipotent. The slogan 'Press On' has solved and always will solve the problems of the human race.

—Calvin Coolidge

Acknowledgements

First of all, I would like to thank my advisor, Professor Paul Goldbart, for introducing me to the fascinating field of theoretical condensed matter physics. Early on in my graduate career, Paul patiently exposed me to the modern ideas of physics that cannot be found in textbooks. In addition, the problems that Paul suggested were both interesting and relevant: the solutions raise more questions than they answer. Finally, in the latter stages of my graduate career, Paul allowed me the freedom to pursue some of my own ideas, and for this I am grateful.

In the fall of 1994, Dr. Alan McKane, a member of the Department of Theoretical Physics at the University of Manchester, spent a semester in Urbana. Alan's research interests and my research interests strongly overlap. The third chapter of this thesis is a consequence of our collaboration. In addition, Alan filled me with confidence and encouragement. I will always be grateful for Alan's friendship and support.

For the last two years of my graduate career, Ken Elder has worked as a post-doctoral research associate. As his office was just a few doors away from mine, I was constantly able to badger him. In addition to being a very astute sounding board, Ken taught me a tremendous amount. His influence on my latter work is significant. Finally, when I needed it most, Ken was always there to provide moral support and encouragement; for this I am eternally grateful.

Another postdoc, Shivaji Sondhi, has also had a strong influence on my career. When times were tough, Shivaji gave me much needed moral support. But he did more. In addition to encouraging me to pursue a postdoctoral research position, Shivaji vollunteered as an unofficial, yet very effective, reference. I will always be grateful for Shivaji's kindness and efforts on my behalf.

It was a great pleasure to work with Efrat Shimshoni, a postdoctoral research associate and Beckman Fellow, on my first major project, which is the subject of the second chapter of this thesis. Efrat's insight in the latter stages of this work was

extremely valuable.

To Cecile (and the guys). Words can never express what our relationship has meant to me for the past six years. You never gave up on me, even when I was ready to give up on myself, and your continuous faith helped keep me afloat during the stormiest times. Together is far better than apart, and together we can cross any river to realize our dreams.

To my family: Mom and Dad, Ian, Lisa and Kent and Steven. Your support has been invaluable. The quality of our lives is not determined by our successes or failures, but rather by the people with whom we share our love. Just knowing that regardless of the outcome of my graduate career, you would still be there for me allowed me to take the risks necesaary to achieve my goal. Thanks!

Thanks to Jim Signore, Marvin Karlow, and Karl Meyer for all of the 5:30 a.m. tee-times. To Jim: Ross Perot once said: 'Never give in, never, never, never...'. I won't if you won't!

I would like to thank the Materials Research Laboratory Center for Computation, and in particular Elena Pourmal, Marc Taylor and Ginny Metze, for all of the help over the years. Your willingness and ability to help greatly facilitated my computational work.

Finally, the work presented here was primarily supported by the United States National Science Foundation through grant DMR-89-20538 (administered by the Materials Research Laboratory of the University of Illinois at Urbana-Champaign, 1992-1994). Additional support was provided by a University Fellowship from the University of Illinois at Urbana-Champaign (1991-1992), as well as a United States Department of Education Graduate Assistantship in Areas of National Need (1994-1995).

Contents

List of Tables

List of Figures

Chapter 1

Introduction

In this thesis we study the behavior of supercurrent flows in mesoscopic superconducting rings, i.e., rings of finite circumference. Two classes of nonequilibrium behavior will be considered: (i) the system is prepared in a nonequilibrium state and subsequently allowed to relax toward equilibrium, and (ii) the system is in contact with an external driving force that does not allow the system to relax toward equilibrium. For concreteness, we imagine that a solenoid penetrates the center of the ring, thereby providing a driving mechanism. For example, if the solenoidal current varies linearly with time, then by Faraday's law of induction a time-independent electromotive force will be induced in the ring.

In Chap. 2 we consider the problem of the lifetime of persistent supercurrents. Here, the system is prepared in a nonequilibrium state and subsequently relaxes toward equilibrium. For the case of wires that are in the thermodynamic limit (i.e., not mesoscopic), this problem has been well studied [1, 2, 3, 4]. Although persistent supercurrents have been observed to flow without decay for over a year, under certain circumstances, e.g., for narrow rings at a temperature slightly below the superconducting transition temperature, the current can decay in a measurable amount of time. The mechanism of current decay, in which energy is dissipated, is via a process whereby thermal fluctuations carry the system over an energy barrier. These processes are known as thermally activated phase-slip processes. Thus, it is thermal fluctuations that are responsible for the dissipation of the kinetic energy of the

supercurrent. For the case of wires that are infinitely long, the dependence of the rate of decay of a persistent current on the temperature and supercurrent has been calculated [2, 3].

In the first part of Chap. 2 we extend the results for the temperature and current dependence of the lifetime to include the dependence on the ring circumference. The main result is that there are substantial length-dependent corrections that have a stabilizing effect, i.e., the decay rate (the inverse of the lifetime) per unit length of the sample, decreases as the length of the wire is reduced. In the second part of Chap. 2 we compare two distinct experimental situations: (i) the superconductor is driven by a voltage source, and (ii) the superconductor is driven by a current source. For an ensemble of systems driven by a voltage source, the solenoidal flux is the independent variable, and for an ensemble of systems driven by a current source, the supercurrent is the independent variable. For wires that are in the thermodynamic limit, a distinction need not be made between a voltage source and a current source [5]. However, we shall see that for mesoscopic wires driven by a voltage source, the lifetimes of the metastable states acquire substantial length-dependent corrections. By contrast, we shall see that for mesoscopic wires driven by a current source, the lifetimes of the metastable states do not acquire substantial length-dependent corrections. This is an explicit example of the general result that for mesoscopic systems, i.e., systems that are not in the thermodynamic limit, the choice of the ensemble is not free, but depends on the experimental circumstances.

In Chap. 3 we present a method for the regularization of the determinants of differential operators. In order to calculate the lifetime of a persistent current, it is necessary to compute the ratio of determinants, with all zero eigenvalues removed, of certain differential operators. The process of factoring the zero eigenvalues out of the determinants involves a step known as regularization. As the eigenvalues of these operators characterize the curvature of the free energy, the determinants are known as fluctuation determinants. The need to calculate fluctuation determinants arises in many scientific problems [6]. Consequently, powerful mathematical tools have been

invented that reduce the problem of the computation of the infinite product of *all* the eigenvalues (i.e., the *unregularized* determinant) to that of finding the solutions to a homogenous differential equation [7, 8, 9, 10]. In these techniques, it is only the boundary values of the homogenous-equation solutions, and their derivatives, that are required. However, in many cases of physical interest, such as the calculation of the lifetime of persistent currents discussed in Chap. 2, it is the *regularized* determinant that is needed. Usually, the regularization is carried out in an *ad hoc* way, either by moving the location of the boundaries (e.g., see Refs. [11, 12]), or by perturbing the operator (e.g., see Refs. [13, 14]). In Chap. 3 we present a *systematic* method of regularization that allows the *regularized* determinant to be expressed in a form that is no more complicated than the form for the *unregularized* determinant.

In the final chapter of this thesis, Chap. 4, we consider the problem of the dynamics of the supercurrent near the critical current. In particular, we imagine that the system is under the influence of an electric field of sufficient strength so that the current is driven to the critical current, at which point the system becomes unstable. (We shall see that this situation is readily obtainable as long as the temperature is not too close to the superconducting transition temperature.) Once the system becomes unstable, there are multiple metastable states that can compete for occupation. We shall find that for 'weak' electric field strengths single phase-slip processes dominate the dynamics, but as the field strength is increased, there is a crossover to double phase-slip domination. In this problem, the important decay processes are from a point of *instability*. This is in contrast to the problem of the lifetime of a persistent current, where it is the decay from a point of *metastability* that is important. The problem of the rate of decay from a metastable state is an old one, and the theoretical approach is by now well known. By contrast, a theory for the decay from an unstable state when multiple metastable states compete for occupation is not available. In the final part of Chap. 4, a possible approach to this problem, inspired by the work of Onsager and Machlup [15], and based on a path integral technique, will be presented.

References

[1] W. A. Little, Physical Review **156**, 396 (1967).

[2] J. Langer and V. Ambegaokar, Physical Review **164**, 498 (1967).

[3] D. McCumber and B. Halperin, Physical Review B **1**, 1054 (1970).

[4] M. Tinkham, *Introduction to Superconductivity* (McGraw-Hill, NY, 1975), Chap. 7.

[5] D. E. McCumber, Phys. Rev. **172**, 427 (1968).

[6] H. Kleinert, *Path Integrals in Quantum Mechanics, Statistics, and Polymer Physics* (World Scientific, 1990).

[7] I. Gel'fand and A. Yaglom, J. Math. Phys. **1**, 48 (1960).

[8] S. Levit and U. Smilansky, Proc. Am. Math. Soc. **65** 299 (1977).

[9] T. Dreyfuss and H. Dym, Duke Math. J. **45**, 15 (1978).

[10] R. Forman, Invent. Math. **88**, 447 (1987).

[11] G. Barton, A. J. Bray and A. J. McKane, Am. J. Phys. **58** 751 (1990).

[12] I. H. Duru, H. Kleinert and N. Uñal J. Low Temp. Phys. **81** 121 (1980).

[13] E. Brézin, J. C. Le Guillou and J. Zinn-Justin, Phys. Rev. D **15**, 1544 (1977).

[14] M. B. Tarlie, E. Shimshoni and P. M. Goldbart, Phys. Rev. B **49** 494 (1994).

[15] L. Onsager and S. Machlup, Phys. Rev. **91**, 1505; *ibid.*, **91**, 1512 (1953).

Chapter 2

Lifetime of Persistent Currents

2.1 Introduction

The physical situation under consideration is that of a narrow superconducting loop of length L threaded by a magnetic flux which is possibly time dependent. The main issue to be addressed is the lifetime of persistent currents in such systems, paying particular attention to the length dependence.

The system is considered to be close to equilibrium if the supercurrent flowing in the wire is much smaller than the critical supercurrent. In addition, what is meant by mesoscopic is that the length L of the wire, when measured in units of the superconducting fluctuation correlation length $\xi(T)$, where T is the temperature, does not greatly exceed one. Finally, we will restrict our attention to narrow wires. More specifically, if σ is the cross-sectional area, then the wire is considered to be narrow if $\sqrt{\sigma}$, the cross-sectional dimension, is much smaller than either $\xi(T)$ or the temperature dependent magnetic penetration depth. This system is therefore termed 'quasi-one-dimensional'.

The basic idea is that the current-carrying states of a quasi-one-dimensional superconductor are metastable (see Ref. [1]). This is illustrated schematically in Fig. 2.1. Hence, the central issue is the rate of transitions between two neighboring metastable states, or, equivalently, the lifetime—the inverse of the transition rate—of a metastable current-carrying state. This is a specific example of the generic problem of the transition rate between two neighboring metastable states; an old problem,

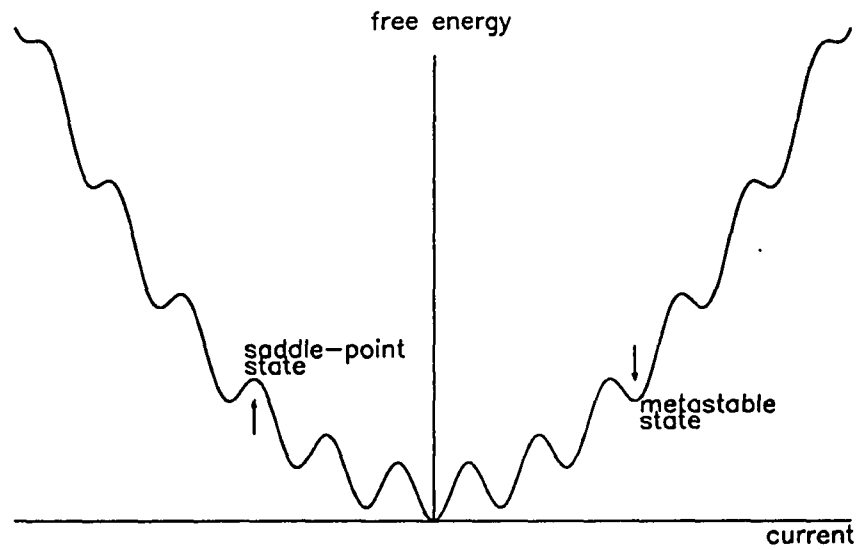

Figure 2.1: Schematic plot of the free-energy as a function of current.

appearing in many areas of science [2, 3]. For example, in the theory of chemical reactions, a reaction is pictured as occuring via a transition between two metastable free energy wells, separated by an energy barrier [4]. In the limit of large damping, the rate for such a reaction is given by the well-known Arrhenius formula of chemical reaction theory [5]. This relation expresses the rate of reaction in terms of two quantities: the energy barrier separating the neighboring metastable states, and a pre-exponential factor, sometimes referred to as the 'attempt frequency'. The expression for the inverse of the lifetime of the supercurrent in a narrow superconducting ring is the multi-dimensional generalization of the Arrhenius equation.

A direct consequence of the metastability of current-carrying states in narrow wires is the concept of the intrinsic resistance of a superconductor [6, 7, 8, 1]. If a wire carrying a supercurrent is isolated, the current will eventually decay. Therefore, in order to maintain a constant current, energy must be supplied to the system; the

rate at which the energy must be supplied, divided by the square of the supercurrent, is a measure of the intrinsic resistance. In other words, the resistance is due to the fact that the system is in the superconducting state. When the resistance of a narrow superconducting wire is measured as a function of temperature, it is found that the resistive transition is not infinitely sharp. Rather, there is a certain range of temperatures for which the resistance is reduced, but still not zero. The combined theoretical work of Langer and Ambegaokar [7], and McCumber and Halperin [8], collectively known as the LAMH theory, was successful in explaining the width (in temperature) of the resistive transition. In the LAMH theory, the ratio L/ξ is assumed to greatly exceed unity. In this chapter we extend the results of LAMH to the situation in which ξ/L is not negligible.

There are two main results to be presented in this chapter. The first concerns the lifetime, or alternatively, the rate of decay, of persistent currents. In this case, as the length of the wire is reduced, we find algebraic (as opposed to exponential) length-dependent corrections that tend to increase both the barrier heights and attempt frequencies [9]. The former corrections tend to reduce the rate, per unit length of the wire, at which transitions occur, whereas the latter will have the opposite effect. Thus, there is a competition between these two tendencies. For cases of practical interest, the barrier height contributions dominate, leaving the final result that as the length of the wire is reduced, the decay rate (per unit length of the sample) will decrease. The second main result concerns the distinction between the situation in which the system is driven by a voltage source, versus that where the system is driven by a current source. For the voltage source we find that there are algebraic length-dependent corrections to both the barrier heights and attempt frequencies, with the net result being dominated by the barrier height corrections. These results are the same as those found for the lifetime of the persistent currents. By contrast, for the current-source we find no algebraic length-dependent corrections. The difference in behavior between a system driven by a voltage source versus that driven by a current source, is a specific example of the general result that for mesoscopic systems, i.e.,

systems that are not in the thermodynamic limit, the choice of ensemble is not free, but depends on the experimental circumstances.

This chapter is organized as follows. In the next section the theoretical model, the Ginzburg-Landau theory of superconductivity, is introduced. Following that, in Sec, 2.3, the central notion of the metastability of the current-carrying states is explained. Presented in Secs. 2.4 and 2.5 the properties of the metastable and saddle-point states, respectively. The length-dependence of the barrier heights is discussed in Sec. 2.6, and in Sec. 2.7 the attempt frequencies are computed. The results of these two sections are summarized in Sec. 2.8. The situations in which the superconductor is driven by a voltage source and by a current source are discussed in Secs. 2.9 and 2.9, respectively. Finally, in Sec. 2.11 the conclusions of this chapter are summarized.

2.2 Theoretical Model

In this section the theoretical model used throughout this thesis will be presented. The theoretical description is based on the Ginzburg-Landau (GL) theory of superconductivity, in which the superconductive state is described by a complex-valued, space- and time-dependent order parameter Ψ [10]. It is sometimes useful to think of Ψ as an 'effective wavefunction' for the superconducting electrons, representing, as it does, the quantum mechanical coherence underlying the phenomenon of superconductivity. The precise relationship between the BCS theory [11], a microscopic quantum mechanical theory, and the phenomenological GL theory, for temperatures close (but not too close) to T_c (the superconducting transition temperature) was established by Gor'kov [12]. Throughout this thesis, it is assumed that the GL theory is adequate.

The basic idea of the GL approach is to apply Landau's theory of second order (i.e., continuous) phase transitions [13, 14] to superconductivity—a second order phase transition in the abscence of a magnetic field. Thus, the order parameter Ψ is considered to be a thermodynamic variable, and the free energy of the superconductor $F[\Psi]$ is expanded in powers of $|\Psi|$ and its spatial gradient $|\nabla\Psi|$. In the presence of a

magnetic field $\mathbf{B} = \nabla \times \mathbf{A}$, where $\mathbf{A}$ is the electromagnetic vector potential, the total energy is a sum of $F[\Psi]$ and the magnetic field energy, where the spatial gradient, which is analogous to the momentum operator in quantum mechanics, is modified to include the momentum $(2e/\hbar c)\mathbf{A}$ of the electromagnetic field [15]. (Here e is the electronic charge, $\hbar$ is Planck's constant, and c is the speed of light.) The total free energy can then be written as

$$F[\Psi, \mathbf{A}] = \int d\mathbf{r}\Big\{|(\nabla - (i2e/\hbar c)\mathbf{A}(\mathbf{r}))\Psi(\mathbf{r})|^2 - \alpha|\Psi(\mathbf{r})|^2 + \frac{\beta}{2}|\Psi(\mathbf{r})|^4\Big\}$$

$$+(8\pi)^{-1}\int d\mathbf{r}(\nabla \times \mathbf{A})^2, \tag{2.1}$$

where $\mathbf{r}$ is a three-dimensional position vector, and α and β are expansion coefficients. The factor of $2e$ in eq. (2.1), rather than a factor of e, accounts for the pairing of electrons into Cooper pairs [16]. The superconducting transition is manifested in the sign of α, which is assumed to be temperature dependent. For temperatures higher than T_c, $\alpha < 0$, whereas for temperatures lower than T_c, $\alpha > 0$. In the former case, the homogeneous part of the free energy density, $-\alpha|\Psi|^2 + (\beta/2)|\Psi|^4$, has a single local minimum at $|\Psi| = 0$. This reflects the notion that for these temperatures the normal state (i.e., $|\Psi| = 0$) is energetically favorable. However, as T is reduced through T_c this single local minimum becomes a local maximum, and at the same time, a one-parameter family of local minima at $|\Psi| = \sqrt{\alpha/\beta}$ evolve continuosly, i.e., $\alpha(T_c) = 0$. In other words, for temperatures below T_c, the superconducting state (i.e., $|\Psi| = \sqrt{\alpha/\beta}$) is energetically favorable. The original Ansatz of Ginzburg and Landau was that $\alpha(T) \propto (T - T_c)$, and the expansion coefficient β was assumed to be independent of T (see below). In this thesis, we will always work in the regime where $T < T_c$.

The celebrated Ginzburg-Landau equations for Ψ and $\mathbf{A}$ are obtained by requiring that the variations ($\delta F[\Psi, \mathbf{A}]/\delta\Psi$ and $\delta F[\Psi, \mathbf{A}]/\delta\mathbf{A}$) of $F[\Psi, \mathbf{A}]$ with respect to Ψ and $\mathbf{A}$ vanish. The conditions that $\delta F/\delta\Psi = 0$ and $\delta F/\delta\mathbf{A} = 0$ are known as stationarity

conditions, and they can be written as

$$(-i\nabla - (2e/\hbar c)\mathbf{A})^2\Psi - \alpha\Psi + \beta|\Psi|^2\Psi = 0 \tag{2.2}$$

$$\nabla \times (\nabla \times \mathbf{A}) = (4\pi/c)\mathbf{J}, \tag{2.3}$$

where the supercurrent *density* $\mathbf{J}$ is given by

$$\mathbf{J}[\Psi] = \frac{4e}{i\hbar}\Big[\Psi^*(\nabla - (i2e/\hbar c)\mathbf{A})\Psi) - \text{c.c.}\Big]. \tag{2.4}$$

At this stage it is convenient to postpone the discussion of the boundary conditions that the stationary configurations must satisfy. This issue is best dealt with at a slightly later stage. Throughout this thesis, the vector potential $\mathbf{A}$ will be treated as a parameter, rather than a dynamical variable. In other words, eqs. (2.2) and (2.3) are not solved self-consistently. Thus, the *conditions* of stationarity for Ψ and $\mathbf{A}$ reduce to a *condition* of stationarity for Ψ (which will depend parametrically on $\mathbf{A}$). For narrow wires, this approximation can be made reasonable (see Appendix A of Ref. [7]). The basic idea is that due to the small cross-sectional area of the wire, the magnetic field generated by the supercurrent does not significantly influence the order parameter. In addition, the magnetic-field energy due to the supercurrent is much smaller than the energy associated with the order parameter. Therefore, the magnetic energy term in eq. (2.1) will be dropped, and $F[\Psi, \mathbf{A}]$ will be written as $F[\Psi]$.

For the specific case of a narrow superconducting ring of cross-sectional area σ and circumference L, the integration in eq. (2.1) over the spatial coordinates perpendicular to the longitudinal coordinate (denoted here by X) of the wire can be performed, with the result that

$$F[\Psi] = \sigma \int_{-L/2}^{L/2} dX\Big\{|(\partial_X - (i2e/\hbar c)A_X)\Psi(X)|^2 - \alpha|\Psi(X)|^2 + \frac{\beta}{2}|\Psi(X)|^4\Big\}, \tag{2.5}$$

where A_X is the component of the vector potential in the longitudinal direction. The requirement that the order parameter be single valued leads to the following periodicity condition for Ψ:

$$\Psi(L + X) = \Psi(X). \tag{2.6}$$

It is convenient, both for notational simplicity and for the purpose of making the physical meaning of the parameters in the equations transparent, to transform the dimensionful variables in eq. (2.5) to dimensionless variables. This transformation proceeds in two steps. First, Ψ, A_x, and X are exchanged for $\tilde{\psi}$, $\tilde{A}_x$, and x via

$$\tilde{\psi} \equiv \sqrt{\beta/\alpha}\,\Psi, \tag{2.7}$$

$$\tilde{A}_x \equiv (2e/\hbar c\sqrt{\alpha})\,A_X, \tag{2.8}$$

$$x \equiv \sqrt{\alpha}\,X. \tag{2.9}$$

Second, the two parameters α and β are exchanged for the more physically meaningful variables $\xi(T)$ and $H_c(T)$, via

$$\xi(T) \equiv 1/\sqrt{\alpha}, \tag{2.10}$$

$$H_c(T) \equiv \sqrt{2\pi\alpha^2/\beta}. \tag{2.11}$$

The quantity $H_c(T)$ is the thermodynamic critical field, so that $H_c^2/8\pi$ is the condensation energy per unit volume, i.e., the energy difference between the higher-energy normal state ($|\Psi| = 0$) and the lower-energy superconducting state ($|\Psi| = \sqrt{\alpha/\beta}$). Using the temperature dependence of α, i.e., $\alpha \propto T_c - T$, and the temperature independence of β, from eqs. (2.10) and (2.11) we see that $\xi(T) \propto (T_c - T)^{-1/2}$ and $H_c(T) \propto T_c - T$. For temperatures close to T_c, the temperature regime in which expect the GL theory is valid, both of these dependences are consistent with the results from BCS theory. This justifies, *a posteriori*, Ginzburg and Landau's original Ansatz.

By using the transformations of eqs. (2.7)-(2.11), the GL free energy given in eq. (2.5) can be written in the form

$$F[\tilde{\psi}] = (4\pi)^{-1}\sigma H_c(T)^2\xi(T)\mathcal{F}[\tilde{\psi}, \tilde{A}_x], \tag{2.12}$$

$$\mathcal{F}[\tilde{\psi}, \tilde{A}_x] \equiv \int_{-\ell/2}^{\ell/2} dx\Big\{|(\partial_x - i\tilde{A}_x)\tilde{\psi}(x)|^2 - |\tilde{\psi}(x)|^2 + \frac{1}{2}|\tilde{\psi}(x)|^4\Big\}, \tag{2.13}$$

where

$$\ell \equiv L/\xi(T). \tag{2.14}$$

The periodicity condition (2.6) is unaffected by the above transformations so that

$$\tilde{\psi}(\ell + x) = \tilde{\psi}(x). \tag{2.15}$$

Using eq. (2.4) for the supercurrent *density* $\mathbf{J}$, the supercurrent $I \equiv \sigma\mathbf{J}$ can be written as

$$I[\tilde{\psi}] = \frac{\sigma\xi H_c^2}{\pi}\frac{e}{\hbar}\tilde{\mathcal{J}}[\tilde{\psi}], \tag{2.16}$$

$$\tilde{\mathcal{J}}[\tilde{\psi}] \equiv \frac{1}{2i}[\tilde{\psi}^*(\partial_x - i\tilde{A}_x)\tilde{\psi}) - c.c.], \tag{2.17}$$

where the quantity $\tilde{\mathcal{J}}[\tilde{\psi}]$ is the dimensionless supercurrent of state $\tilde{\psi}$. Finally, the equation of stationarity (2.2) becomes

$$(\partial_x - i\tilde{A}_x)^2\tilde{\psi}(x,t) + \tilde{\psi}(x,t) - \tilde{\psi}(x,t)|\tilde{\psi}(x,t)|^2 = 0. \tag{2.18}$$

At this stage it is convenient to discuss the boundary conditions associated with the stationarity condition (2.18). Certainly, the requirement that $\tilde{\psi}$ be single-valued implies that $\tilde{\psi}$ satisfy eq. (2.15). However, (2.18) is a second order differential equation, so that an additional boundary condition is required. This condition is determined by the requirement that F be stationary at the boundaries. To be more explicit, the term $(\partial_x - i\tilde{A}_x)^2\tilde{\psi}$ in eq. (2.18) is obtained by requiring that $\mathcal{F}[\tilde{\psi}]$ be stationary with respect to variations $\delta\tilde{\psi}^*$ of $\tilde{\psi}^*$; this procedure generates a term of the form $[(\partial_x - i\tilde{A}_x)\tilde{\psi}][\partial_x\delta\tilde{\psi}^*]$, which when integrated by parts, generates the boundary term $\delta\tilde{\psi}^*(\partial_x - i\tilde{A}_x)\tilde{\psi}|_{-\ell/2}^{\ell/2}$. This term can be made to vanish if (i) $\delta\tilde{\psi}$ satisfy eq. (2.15), which implies that $\tilde{\psi}$ must also satisfy eq. (2.15), and if (ii)

$$(\partial_x - i\tilde{A}_x)\tilde{\psi}|_{\ell+x} = (\partial_x - i\tilde{A}_x)\psi|_x. \tag{2.19}$$

Equation (2.19) is the so-called natural boundary condition, and is the additional condition that was sought. Thus, the stationary states must satisfy the (differential) eq. (2.18), subject to the periodicity conditions given in eqs. (2.15) and (2.19).

The form of the GL free energy given in eq. (2.13), and the form of the boundary condition given in eq. (2.15), will be most useful in Chap. 4 where the dynamics of the supercurrent is studied. However, in this chapter it is convenient to make one final change of variables to eliminate the explicit dependence of the free energy on the vector potential. Changing from $\tilde{\psi}$ to ψ, via

$$\psi \equiv e^{-i\int^x dx' \tilde{A}_x}\tilde{\psi}, \tag{2.20}$$

the free energy becomes

$$\mathcal{F}[\psi] \equiv \int_{-\ell/2}^{\ell/2} dx\Big\{|\partial_x\psi(x)|^2 - |\psi(x)|^2 + \frac{1}{2}|\psi(x)|^4\Big\}, \tag{2.21}$$

and the boundary condition (2.15) becomes

$$\psi(\ell + x) = e^{i\Phi}\psi(x), \tag{2.22}$$

$$\Phi \equiv \frac{2e\xi}{\hbar c}\int_{-\ell/2}^{\ell/2} dx\, A_x, \tag{2.23}$$

where Φ is a dimensionless measure of the magnetic flux through the ring. In addition, the equation of stationarity (2.18) and the natural boundary condition (2.19) become

$$\psi'' + \psi - \psi|\psi|^2 = 0, \tag{2.24}$$

$$\psi'(\ell + x) = e^{i\Phi}\psi'(x), \tag{2.25}$$

where the prime denotes differentiation with respect to x. Finally, the dimensionless supercurrent $\tilde{\mathcal{J}}$ given in eq. (2.17) becomes

$$\mathcal{J}[\psi] \equiv \frac{1}{2i}[\psi^*\partial_x\psi - \psi\partial_x\psi^*]. \tag{2.26}$$

Thus, the effect of the vector potential has been taken into account via a transformation that alters the boundary conditions from periodic [eq. (2.15)], to twisted periodic [eq. (2.22)]. For most of this chapter Φ is taken to be static; in Sections 2.9 and 2.10, where the voltage and current sources are discussed, the flux Φ is endowed with time dependence.

For the purposes of this chapter, there are two types of characteristic feautures on the free energy landscape: local minima and saddle-points. The local minima correspond to the metastable current-carrying states of the superconductor (see Sec. 2.3), and the saddle-points correspond to the points of lowest free energy that connect two neighboring metastable states (see Sec. 2.4). As will be seen in the following sections, the lifetime of the persistent currents depends on the properties of these states. Both classes of states make the free energy stationary, i.e., both classes of states satisfy eqs. (2.24)-(2.25). We will denote by ψ_e (the e stands for extremal) a stationary state that is either a saddle-point or a metastable point, so that if $e = m$ then the state is metastable, and if $e = s$ the state is a saddle-point. In other words, ψ_m is a metastable state and ψ_s is a saddle-point state.

In order that the characteristics of the stationary states may be understood more fully when they are introduced in Secs. 2.4 and 2.5, we discuss the stationarity condition (2.24) in detail. By introducing a polar decomposition $\psi(x) \equiv f(x)e^{i\phi(x)}$, the stationarity condition (2.24) for ψ can be written in terms of f and ϕ as

$$E' \equiv \partial_x[(f')^2 + f^2 - \frac{1}{2}f^4 + f^2(\phi')^2] = 0, \tag{2.27}$$

$$J' \equiv \partial_x[f^2\phi'] = 0. \tag{2.28}$$

The equations of stationarity, eqs. (2.27) and (2.28), are analogous to the classical equations of motion for a particle moving in two dimensions under the influence of a radial potential. This mechanical analogy will prove to be a useful aid in the visualization of the stationary states. In the analogy, f is interpreted as a radial coordinate, ϕ as an angular coordinate, and x as time. The quantity E is the mechanical energy of the classical particle, and J is its angular momentum. Both of these quantities are 'conserved' in the sense of the mechanical analogy, i.e., they are independent of the 'time' x. The conservation of E and J allows the stationary states to be determined explicitly (see Secs. 2.4 and 2.5 and App. B). The conservation of J allows ϕ to be eliminated from eqs. (2.27) and (2.28), leaving a second-order differential equation

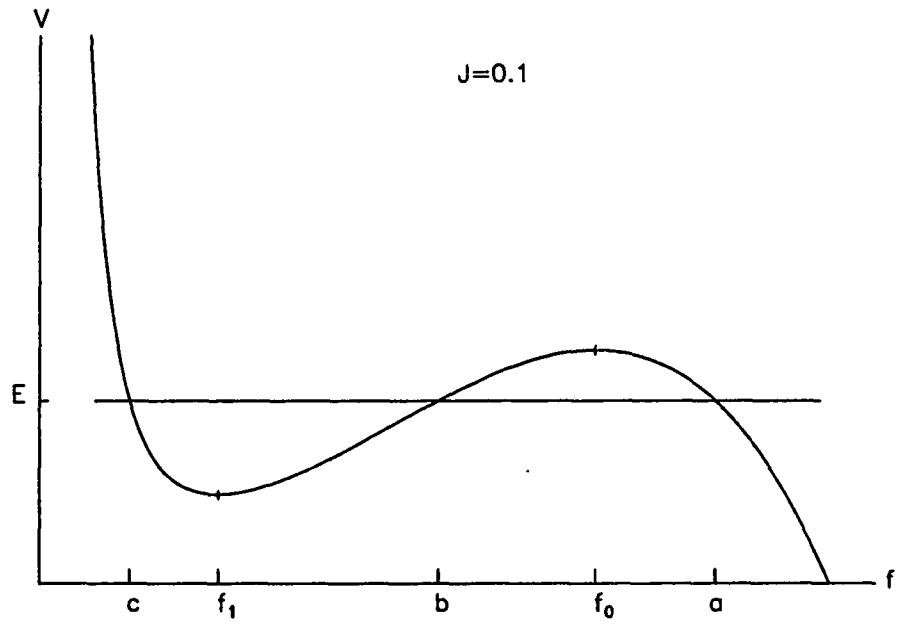

Figure 2.2: Effective potential $V(f;J)$ as a function of f, for $J = 0.1$.

for f that can be written in the form

$$\begin{aligned} f'' &= -\partial_f V(f;J) \\ &= -\partial_f(f^2/2 - f^4/4 + J^2/2f^2). \end{aligned} \tag{2.29}$$

The effective radial potential $V(f;J)$ is pictured in Fig. 2.2. For $J < 2/\sqrt{27}$ there are two positive roots of $-\partial_f V(f;J) = 0$, namely f_0 and f_1. The radial force $-\partial_f V(f;J)$ vanishes at these two points. If $J > 2/\sqrt{27}$ then $f_0 = f_1$ and the two roots merge. Their significance will be discussed in Sec. 2.4.

2.3 Metastability

The key idea, due to Little [6], is that the current-carrying states in a quasi-one-dimensional superconductor are metastable. In other words, thermal fluctuations can carry the system from one metastable current-carrying state, to another. This is

illustrated schematically in Fig. 2.1. In order for a transition to occur, the system must overcome an energy barrier that protects two neighboring metastable states from one another. As the barrier heights protecting a particular state from current-decreasing transitions are smaller than the barriers protecting from current-increasing transitions, the current-decreasing transitions are more likely. Thus, on average, the current decays with time, with the kinetic energy of the current being lost to the environment in the form of heat. The current-altering processes are therefore dissipative. The transition process requires that the superconducting condensate acquire energy. This is possible because the condensate interacts with the phonons and quasiparticles of the metal, which act as a heat bath [7]. Thus, the condensate can absorb energy from these other degrees of freedom, thereby acquiring the energy required to overcome the barrier. These transitions are usually referred to as 'thermally activated' because the requisite energy is provided by the thermal bath (phonons and quasiparticles).

The theoretical description of the thermally activated processes requires a dynamical description of the condensate. This is provided by the time-dependent Ginzburg-Landau theory (TDGL) [17, 18], which, in its simplest form, is relaxational dynamics:

$$\begin{aligned} \frac{\partial\tilde{\psi}(x,t)}{\partial t} &= -2\frac{\delta\mathcal{F}[\tilde{\psi}]}{\delta\tilde{\psi}^*(x,t)} \\ &= (\partial_x - i\tilde{A}_x)^2\tilde{\psi} + \tilde{\psi} - \tilde{\psi}|\tilde{\psi}|^2, \end{aligned} \tag{2.30}$$

where $\mathcal{F}[\tilde{\psi}]$ is given in eq. (2.13), and where the (dimensionless) time t is measured in units of the the Ginzburg-Landau time

$$\tau_{GL} = \frac{\pi\hbar}{8k_B(T_c - T)}, \tag{2.31}$$

where k_B is Boltzmann's constant. The effect of the heat bath is taken into account by adding to the right hand side of eq. (2.30) a space- and time-dependent Gaussian noise term, $\tilde{\eta}(x,t)$, Dirac-delta correlated in both space and time with mean zero and

variance $2D$, where D is determined by the fluctuation-dissipation theorem and is given by [8]

$$D = \frac{4\pi k_B T}{\sigma \xi(T) H_c(T)^2}. \tag{2.32}$$

The resulting stochastic time-dependent Ginzburg-Landau (STDGL) equation can be written in the form

$$\frac{\partial \tilde{\psi}(x,t)}{\partial t} = -2\frac{\delta \mathcal{F}[\tilde{\psi}, \tilde{A}_x]}{\delta \tilde{\psi}^*(x,t)} + \tilde{\eta}(x,t). \tag{2.33}$$

The stochastic time-dependent Ginzburg-Landau equation (2.33) is in the form of a Langevin equation. An alternative dynamical description can be achieved by studying the associated Fokker-Planck equation for the probability density functional $P[\psi]$ [3]. In this description, the dynamical equation for $P[\psi]$ is in the form of a continuity equation, thereby allowing the identification of a probability current (see App. C). Under conditions of steady-state (i.e., $\partial P/\partial t = 0$), there can be a non-zero probability current through the saddle-point. The resulting probability flux will determine the rate of transition from the associated metastable state. If the barrier height—the difference in energy between the saddle-point state and the associated metastable state—is much larger than the thermal energy $k_B T$, then the rate expression is of the Arrhenius type: an 'attempt frequency' pre-exponential factor divided by the exponential of the ratio of the barrier height to $k_B T$ [19, 20, 21]. In our case, the expression for the rate $\ell\Gamma_{-(+)}$ at which current decreasing (increasing) transitions occur can be written as [8]

$$\ell\Gamma_{\pm} = \Omega_{\pm} \exp(-U_{\pm}/k_B T). \tag{2.34}$$

This equation, for the specific case considered here, is derived in App. C. As the fluctuation rate is proportional to ℓ, for convenience in exhibiting the length-dependent corrections to the rate, we have defined $\Gamma_{\pm}$ to be the fluctuation rate per unit length. The quantity $U_{-(+)}$ in eq. (2.34) is the energy barrier protecting the metastable state from current decreasing (increasing) transitions. More specifically, U is the difference in (free) energy between the transition (i.e., saddle-point) state, and the associated

metastable state. The quantity $\Omega_{\pm}$ is the so-called attempt frequency prefactor, and depends on, among other things, the curvature of the free energy about the metastable and saddle-point states. Both U and Ω will be discussed in detail in the following sections.

For the situation in which $\ell \gg 1$, the barrier heights U, and their dependence on current, were computed by Langer and Ambegaokar [7]. The main qualitative feature of their result is that the barriers are a decreasing function of the current, vanishing at the critical current. (The behavior for currents near the critical current is the subject of Chapter 4.) In this same limit, i.e., $\ell \gg 1$, the attempt frequencies Ω, and their dependence on current, were first calculated by McCumber and Halperin [8], and subsequently by Duru, Kleinert and Uñal [22]. Again, the main qualitative feauture of both results is that Ω vanishes at the critical current.

In the present, we determine the length-dependent corrections to the barrier heights and attempt frequencies. We find that as the length of the wire is reduced, the barrier heights increase. This has the effect of *decreasing* Γ, the fluctuation rate per unit length. On the other hand, as the length of the wire is reduced, the attempt frequency prefactor acquires length-dependent corrections that tend to increase Ω/ℓ. This has the effect of *increasing* Γ. Thus, these two effects compete. As we shall see, the effect due to the barrier heights is dominant, and so the final conclusion is that as the length of the wire is reduced, the decay rate (per unit length of the wire) decreases.

2.4 Metastable States

The fluctuation rates are determined by the properties of the two distinguishing features on the free energy landscape: the local minima and the saddle-points. The metastable states are the subject of this section. These states are a subset of the simplest stationary states: uniformly twisted plane waves. These configurations have a constant amplitude, either f_0 or f_1 (see Fig. 2.2), and a phase that is linearly

proportional to x. In the mechanical analogy, the uniformly twisted plane waves correspond to a particle executing circular motion with constant radius f_0 or f_1, and a constant angular velocity. In addition, the mechanical energy E_m is equal to either $V(f_0, J)$ or $V(f_1, J)$. Denoting these states by ψ_m, they can be written as

$$\psi_m(x; k, \phi_{m,0}) = f_m \exp i\phi_m(x) \tag{2.35}$$

$$f_m^2 = u(k_m), \tag{2.36}$$

$$\phi_m(x) = \phi_{m,0} + k_m x, \tag{2.37}$$

where $u(q) \equiv (1-q^2)$, and $\phi_{m,0}$ is an arbitrary phase (which can be taken to be zero). A useful visualization of these states can be achieved by constructing a parametric plot of the real and imaginary parts of ψ_m, as a function of x. The resulting plot is a helix with $\ell k_m/2\pi$ loops, as shown schematically in Fig. 2.3.

The wavevector k_m characterizes the uniformly twisted states. The supercurrent $\mathcal{J}_m \equiv \mathcal{J}[\psi_m]$ is obtained by inserting eq. (2.35) into eq. (2.26), yielding

$$\mathcal{J}_m(k_m) = k_m(1 - k_m^2). \tag{2.38}$$

Notice that $\mathcal{J}_m$ achieves a maximum value of $\mathcal{J}_c = 2/\sqrt{27}$, the so-called critical current, at the critical wavevector $k_c = 1/\sqrt{3}$. For a given $\mathcal{J}_m < \mathcal{J}_c$, there are two values of k_m that satisfy this relation, one smaller than k_c, and the other larger. The smaller of these determines f_0, and the larger, f_1 (see Fig. 2.2).

The free energy $\mathcal{F}_m \equiv \mathcal{F}[\psi_m]$ of the uniformly twisted states can also be expressed in terms of the wavevector k_m. The desired expression is obtained by inserting eq. (2.35) into eq. (2.21), yielding

$$\mathcal{F}_m(k_m) = -\frac{\ell}{2}(1 - k_m^2)^2. \tag{2.39}$$

As a function of k_m, $\mathcal{F}_m(k_m)$ has a point of inflection at $k = k_c$; for $k < (>)k_c$, the curvature of $\mathcal{F}_m$ is positive (negative). Thus, the metastable states are those uniformly twisted states for which $k < k_c$. This implies that the mechanically stable

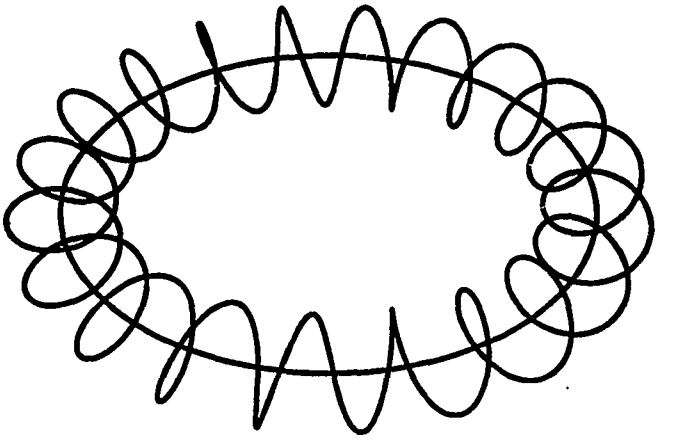

Figure 2.3: Schematic parametric (in x) plot of the real and imaginary parts of state ψ_m. The simple circle represents the wire.

states (in the sense of the mechanical analogy) for which $f_m = f_1$ are thermodynamically *unstable*. Furthermore, the mechanically unstable states for which $f_m = f_0$ are (thermodynamically) *metastable*. The stability of the uniformly twisted states is treated in more detail in Sec. 4.5.

In the physical situation of a ring-shaped wire of circumference $L = \ell\xi(t)$ (see eq. (2.14)), threaded by a static magnetic flux $\hbar\Phi/2e$ (see eq. (2.23)), the two (dimensionless) independent variables are ℓ and Φ. Imposing the boundary condition of eq. (2.22) relates k_m to both of these via

$$k_m\ell = 2\pi n_m + \Phi, \tag{2.40}$$

where n_m is an integer. Thus, once ℓ and Φ are given, the properties of the metastable states, i.e., their currents $\mathcal{J}_m$ and free-energies $\mathcal{F}_m$, are completely determined. Moreover, these states are quantized, in a manner analogous to the quantization of angular

momentum in quantum mechanics. In other words, for a system of finite length, there are a fixed number of metastable states, in which the system can reside for extended periods of time (illustrated schematically in Fig. 2.1). The duration of such stays are what we intend to compute.

In the present chapter we focus on the decay of a metastable current-carrying state. A useful visualization of this process can be obtained by referring to the helical plot of ψ_m shown in Fig. 2.3. In this representation, the decay of a metastable current carrying state is associated with the loss of a loop of the helix. In order for this to occur, the amplitude of ψ_m must vanish at some point in the sample. (Recall that the boundary condition given in eq. (2.22) precludes the unwinding at the boundaries.) The vanishing of $|\psi_s|$ implies that the phase of the order parameter becomes undefined at the point at which $|\psi_s| = 0$. In this way, the total phase-difference can change by an integral multiple of 2π. In this chapter, we will only consider phase changes of 2π. These processes are often referred to as 'phase-slip' processes. Physically, a phase-slip is associated with the creation of a region of normal (i.e., nonsuperconducting) metal, and is therefore dissipative. More specifically, the kinetic energy of the condensate is lost to the environment (quasi-particles and phonons), and is dissipated as thermal energy (i.e., heat). In order to fully understand the phase-slip process, we now need to turn our attention to the transition states.

2.5 Transition States

The transition states are the points of lowest free energy connecting two neighboring metastable states. In other words, these states are saddle-points of $\mathcal{F}$ and are characterized by the existence of a single 'downhill' direction in function space—the reaction coordinate. One way to picture a current-altering transition is to view the system point as (mainly) executing small random excursions about a metastable state ψ_m. Occasionally however, the fluctuating environment can supply enough energy so that it is possible for the system to explore the neighborhood of the saddle-point, and

thus make the transition to a neighboring local minimum of $\mathcal{F}$.

The saddle-point states are obtained by solving the stationary equations (2.27) and (2.28). In contrast to the metastable states, which have a constant amplitude, the saddle-point states have an amplitude that varies with x. Referring to the mechanical analogy (see Fig. 2.2), the saddle-point trajectories have a mechanical energy $E < V(f_0, J)$. Thus, f_s, the amplitude of the saddle-point state, is bounded below by c, and above by b. As the boundary conditions require that $f_s(-\ell/2) = f_s(\ell/2)$, the radial motion must be periodic, with period ℓ. As an example, suppose that at 'time' $x = -\ell/2$, the radius of the mechanical particle is b. Then, at 'time' $x = 0$, the particle radius will have reached the turning point, and $f_s = c$. At this point, the radius will continue to increase again until reaching the other turning point at $f_s = b$. These trajectories are sometimes referred to as bounce (or instanton) solutions [23, 24]. Here, we will only consider trajectories that 'bounce' once.

The conservation of E and J allows ψ_s to be determined by quadratures, with the result that (see App. B)

$$\psi_s(x; k_s, m, x_0, \phi_{s,0}) = f_s(x) \exp i\phi_s(x), \tag{2.41}$$

$$f_s(x)^2 = 2k_s^2 + \frac{1}{3} m_1 \Delta(k_s) + m\, \Delta(k_s)\, \mathrm{sn}(\sqrt{\Delta(k_s)/2}\,(x - x_0)|m)^2, \tag{2.42}$$

$$\phi_s(x) = \phi_{s,0} + \mathcal{J}_s(k_s, m) \int_{x_0}^{x} dx' f_s(x')^{-2}, \tag{2.43}$$

where

$$\mathcal{J}_s \equiv \mathcal{J}[\psi_s] \tag{2.44}$$

is the dimensionless supercurrent of the saddle-point state [see eq.)2.26)]. The function sn in eq. (2.42) is a Jacobi elliptic function [25, 26], $\Delta(q) \equiv (1 - 3q^2)$ and $m_1 \equiv (1 - m)$. As with the metastable states, it is useful to construct a parametric plot of the real and imaginary parts of ψ_s as a function of x (see Fig. 2.4). In this figure we can see that the helix is in the process of losing a loop. However, as the amplitude of $|\psi_s|$ is not zero, the phase-slip has not yet occured.

The states ψ_s depend on four constants of integration: k_s, m, x_0, and $\phi_{s,0}$. The position x_0 locates the point at which $|\psi(x)|$ achieves its minimum value; due to the

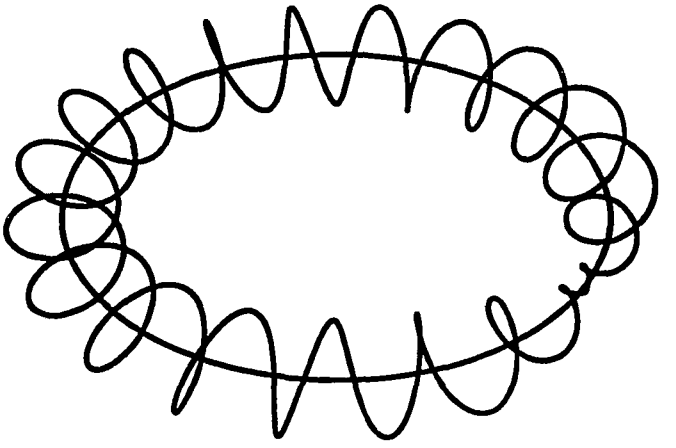

Figure 2.4: Schematic parametric (in x) plot of the real and imaginary parts of state ψ_s. The simple circle represents the wire.

assumed translational invariance of the wire this point is arbitrary, and can be set to zero. The constant $\phi_{s,0}$ is an arbitrary phase-reference; due to the U(1) symmetry of the integrand of $\mathcal{F}$, this phase is arbitrary, and can also be set to zero. These two symmetries, translational and gauge, are however, important. They each give rise to a Goldstone mode [27], and this will be important when we consider the attempt frequency in Sec. 2.7. The constant k_s is an effective wavevector, and m is related to the mechanical energy E_s of eq. (2.27); both of these will be discussed below.

The relationship between the constants k_s and m and the independent variables ℓ and Φ is obtained by requiring that ψ_s satisfy the boundary condition given in eq. (2.22), which gives

$$\ell(k_s, m) = \sqrt{8/\Delta(k_s)}\, K(m), \tag{2.45}$$

$$\phi_s(\ell/2; k_s, m) = \Phi + 2\pi n_s, \tag{2.46}$$

in which K is the complete elliptic integral of the first kind [26], and n_s is an integer. In the limit that $m \to 1$, $2K(m) \to \ln(16/m_1)$, so that eq. (2.45) reduces to

$$m_1 \approx \frac{1}{16} \exp(-\sqrt{\Delta(k_s)/2}\,\ell). \tag{2.47}$$

Thus, if the exponent of eq. (2.47) is much larger than one, ignoring terms of order m_1 is valid. As we are interested in possible algebraic length-dependent corrections to the lifetime of the current-carrying states, we will assume that $m_1 \ll 1$. This condition requires that $\ell\sqrt{\Delta(k_s)/2} \gtrsim 1$; this condition is violated if k_s is too close to $1/\sqrt{3}$. Therefore, we are restricted to near-equilibrium regime where the current $\mathcal{J}_s$ is far from the critical current. In the limit that $m \to 1$, eq. (2.46) reduces to

$$k_s\ell + 2\chi(k_s) = 2\pi n_s + \Phi, \tag{2.48}$$

$$\chi(q) \equiv \arctan\sqrt{\Delta(q)/2q^2}. \tag{2.49}$$

Thus, as we found previously (in Sec. 2.4) for the metastable states, the saddle-point states are quantized. Notice that eq. (2.48) differs from the corresponding equation for k_m, eq. (2.40), by the term $2\chi(k_s)$. Thus, the parameter k_s is interpreted as an effective wavevector.

The free energy $\mathcal{F}_s \equiv \mathcal{F}[\psi_s]$ of the saddle-point states is given by [28]

$$\begin{aligned}\mathcal{F}_s(k_s,m) \;=\; & -\frac{2K(m)}{a^2}\left[\frac{c^4}{2} + \frac{b^2c^2}{m} + \left(\frac{2+m}{6}\right)\frac{b^4}{m^2}\right] + \\ & E(m)\left[\frac{2b^2c^2}{ma^2} + \frac{2(1+m)b^4}{3a^2m^2}\right],\end{aligned} \tag{2.50}$$

and the current $\mathcal{J}_s$ [see eq. (2.44)] is given by

$$\mathcal{J}_s(k_s,m) = abc/\sqrt{2}, \tag{2.51}$$

where $E(m)$ is the complete elliptic integral of the second kind [26]. The three constants a, b, and c are pictured in Fig. 2.2, and are defined in terms of terms of m and k_s in App. B. In the limit that $m \to 1$, eqs. (2.50) and (2.51) reduce considerably, yielding the forms

$$\mathcal{F}_s(k_s) = -\frac{\ell}{2}(1-k_s^2)^2 + \frac{4}{3}\sqrt{2\Delta(k_s)} \tag{2.52}$$

and

$$\mathcal{J}_s(k_s) = k_s(1 - k_s^2). \tag{2.53}$$

Thus, in this limit, the free energy and the current of the saddle-point states are completely determined by k_s and ℓ, with k_s being the effective wavevector characterizing ψ_s.

In order to compute the barrier heights and attempt frequencies, it is necessary to make the connection between a given metastable state and its associated saddle-point states. This connection is made in the following way. The key notion is that all states, by virtue of the boundary condition given in eq. (2.22), have the same phase (modulo 2π). Suppose that the metastable state ψ_m under consideration has a wavevector $k_m = \Phi/\ell$ [see eq. (2.40)]. Then the saddle-point state ψ_s^- protecting ψ_m from current-reducing fluctuations will have a current $\mathcal{J}_s^-$, and hence wavevector k_s^-, that is slightly smaller than k_m. On the other hand, the saddle-point state ψ_s^+ protecting ψ_m from current-increasing fluctuations will have a current $\mathcal{J}_s^+$, and hence wavevector k_s^+, that is slightly larger than k_m. Thus, k_s^- can be obtained by setting $n_s = 0$ in eq. (2.48), and equating this expression with that from eq. (2.40). This gives $k_s^-\ell + 2\chi(k_s^-) = k_m\ell$. As k_s^+ is slightly larger than k_m, we have that $n_s = 1$, and so $k_s^+\ell + 2\chi(k_s^+) - 2\pi = k_m\ell$. These two expressions can be combined into the compact form

$$k_m\ell = k_s^\pm\ell + 2\chi(k_s^\pm) - (\pi \pm \pi), \tag{2.54}$$

up to terms of order m_1. Equation (2.54) gives k_m in terms of k_s; we seek k_s in terms of k_m. Inverting eq. (2.54) gives, to second order in ℓ^{-1},

$$k_s^\pm = k_m - \ell^{-1}\chi_\pm(k_m) - \ell^{-2}\frac{2\sqrt{2}\chi_\pm(k_m)}{u(k_m)\sqrt{\Delta(k_m)}} + \mathcal{O}(\ell^{-3}), \tag{2.55}$$

$$\chi_\pm(q) \equiv 2\chi(q) - (\pi \pm \pi). \tag{2.56}$$

This relationship is central. It is the length-dependence of the relationship between k_m and $k_s^\pm$ that gives rise to the algebraic length-dependences of the barrier heights and attempt frequencies.

Finally, the main results of this section, for the particular case of a saddle-point protecting a metastable state from a current-decreasing transition, are summarized visually in Fig. 2.5. In this figure, the amplitude and phase of a metastable state (dotted curves) and its associated (current-decreasing) saddle-point state (solid curves) are plotted as a function of x. Here we see that f_s is reduced over a spatial region of width $\mathcal{O}(\xi)$ around x_0, which in this case is zero. This reduction in f_s means that the phase ϕ_s must wind more rapidly in this region. However, in order to compensate for this, i.e., in order that k_s—the slope of ϕ_s in the outer regions—satisfy eq. (2.48), the phase must wind less rapidly in the region over which $|\psi_s(x)|$ varies. This implies that $k_s < k_m$, as can be seen in Fig. 2.5.

2.6 Barrier Heights

The barrier heights are determined by the difference in free energy between the metastable and saddle-point states, i.e.,

$$U = D^{-1} k_B T (\mathcal{F}[\psi_s] - \mathcal{F}[\psi_m]) \equiv D^{-1} k_B T \Delta\mathcal{F}. \tag{2.57}$$

Although $\mathcal{F}_m$ and $\mathcal{F}_s$ are given in eqs. (2.39) and (2.50), respectively, we seek the barrier heights protecting a given metastable state ψ_m from current-altering transitions. Thus, we are required to determine the relationship between a given state ψ_m and its associated saddle-points. This was accomplished in the previous section [see eq. (2.55)], where we restricted our attention to the nearest-neighbor saddle-points. Combining eqs. (2.55), (2.39) and (2.50), we find

$$\Delta\mathcal{F}_\pm = \Delta\mathcal{F}_\pm^{(0)} + \ell^{-1}\Delta\mathcal{F}_\pm^{(1)} + \mathcal{O}(\ell^{-2}), \tag{2.58}$$

$$\Delta\mathcal{F}_\pm^{(0)} = \frac{4}{3}\sqrt{2\Delta(k_m)} - 2\chi_\pm(k_m)k_m u(k_m), \tag{2.59}$$

$$\Delta\mathcal{F}_\pm^{(1)} = \chi_\pm(k_m)^2\Delta(k_m), \tag{2.60}$$

where $\Delta\mathcal{F}_{+(-)}$ is the barrier height associated with current increasing (decreasing) transitions. Although only the $\mathcal{O}(\ell^{-1})$ correction to the barrier is exhibited, it is

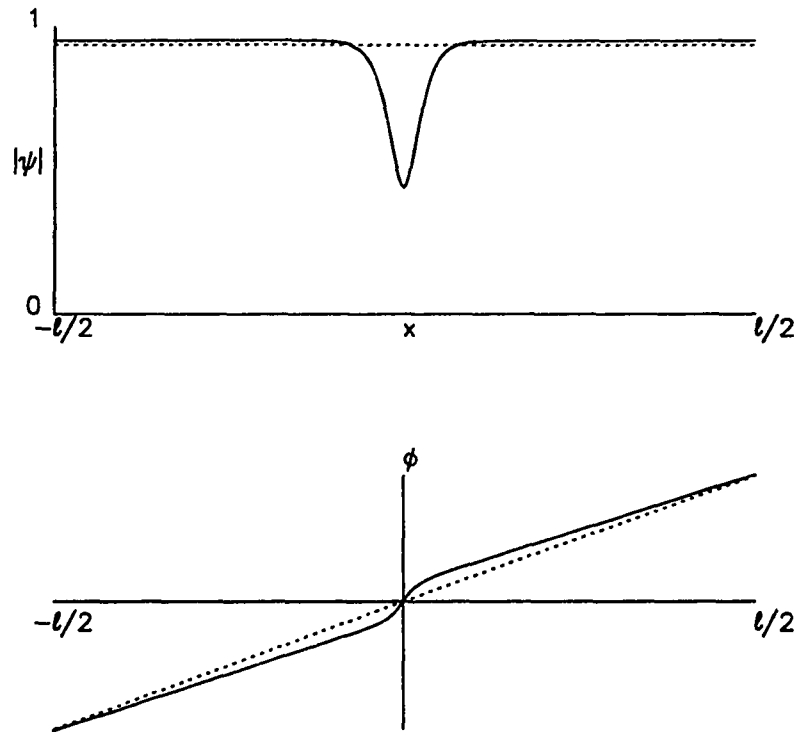

Figure 2.5: $|\psi_s|$ and ϕ_s as a function of x for a saddle-point associated with a current decreasing transition. The dotted lines are the corresponding amplitude and phase for the associated metastable state.

straightforward to compute the subsequent (algebraic) corrections. In order to compute the n^{th} order correction, it is necessary to find k_s as a function of k_m, to the $(n+1)^{th}$ order, as the free energies $\mathcal{F}_m$ and $\mathcal{F}_s$ are proportional to ℓ [see eqs. (2.39) and (2.50)].

Evidently, the barrier heights are increased relative to their infinite-length value. In the small current limit, i.e., when $k_m \to 0$, we find that $\Delta\mathcal{F}_{\pm}^{1} \to \pi^2$; thus, the corrections can be numerically significant. At first sight, it is not obvious that, in the $m = 1$ approximation [see eq. (2.47)], any nonexponential length-dependent correc-

tions should arise. One might expect that, due to the fact that the spatial variation is localized to a spatial region of order $\xi(T)$, the system would be sensitive to the size only when $L \sim \xi(T)$. If this reasoning were valid, we would expect that the leading length-dependent corrections would be exponential in ℓ^{-1}. That they are algebraic results from the presence of the phase degree of freedom, and the consequent requirement that the metastable and transition states have the same winding angle, modulo 2π. More specifically, the length-dependence of the barrier heights arises solely from the relationship, given in eq. (2.55), between k_m and k_s; it is precisely this relationship that is the source of the algebraic length-dependence.

2.7 Attempt Frequencies

The prefactor Ω in the Arrhenius-type expression for the fluctuation rate $\ell\Gamma$ is given by

$$\Omega = \frac{1}{\tilde{\tau}(T)} \frac{\mathcal{V}_s^{(1)} \mathcal{V}_s^{(2)}}{\mathcal{V}_m^{(1)}} |\lambda_{s0}| \left| \frac{\det' L_s}{\det' L_m} \right|^{-1/2} . \tag{2.61}$$

(This equation is derived in App. C.) The quantity $\tilde{\tau}(T) \equiv \tau_{GL}(T)\sqrt{D4\pi^3}$ is a characteristic time [see eq. (2.31)]. The $\mathcal{V}$-factors appearing in eq. (2.61) arise from integrations over the so-called zero modes (see [29] and App. C); $\mathcal{V}_s^{(1)}$ and $\mathcal{V}_m^{(1)}$ result from integrating over the collective coordinates associated with gauge invariance, and $\mathcal{V}_s^{(2)}$ results from integrating over the collective coordinate associated with translational invariance. This latter symmetry gives rise to the overall scaling of Ω with ℓ. The quantity λ_{s0} is the negative eigenvalue associated with the reaction coordinate (see below). The fact that Ω is proportional to λ_{s0} is consistent with the intuitive notion that an increase in the curvature of the free energy at the saddle-point, in the 'downhill' direction, will result in an increased fluctuation rate. As we are interested in algebraic corrections to Ω, the value of λ_{s0} obtained for $\ell = \infty$ is sufficient, as any corrections are $\mathcal{O}(m_1)$. Based on this, it is tempting to argue that since any individual eigenvalue should only acquire corrections of $\mathcal{O}(m_1)$, the overall length-dependent corrections to Ω will be of this same order, i.e., not of interest here. This is not in

fact the situation, as will be borne out by the explicit exhibition of algebraic length-dependent corrections to Ω. The reason is that the exponentially small corrections to an individual eigenvalue accumulate in the infinite product of eigenvalues to generate an algebraic dependence on the length.

The quantities L_m and L_s appearing in eq. (2.61) are the so-called fluctuation operators that are associated with the second variation

$$\delta\mathcal{F}_c^{(2)} = \int_{-\ell/2}^{\ell/2} dx \delta\Psi^\dagger L_c \delta\Psi$$

of the free energy. The two components of $\delta\Psi$ are $\delta\psi$ and its complex conjugate, so that

$$L_c = \begin{bmatrix} -\partial_x^2 - 1 + 2f_c^2 & f_c^2\, e^{2i\phi_c} \\ f_c^2\, e^{-2i\phi_c} & -\partial_x^2 - 1 + 2f_c^2 \end{bmatrix}. \tag{2.62}$$

The metastable states ψ_m are those states for which all eigenvalues of L_m are non-negative. In other words these states are local minima of $\mathcal{F}$. The saddle-point states ψ_s are characterized by the existence of a single negative eigenvalue (λ_{s0}) in the spectrum of L_s. The associated negative eigenvector is the so-called reaction coordinate representing the direction (in function space) of largest decrease of $\mathcal{F}$.

Whereas it was straightforward to compute the barrier heights, the same is not true for the attempt frequencies. The difficulty is in the computation of the ratio of functional determinants

$$R' \equiv \det' L_s / \det' L_m, \tag{2.63}$$

that appears in eq. (2.61. The primes on det indicate that no zero eigenvalues are included in the computation of the determinants. The dependence of Ω on the ratio R' can be understood intuitively, in the following way. First of all, the proportionality of Ω to $\sqrt{\det' L_m}$ is actually what gives rise to the labelling of Ω as an attempt frequency. (Strictly speaking, it is only this term, divided by the dimensionful time $\tilde{\tau}(T)$, that should be called an attempt frequency.) The idea is that as the curvature of the free energy about the metastable state increases, the frequency with which the system fluctuates about the state ψ_m increases, thus leading to an increase in the number

of attempts, per unit time, to cross the barrier. On the other hand, Ω is inversely proportional to $\sqrt{\det' L_s}$. This dependence reflects the notion that if the curvature of the free energy at the saddle-point, *perpendicular to the reaction coordinate*, is decreased, the system has more configuration space through which to pass over the top of the barrier, and hence the result will be an increase in the fluctuation rate.

A useful interpretation of $\sqrt{\det' L_e}$ is in terms of an entropy [8]. That is, $S_e \equiv -k_B \ln \sqrt{\det' L_e}$ is interpreted as the entropy associated with order parameter fluctuations about state ψ_e [8]. Then, if $\mathcal{F}_{tot}[\psi_e] \equiv \mathcal{F}[\psi_e] + TS_e$ is defined to be the *total* free energy (where $\mathcal{F}$ is now interpreted as an energy, rather than a free energy), then the fluctuation rate $\ell\Gamma$ can be written in the form

$$\ell\Gamma = \frac{1}{\tilde{\tau}(T)} \frac{\mathcal{V}_s^{(1)} \mathcal{V}_s^{(2)}}{\mathcal{V}_m^{(1)}} |\lambda_{s0}| e^{-U_{tot}/k_B T}, \tag{2.64}$$

where $U_{tot} \equiv (\mathcal{F}_{tot}[\psi_s] - \mathcal{F}_{tot}[\psi_m])/D$. This interpretation of the ratio of fluctuation determinants, and hence the fluctuation rate Γ, will be useful when the current source is discussed in Sec. 2.10.

At first sight, the calculation of R' is daunting. There are two main issues. The first is that R' is the ratio of two infinite products of eigenvalues of differential operators, which are in general difficult to diagonalize directly. The second is that any zero eigenvalues must be omitted from the ratio of products. In the work of McCumber and Halperin [8], R' was computed directly. However, their result only applies to the situation in which $\ell = \infty$, and it is not clear how to generalize their results to the case of finite ℓ.

Fortunately, however, there is a recent mathematical result, due to Forman [30], that expresses R (the ratio of determinants including *all* eigenvalues) in terms of the boundary conditions and the solutions of the homogeneous equation

$$L_e \eta_e = 0. \tag{2.65}$$

Forman's result is that

$$R = \frac{\det [M + NY_s(\ell/2)]}{\det [M + NY_m(\ell/2)]}. \tag{2.66}$$

Here the (4×4) matrices N and M encode the boundary conditions, and $Y_e(x)$ is the so-called fundamental matrix, constructed from the η_e (see Chap. 3 and App. D). Thus, the ratio of infinite dimensional matrices has been reduced to the ratio of finite- (in this case four-) dimensional matrices. In addition, Forman's equation (2.66), a generalization of the Gel'fand-Yaglom formula [31], is particularly useful in that it emphasizes the independent roles of the boundary conditions and the solutions η_e, which, by definition, have no dependence on boundary conditions.

The first issue discussed in the previous paragraph, viz., the computation of the determinant of an infinite-dimensional matrix, is resolved by Forman's equation (2.66). However, in order to compute Ω, R' is needed, not R, which in the presence of zero modes would be 0/0, and thus not well-defined. Thus, eq. (2.66) must be modified in some way. One natural approach is to 'regularize the problem'. Generally, this consists of perturbing the problem in some way so that what were once zero eigenvalues are no longer zero, in which case eq. (2.66) can be used to obtain a meaningful result. Next, the pseudo-zero eigenvalues are computed, usually perturbatively, and factored out of the perturbed result. Finally, the perturbation parameter can be taken to zero, leaving a well-defined result for the ratio R'.

There are at least three distinct schemes by which to accomplish the regularization. One way to proceed is to to move the location of the boundaries. This is essentially the procedure followed by Duru, Kleinert, and Uñal [22]. In their approach they made use of the Gel'fand-Yaglom formula [31]; in this sense their approach is similar to the approach presented here. However, their approach, which requires integrating out the phase degree of freedom (leaving 1×1 matrix-differential operators, as opposed to the 2×2 matrix-differential operators L_e [see eq. (2.62)] under consideration here) is only valid in the limit that $\ell = \infty$. Another option is to perturb the operator in such a way so that the determinant of the perturbed operator can be calculated using Forman's equation. What was a zero mode will now be non-zero, in proportion to the strength of the perturbation; the psuedo-zero eigenvalue can then be calculated perturbatively. This is the approach that we have followed in computing Ω [9]. The

utility of our approach, discussed in detail in Appendix D, is our perturbation scheme, which allowed us to make use of Forman's equation (2.66). A third approach is to perturb the form of the boundary conditions, while leaving the form of the operator unchanged (see Chap. 3). The utility of this approach is that it allows the derivation of remarkably simple equations for R', which only depend on the η_i at the boundaries. This approach, which was developed in collaboration with A. J. McKane, will be explained in detail in Chapter 3.

The second approach mentioned in the previous paragraph, namely regularizing by perturbation of L_e, yields the following form for $\Omega_\pm$, accurate to $\mathcal{O}(m_1)$:

$$\begin{aligned}\Omega_\pm &= 2^{7/4}\tilde{\tau}(T)^{-1}\ell\Lambda(k_s^\pm)\Delta(k_s^\pm)^{7/4}\, e^{\sqrt{\Delta(k_m)/2}\ell-\sqrt{\Delta(k_s^\pm)/2}\ell} \\ &\quad\times\left[\frac{\Delta(k_s^\pm)}{\Delta(k_m)}\frac{u(k_m)}{u(k_s^\pm)}\right]^{1/2}\left[1-\frac{2\sqrt{2}}{u(k_s^\pm)\sqrt{\Delta(k_s^\pm)}}\frac{1}{\ell}\right]^{-1/2}, \qquad (2.67)\end{aligned}$$

where $\Lambda(q) \equiv -1-q^2+[3\Delta(q)^2+(1+q^2)^2]^{1/2}$. The details of the derivation of eq. (2.67) are provided in App. D. Equation (2.67) gives the prefactor $\Omega_\pm$ in terms of k_s which, by virtue of eq. (2.55), can be expressed solely in terms of k_m and ℓ. Thus, it is possible to expand $\Omega_\pm(k_m)$ in powers of ℓ^{-1}, to any desired order, yielding the result that the length-dependent corrections have the effect of increasing Ω/ℓ. In the limit that $k_m \to 0$, the expression for $\Omega_\pm$ simplifies considerably to the form

$$\Omega_\pm = \frac{\ell}{\tilde{\tau}}\left[1+\ell^{-1}\frac{4+3\pi^2}{2\sqrt{2}}+\mathcal{O}(\ell^{-2})\right]. \qquad (2.68)$$

The evident increase of the prefactor as the length is reduced is interpreted as the flattening out of the free energy at the saddle-point, *in the directions perpendicular to the reaction coordinate*, thereby providing the system with more configuration space through which to pass over the barrier. Thus, the length-dependent correction to $\Omega_\pm/\ell$ has the effect of tending to increase $\Gamma_\pm$. This is in contrast to the effect from the barrier height corrections which, as was found in Sec. 2.6, tend to reduce $\Gamma_\pm$.

2.8 Results

In Sec. 2.6 we found that as the length of the wire is reduced, the length-dependent corrections to the barrier heights tend to reduce the fluctuation rate per unit length, whereas, in Sec. 2.7 we found that the length-dependent corrections to the pre-exponential factor, or attempt frequency, have the effect of increasing the fluctuation rate per unit length. Thus, these two effects compete. In order to quantify this competition, it is useful to expand, viz.,

$$\Delta\mathcal{F} \approx \Delta\mathcal{F}^{(0)} + \ell^{-1}\Delta\mathcal{F}^{(1)}, \tag{2.69}$$

$$\Omega \approx \Omega^{(0)} + \ell^{-1}\Omega^{(1)}. \tag{2.70}$$

Thus, we find

$$\ln[\Gamma(\ell)/\Gamma(\infty)] \approx \ell^{-1}\{ - D^{-1}\Delta\mathcal{F}^{(1)} + \Omega^{(1)}/\Omega^{(0)}\}, \tag{2.71}$$

$$\Gamma(\infty) \equiv \Omega^{(0)}\exp(-g\Delta\mathcal{F}^{(0)}). \tag{2.72}$$

The competition between the barrier height and attempt frequency corrections is a consequence of the positivity of $\Delta\mathcal{F}^{(1)}$ and $\Omega^{(1)}$. However, in order for the Ginzburg-Landau approach to be valid, we should have $D \ll 1$ [8]. Thus, the length-dependent corrections to the fluctuation rate, and hence the lifetime of the persistent currents, are essentially determined by the length-dependent corrections to the barrier heights.

For the sake of illustration, we suppose that $T_c = 1\,K$, $H_c = 100\,G$, $\xi(0) = 1000\,\mathring{A}$, $\sqrt{\sigma} = 750\,\mathring{A}$, and $T/T_c = 0.99$, so that $D \approx 0.10$. In the low-current limit, $\Delta\mathcal{F}^{(1)} = \pi^2$, so that $\Gamma(\ell)/\Gamma(\infty) \approx \exp(-D^{-1}\Delta\mathcal{F}^{(1)}/\ell) \approx \exp(-99/\ell)$, i.e., roughly 0.14 when $L = 50\,\mu$m. It is worthwhile to note that Γ is extremely sensitive to the temperature; this is due to the temperature dependence of D. For example, for the parameters introduced above, $\Gamma(\infty) \approx 6\,$Hz. However, if we reduce T from 0.99 K to 0.98 K, then D changes from ≈ 0.10 to ≈ 0.035 and now $\Gamma(\infty) \approx 10^{-14}\,$Hz. Thus, it is only for temperatures reasonably close to T_c that the lifetime of a current carrying state is measurable.

2.9 Voltage Source

So far in this chapter we have considered the situation in which the magnetic flux penetrating the ring is static in time. This allowed us to compute the length-dependent corrections to the lifetime of the persistent currents in the ring. If we now allow the (dimensionless) flux Φ [see eq. (2.23)] to increase linearly with time, then, by Faraday's law of induction, a constant electromotive force (emf)

$$V = (\hbar/2e\tau_{GL})\frac{d\Phi(t)}{dt} \tag{2.73}$$

will be induced in the ring. (See Chap. 4 for a more detailed discussion.)

The induced emf will accelerate the superconducting condensate, according to the first London equation (i.e., Newton's law of motion applied to the condensate) [16]. However, as we have seen, the current-carrying states are metastable, i.e., the current can decay. Thus, if the current-altering transitions occur sufficiently frequently, it is possible to establish a nonequilibrium steady state, in which the increase in current resulting from the acceleration due to the emf is balanced, on the average, by the net decrease in current due to thermally activated phase-slip processes. In general, the fluctuation rates will depend on both the current of the metastable state, as well as the externally applied emf. If we denote by $\ell\Gamma_{-(+)}(I,V)$ the (current and voltage dependent) fluctuation rate for current-decreasing (increasing) transitions, then the emf V required to maintain a certain average supercurrent I is given by [32]

$$V = \frac{\ell h}{2e}\big[\Gamma_-(I,V) - \Gamma_+(I,V)\big]. \tag{2.74}$$

Equation (2.74) is complicated by the fact that right-hand-side depends on V. This situation can be simplified considerably if we make a quasi-static approximation. To do so, we identify two time scales. The first is $h/2eV$; this is the time required for the emf to advance the phase of the order parameter by 2π. The second is the time-scale for an individual phase-slip process, which we estimate as being of $\mathcal{O}(\tau_{GL})$. Now, if $\tau_{GL} \ll h/2eV$, then during a particular phase-slip event, the phase is essentially

static. This defines the quasi-static approximation. Under these conditions, eq. (2.74) can be replaced by

$$V = \frac{h}{2e}\big(\Gamma_-(I,0) - \Gamma_+(I,0)\big). \tag{2.75}$$

But, $\Gamma_\pm(I,0)$ are the rates per unit length that we have computed previously. Thus, using eq. (2.64), we can write eq. (2.75) in the form

$$V = \Big(\frac{h}{2e}\Big)\ell\Gamma_-\Big(1 - \frac{\Omega_+}{\Omega_-}e^{-(U_+-U_-)/k_BT}\Big). \tag{2.76}$$

Using the results in eqs. (2.58) and (2.68), in the limit that $k_m \ll 1$, the above expression reduces to

$$V = IR_{int} \tag{2.77}$$

$$R_{int} = R_0\Big(1 + \frac{1}{\ell}\frac{12+3\pi^2}{2\sqrt{2}} + \mathcal{O}(\ell^{-2})\Big)e^{-\Delta\mathcal{F}_-/D} \tag{2.78}$$

where $R_0 \equiv \ell(h/2e)^2/\tilde{\tau}k_BT$, $I = k_m 4ek_BT/D\hbar$ [see eq. (2.16)], and $\Delta\mathcal{F}_-$ is given in eq. (2.58). The quantity R_{int} is the intrinisc resistance of the superconductor. (Using the parameters of Sec. 2.8 and for $T = 0.99$K, in order of magnitude $R_{int}/\ell \approx 1.8\mu\Omega$.) Thus, as we found previously for the length-dependent corrections to the lifetimes of the current-carrying states, the length-dependent correction to the barrier height $\Delta\mathcal{F}_-$ will dominate. Thus, we see that as the length of the wire is reduced, R_{int}/ℓ, the intrinsic resistance per unit length, will decrease.

2.10 Current Source

In this section we imagine that the superconducting ring is driven by a current-source. In particular, we imagine that the solenoidal flux can respond to the supercurrent fluctuations, by inserting or removing flux, so as to maintain a constant supercurrent. This requires some type of feedback mechanism whereby the magnetic moment of the ring is monitored (e.g., using a SQUID magnetometer) and any time a fluctuation in the magnetic moment is detected, the feedback mechanism responds in just such a way as to counteract the intrinsic fluctuation. In this case, the independent variable

is the (dimensionless) supercurrent $\mathcal{J}$, in contrast to the voltage source, where the independent variable is the (dimensionless) flux Φ. In other words, for a current-source, the flux Φ fluctuates and the current $\mathcal{J}$ is determined, in contrast to a voltage-source, where Φ is determined and $\mathcal{J}$ fluctuates.

In order to compute the fluctuation rates when $\mathcal{J}$ is the independent variable, we need to change the ensemble from one in which Φ is constant to one in which $\mathcal{J}$ is constant. Referring to eq. (2.64), this means that we need to compute the *total* free energy when the current is the independent thermodynamic variable. This is accomplished by introducing a (generalized) fugacity $\exp(2D^{-1}\mathcal{J})$, multiplying the numerator and denominator by this quantity, and integrating each over the now unconstrained (i.e., fluctuating) variable Φ:

$$\ell\Gamma = \frac{1}{\tilde{\tau}(T)} \frac{\int_0^{2\pi} d\Phi\, e^{2D^{-1}\mathcal{J}\Phi} \left\{ e^{-D^{-1}\mathcal{F}[\psi_s]}\, \mathcal{V}_s^{(1)} \mathcal{V}_s^{(2)} |\lambda_{s0}| |\det' \mathrm{L}_s|^{-1/2} \right\}\Big|_\Phi}{\int_0^{2\pi} d\Phi\, e^{2D^{-1}\mathcal{J}\Phi} \left\{ e^{-D^{-1}\mathcal{F}[\psi_m]}\, \mathcal{V}_m^{(1)} |\det' \mathrm{L}_m|^{-1/2} \right\}\Big|_\Phi}. \tag{2.79}$$

The integrations over Φ may be performed using Laplace's method because $D \ll 1$ [33]. The maximum values of the exponents, i.e., (minus) the Gibbs free energies [34]

$$\mathcal{G}[\psi_e] \equiv \mathcal{F}[\psi_e] - 2\mathcal{J}\Phi_e \tag{2.80}$$

occur at

$$\Phi_s = k\ell + 2\chi(k) \pmod{2\pi} \tag{2.81}$$

and

$$\Phi_m = k\ell \pmod{2\pi}, \tag{2.82}$$

where $k(< 1/\sqrt{3})$ satisfies $\mathcal{J} = k\,u(k)$. This can be seen by first noting that the Φ_e satisfy

$$2\mathcal{J} = \left.\frac{\partial \mathcal{F}[\psi_e]}{\partial \Phi}\right|_{\Phi_e} = \left.\frac{\partial \mathcal{F}_e}{\partial k_e} \frac{\partial k_e}{\partial \Phi}\right|_{\Phi_e}. \tag{2.83}$$

Using eqs. (2.39) and (2.50) for $\mathcal{F}_m$ and $\mathcal{F}_s$, respectively, and eqs. (2.40) and (2.48) for $k_m(\Phi)$ and $k_s(\Phi)$, respectively, and defining k to be the smallest positive root of

$\mathcal{J} - k(1-k^2) = 0$ (for $\mathcal{J} < 2/\sqrt{27}$), eq. (2.83) yields the result that

$$k_e = k. \tag{2.84}$$

Equation (2.84), when combined with eqs. (2.81) and (2.82), yields the values for Φ_e given in eqs. (2.81) and (2.82). The interpretation is that the current source responds to a fluctuation by inserting (or removing) flux so as to maintain a constant current. Thus, Φ_m and Φ_s differ. Using Laplace's method, eq. (2.79) can be written as

$$\ell\Gamma = \tau(T)^{-1}\sqrt{\frac{\mathcal{F}_m''}{\mathcal{F}_s''}}\frac{\left\{\mathcal{V}_s^{(1)}\mathcal{V}_s^{(2)}|\lambda_{s0}||\det' L_s|^{-1/2}\right\}\Big|_{\Phi_s}}{\left\{\mathcal{V}_m^{(1)}|\det' L_m|^{-1/2}\right\}\Big|_{\Phi_m}} e^{-(\mathcal{G}_s-\mathcal{G}_m)/D} \tag{2.85}$$

where $\mathcal{F}_e'' \equiv \partial^2\mathcal{F}[\psi_e]/\partial\Phi^2|_{\Phi_e}$. This quantity takes into account the phase fluctuations that are required to maintain a constant current $\mathcal{J}$. Using eq. (2.39) for $\mathcal{F}_m$, and eq. (2.40) for $k_m(\Phi)$, we find that

$$\mathcal{F}_m'' = \frac{2\Delta(k)}{\ell}. \tag{2.86}$$

Similarly, using eq. (2.50) for $\mathcal{F}_s$ and eq. (2.48) for $k_s(\Phi)$, we find that

$$\mathcal{F}_s'' = \frac{2\Delta(k)}{\ell}\left(1 - \frac{2\sqrt{2}}{u(k)\sqrt{\Delta(k)}}\frac{1}{\ell}\right). \tag{2.87}$$

Now, the the third factor in the right-hand-side of eq. (2.85) can be obtained from eq. (2.67) by replacing k_m and k_s by k [see eq. (2.84)], which when combined with eqs. (2.86) and (2.87) yields

$$\ell\Gamma_\pm = 2^{7/4}\tilde{\tau}(T)^{-1}\ell\Lambda(k)\Delta(k)^{7/4}e^{-U_\pm/k_BT}, \tag{2.88}$$

where the barrier heights $U_\pm$ are given by

$$U = D^{-1}k_BT(\mathcal{G}[\psi_s] - \mathcal{G}[\psi_m]) \equiv D^{-1}k_BT\Delta\mathcal{G}_\pm, \tag{2.89}$$

and where

$$\Delta\mathcal{G}_\pm = \frac{4}{3}\sqrt{2\Delta(k)} - 4\chi_\pm(k)k\,u(k) + \mathcal{O}(m_1). \tag{2.90}$$

The $+(-)$ subscript stands for flux-increasing (decreasing) transitions. As $\Delta\mathcal{G}_- < \Delta\mathcal{G}_+$, the flux-decreasing transitions are more likely than the flux-increasing transitions, which implies that on average, the current-source must add flux to the system; in other words, the system is dissipative. From eq. (2.88), we see that although the pre-exponential factors in the integrands of eq. (2.79) depend algebraically on ξ/L, this algebraic dependence is *exactly cancelled* by the ratio $\sqrt{\mathcal{F}_m''/\mathcal{F}_s''}$ that arises from the Gaussian fluctuations of Φ. Thus, in contrast with the voltage-source case, we see that the rate per unit length Γ is insensitive to the sample circumference, up to terms $\mathcal{O}(m_1)$.

The different behavior of mesoscopic superconducting rings under the influence of voltage and current sources is a specific example of the general result that for systems that are not in the thermodynamic limit, i.e. mesoscopic systems, the choice of ensemble is not free. In thermodynamics, the different thermodynamic potentials that are associated with different ensembles, which are distinguished by their independent variables, are related by a Legendre transformation. However, when the system is not in the thermodynamic limit, the change of ensemble is implemented as above, by introducing a generalized fugacity, and integrating over the variable conjugate to the independent variable. This allows the effect of the fluctuations of the conjugate-variable to be taken into account. As we have seen explicitly above, where the fluctuations in Φ are responsible for the exact cancellation of the explicit time dependence of the attempt frequency, these fluctuations can be important in the mesoscopic regime.

2.11 Conclusions

In this chapter we have studied the length-dependence of the lifetime of persistent currents in superconducting rings. We found algebraic length-dependent corrections to both the energy barriers and attempt frequencies that enhance both quantities. The increase in the barrier heights has the effect of reducing the transition rate (per

unit length), whereas the increase in the attempt frequencies (per unit length) has the effect of increasing the transition rate (per unit length). Thus, a competition arises. In practise, we found that it is the barrier heights that dominate, so our conclusion was that as the length of the wire is reduced, the transition rate (per unit length) decreases.

In the second part of the chapter we considered two distinct experimental situations: (i) the system is driven by a voltage source, and (ii) the system is driven by a current source. We found that for the voltage source case, the lifetimes of the metastable current-carrying states acquire algebraic length-dependent corrections that are identical to those found for the persistent currents. On the other hand, we found that in the case of the current source, there are no algebraic length-dependent corrections. This is a specific example of the general result that for systems that are not in the thermodynamic limit, the choice of ensemble is not free, but depends on the experimental circumstances.

In order to carry out the computations, we made use of two mathematical results: Forman's equation and Jacobi's theorem. The former is relatively new, and is a powerful generalization of previous results that express functional determinants in terms of the solutions to homogenous differential equations. The latter, Jacobi's theorem, is much older. Nevertheless, it was an important component in our computation because it provided an algorithmic method for solving the homogenous differential equation that arises through the use of Forman's equation.

References

[1] M. Tinkham, *Introduction to Superconductivity* (McGraw-Hill, NY, 1975), Chap. 7.

[2] J. Frenkel, *Kinetic Theory of Liquids* (Dover, New York, 1955).

[3] C. W. Gardiner, *Handbook of Stochastic Methods* (Springer-Verlag, Berlin, 1990).

[4] H. A. Kramers, Physica **7**, 284 (1940).

[5] See Chapter 5 of [3].

[6] W. A. Little, Phys. Rev. **156**, 396 (1967);

[7] J. Langer and V. Ambegaokar, Phys. Rev. **164**, 498 (1967).

[8] D. McCumber and B. Halperin, Phys. Rev. B **1**, 1054 (1970).

[9] M. B. Tarlie, E. Shimshoni and P. M. Goldbart. Phys. Rev. B **49**, 494 (1994).

[10] V. Ginzburg and L. Landau, J. Exptl. Theoret. Phys. (USSR), **20**, 1064 (1950); for a reprint of this paper, that of ref. [13], and many other of Landau's papers, see D. ter Haar, *Men of Physics: L. D. Landau I and II* (Pergamon Press, 1962).

[11] J. Bardeen, L. N. Cooper, and J. R. Schrieffer, Phys. Rev. **108**, 1175 (1957).

[12] L. P. Gor'kov, J. Exptl. Theoret. Phys. (USSR) **36**, 1918 (1959) [*Soviet Phys.-JETP* **9**, 1364 (1959)].

[13] L. D. Landau, Phys. Z. Soviet Un. **11**, 26 (1937).

[14] N. Goldenfeld, *Lectures on Phase Transitions and the Renormalization Group* (Addison-Wesley, Reading, MA, 1992).

[15] C. Kittel, *Introduction to Solid State Physics* (Wiley, New York, 1986), App. G.

[16] J. R. Schrieffer, *Theory of Superconductivity* (Bejamin/Cummings, Reading, MA, 1964).

[17] E. Abrahams and T. Tsuneto, Phys. Rev. **152**, 416 (1966).

[18] R. Tidecks, *Current Induced Nonequilibrium Phenomena in Quasi One Dimensional Superconductors*, (Springer-Verlag, Berlin, 1990).

[19] R. Landauer and J. A. Swanson, Phys. Rev. **121**, 1668 (1961).

[20] J. S. Langer, Phys. Rev. Lett. **21**, 973 (1968).

[21] J. S. Langer, Ann. Phys. (NY) **54**, 258 (1969).

[22] I. H. Duru, H. Kleinert, and N. Ünal, J. Low Temp. Physics **42**, 137 (1980); H. Kleinert and T. Sauer, J. Low Temp. Physics **81**, 123 (1990).

[23] S. Coleman, *Aspects of Symmetry* (Cambridge, 1990).

[24] R. Rajaraman, *Solitons and Instantons* (North Holland, Amsterdam, 1982).

[25] See, e.g., E. H. Neville, *Jacobian Elliptic Functions* (Clarendon, Oxford, 1944), Chap. 15; P. F. Byrd and M. D. Friedman, *Handbook of Elliptic Integrals for Engineers and Scientists* (Springer, Berlin, 1971); and H. Hancock, *Elliptic Integrals* (Dover, NY, 1958).

[26] M. Abramowitz and I. Stegun, *Handbook of Mathematical Functions* (Dover, New York, 1970), Chaps. 16 and 17.

[27] J. W. Negele and H. Orland, *Quantum Many-Particle Systems* (Addison-Wesley, redwood City, CA, 1988).

[28] I. Gradshteyn, I. Ryzhik, *Table of Integrals, Series and Products*

[29] J. S. Langer, Ann. Phys. (NY) **41**, 108 (1967).

[30] R. Forman, Invent. Math. **88**, 447 (1987).

[31] I. Gel'fand and A. Yaglom, J. Math. Phys. **1**, 48 (1960). Gel'fand and Yaglom seem to have been the first to relate the determinant of a differential operator to the solutions of a homogeneous differential equation.

[32] A proper treatment of this situation requires an analysis based on a Master equation [7]. However, the essence of the problem can be understood in a simple way by requiring that, on average, the total change in phase of the order parameter, and hence the supercurrent, be zero. On average, the phase will increase by an amount $2eV/\hbar + 2\pi\Gamma_+$, whereas, on average, it will decrease by $2\pi\Gamma_-$. Equating these two expressions and rearranging gives eq. 2.74.

[33] C. M. Bender and S. Orszag, *Advanced Mathematical Methods for Scientists and Engineers* (McGraw-Hill, New York, 1978).

[34] D. E. McCumber, Phys. Rev. **181**, 716 (1969).

Chapter 3

Regularization of Functional Determinants using Boundary Perturbations

3.1 Introduction

In this chapter I present a method for regularizing functional determinants using boundary perturbations. This work was done in collaboration with A. J. McKane (Univ. Manchester, U. K.). We were motivated by the increasing use of path integrals as a calculational tool, which has led to a corresponding increase in interest in the evaluation of functional determinants. This is simply because the evaluation of Gaussian path integrals typically gives such determinants. The first results were obtained over thirty years ago: Gel'fand and Yaglom [1] derived expressions for the functional determinants obtained from evaluating path integrals with the simplest type of quadratic action. In subsequent years the results became more general and the formalism more elaborate [2, 3], culminating with the work of Forman [4] who gave a remarkably simple prescription which can be applied to a rather general operator and boundary conditions.

However, in many calculations involving Gaussian integrals that are currently carried out, these results are not directly applicable. The reason is that the Gaussian nature of the integral is frequently a consequence of expanding about some non-trivial "classical" solution of the model (e.g., a soliton or instanton). Typically this results in a particular point (in space or time) being selected, which breaks the translational invariance of the theory, and so gives rise to a Goldstone mode. There are other

possible ways that such a zero mode could come about, but in all cases the Gaussian approximation breaks down. The remedy is to first extract this mode as a collective coordinate [5] and to treat only the non-zero modes in the Gaussian approximation. Therefore, it is not the functional determinant that is required in these cases — it will in any case be identically zero — but the functional determinant with the zero mode extracted.

In this chapter we present a systematic method to calculate this quantity. The most obvious way to proceed is to "regularise" the theory in some way, so that the eigenvalue of the operator under consideration, which was previously zero, is now non-zero. The determinant is now also non-zero and the pseudo-zero eigenvalue can be factored out, the regularisation removed, and a finite result obtained. Previous approaches have been rather *ad hoc*, being performed on a case by case basis as the need arose. For example, it may be possible in certain cases to modify the form of the operator in such a way that the zero mode is regularised, but also that the calculation may still be performed [6, 7]. This is the approach that we used to compute the fluctuation determinant that arises in the expression for the rate of decay of a persistent current in a quasi-one-dimensional superconducting ring (see Chap. 2 and App. D). In other cases, it may be possible to move the boundaries to achieve the same end [8, 9]. Here we adopt an approach which applies to very general situations and which, we believe, is the simplest and most systematic regularisation and calculational procedure. This is because the method is the least intrusive — the operator and the position of the boundaries are left unchanged — only the form of the boundary conditions are modified in the regularisation procedure. We use the notation and general approach of Forman to calculate the regularised functional determinant, as it is ideally suited to this form of regularisation, emphasising as it does the separation of the boundary conditions from the solutions of a homogeneous differential equation.

In Sec. 3.2 we develop our method in one of the simplest situations in order to clearly illustrate it. The calculation of the regularised expression for the formerly

zero eigenvalue is derived, for the most general case that will interest us, in Sec. 3.3 and the general procedure for finding the functional determinant with the zero mode extracted is described in Sec. 3.4. In Sec. 3.5 we apply the method to certain specific cases and we conclude in Sec. 3.6 with some general remarks.

3.2 A Simple Example

In this section we will explain the method by carrying out an explicit calculation on what is perhaps the simplest example. Suppose that we wish to calculate the determinant of an operator of the form

$$L = \frac{d^2}{dt^2} + P(t), \qquad t \in [a, b], \tag{3.1}$$

where $P(t)$ is a known real function. We suppose that the boundary conditions on the functions on which L operates are homogeneous Dirichlet, i.e., $u(a) = u(b) = 0$. In particular, the eigenfunctions of L have to satisfy these conditions.

We now give Forman's prescription for calculating $\det L$. A more detailed discussion is given in Sec. 3.4, where our approach is explained in greater generality. The recipe has two ingredients:

(i) Write the boundary conditions on L in the form:

$$M \begin{bmatrix} u(a) \\ \dot{u}(a) \end{bmatrix} + N \begin{bmatrix} u(b) \\ \dot{u}(b) \end{bmatrix} = \begin{bmatrix} 0 \\ 0 \end{bmatrix}, \tag{3.2}$$

where M and N are 2×2 matrices and $\dot{u} = du/dt$. These two matrices are not unique; for the case of our boundary conditions $u(a) = u(b) = 0$ we choose them to be

$$M = \begin{bmatrix} 1 & 0 \\ 0 & 0 \end{bmatrix}, \quad N = \begin{bmatrix} 0 & 0 \\ 1 & 0 \end{bmatrix}. \tag{3.3}$$

(ii) Now consider a different problem. Let $y_1(t)$ and $y_2(t)$ be two independent solutions of the homogeneous differential equation

$$Lh = 0. \tag{3.4}$$

Construct the matrix $H(t)$ defined by

$$H(t) \equiv \begin{bmatrix} y_1(t) & y_2(t) \\ \dot{y}_1(t) & \dot{y}_2(t) \end{bmatrix}, \tag{3.5}$$

and the 2×2 matrix $Y(b) \equiv H(b)H^{-1}(a)$.

Forman then proves that [4]

$$\frac{\det L}{\det \hat{L}} = \frac{\det(M + NY(b))}{\det(M + N\hat{Y}(b))}. \tag{3.6}$$

We would expect that $\det L$ itself is divergent, being a product of an infinite number of eigenvalues of increasing magnitude. Therefore it is only when it is defined relative to the determinant of an operator of a similar type (denoted here by $\hat{L}$), that it has any meaning. In applications to path integrals, ratios of determinants such as the one on the left-hand-side of eq. (3.6) naturally arise from the normalisation of the path integral itself. In general, they will relate to a simple quantum mechanical system or stochastic process, such as the harmonic oscillator or Ornstein-Uhlenbeck process. In these cases, $\hat{P}(t)$ is independent of t and will not, in general, have a zero mode.

For the matrices M and N of our simple example,

$$\begin{aligned} \det(M + NY(b)) &= Y_{12}(b) \\ &= \frac{y_1(a)y_2(b) - y_2(a)y_1(b)}{y_1(a)\dot{y}_2(a) - y_2(a)\dot{y}_1(a)}. \end{aligned} \tag{3.7}$$

The denominator of this expression is the Wronskian, which does not vanish as the two solutions $y_1(t)$ and $y_2(t)$ are presumed independent. If we take $y_1(t)$ to be a solution for which $y_1(a) = 0$, then (3.7) can be simplified to $y_1(b)/\dot{y}_1(a)$, so that, if $\hat{y}_1(a)$ also vanishes,

$$\frac{\det L}{\det \hat{L}} = \frac{y_1(b)\dot{\hat{y}}_1(b)}{\dot{y}_1(b)\hat{y}_1(b)} \tag{3.8}$$

This simple expression is particularly useful, since it only involves $y_1, \hat{y}_1$ and their first derivatives at one of the boundaries. We should stress that results such as this have been known since the work of Gel'fand and Yaglom — our purpose here is to introduce the formalism required to describe our approach, in as simple a way as possible.

Now suppose that $y_1(b) = 0$ (as well as $y_1(a) = 0$). Then $y_1(t)$ is an eigenvalue of L with zero eigenvalue. This is the situation of interest to us in this chapter. To extract this zero mode, we first regularise the problem by modifying it so that the operator is unchanged, but the boundary conditions $u(a) = u(b) = 0$ become

$$u^{(\epsilon)}(a) = 0, \quad u^{(\epsilon)}(b) = \epsilon \dot{u}^{(\epsilon)}(b) \tag{3.9}$$

where ϵ is some small number. Now $y_1(t)$ is no longer an eigenfunction of L with zero eigenvalue. Let $y_1^{(\epsilon)}(t)$ be the corresponding eigenfunction (i.e., the one that reduces to $y_1(t)$ when $\epsilon \to 0$) and let it have eigenvalue $\lambda^{(\epsilon)}$. To find $\det L$ with these boundary conditions we first note that $Y(b)$ is unchanged, as it does not involve boundary conditions at all; it only depends on two independent solutions to the homogeneous differential equation $Lh = 0$. Modifying the boundary conditions as in (3.9) only changes M and N to

$$M^{(\epsilon)} = \begin{bmatrix} 1 & 0 \\ 0 & 0 \end{bmatrix}, \quad N^{(\epsilon)} = \begin{bmatrix} 0 & 0 \\ 1 & -\epsilon \end{bmatrix}. \tag{3.10}$$

This gives $\det(M^{(\epsilon)} + N^{(\epsilon)}Y(b)) = Y_{12}(b) - \epsilon Y_{22}(b)$. But as $y_1(a) = y_1(b) = 0$, $Y_{12}(b) = 0$, and so

$$\begin{aligned} \det(M^{(\epsilon)} + N^{(\epsilon)}Y(b)) &= -\epsilon Y_{22}(b) \\ &= -\epsilon \frac{\dot{y}_1(b)}{\dot{y}_1(a)} \end{aligned} \tag{3.11}$$

This is the regularised form of the determinant. In the next section we will give a general method for finding $\lambda^{(\epsilon)}$. In this simple problem it turns out that, to lowest order in ϵ,

$$\lambda^{(\epsilon)} = -\epsilon \frac{\dot{y}_1^2(b)}{\langle y_1 | y_1 \rangle}, \tag{3.12}$$

where $\langle y_1 | y_1 \rangle$ is the norm of the zero mode:

$$\langle y_1 | y_1 \rangle = \int_a^b dt\, y_1^2(t). \tag{3.13}$$

From (3.11) and (3.12) we have:

$$\lim_{\epsilon \to 0} \frac{\det(M^{(\epsilon)} + N^{(\epsilon)}Y(b))}{\lambda^{(\epsilon)}} = \frac{\langle y_1 | y_1 \rangle}{\dot{y}_1(a)\dot{y}_1(b)} \tag{3.14}$$

This remarkably simple result is the one that we sought. Note that, apart from the norm, it is only involves $\dot{y}_1$ at the boundaries. In applications, it will usually be the case that the norm in eq. (3.14) will cancel with an identical factor coming from the lowest order form of the Jacobian of the transformation to collective coordinates. Therefore $\langle y_1|y_1\rangle$ need not be calculated. Denoting the determinant of L with the zero mode extracted by $\det' L$ and normalising by $\det \hat{L}$, we finally obtain

$$\frac{\det' L}{\det \hat{L}} = \frac{\langle y_1|y_1\rangle}{\dot{y}_1(a)\dot{y}_1(b)} \frac{\dot{\hat{y}}_1(b)}{\hat{y}_1(b)} \tag{3.15}$$

The method we have described to find the regularised form of $\det(M + NY(b))$ is hardly more complicated than finding the unregularised form. The key to achieving this happy state of affairs was firstly the decision to modify only the boundary conditions, and secondly, the choice of regularised boundary conditions, which gave simple forms for $M^{(\epsilon)}$ and $N^{(\epsilon)}$. We shall now show that these choices also allow $\lambda^{(\epsilon)}$ to be determined in a very simple and elegant way.

3.3 The Regularisation of the Eigenvalue

While the regularised form of the determinant could be found by use of Forman's method, a new technique for calculating the previously vanishing eigenvalue $\lambda^{(\epsilon)}$ has to be developed. It is natural to attempt to calculate it perturbatively in ϵ, but it is not at all obvious that a general procedure can be set up. Fortunately, it will turn out that choosing the regularised boundary conditions in the manner illustrated in Sec. 3.2 on a simple example, enables $\lambda^{(\epsilon)}$ to be found to lowest order almost without calculation.

Let us begin describing the method where the operator is of the simple form eq. (3.1); we will generalise to more complicated operators later in this section. There is no need to specify the boundary conditions at this stage, because, as we will see, a useful formula for $\lambda^{(\epsilon)}$ can be derived without having to make any choices of boundary conditions. Using the notation introduced in the last section:

$$L y_1^{(\epsilon)} = \lambda^{(\epsilon)} y_1^{(\epsilon)}, \tag{3.16}$$

where $y_1^{(\epsilon)}(t) \to y_1(t)$ and $\lambda^{(\epsilon)} \to 0$ as $\epsilon \to 0$. From eq. (3.16) we have

$$\begin{aligned} \int_a^b dt\, y_1 L y_1^{(\epsilon)} &= \lambda^{(\epsilon)} \int_a^b dt\, y_1\, y_1^{(\epsilon)} \\ &= \lambda^{(\epsilon)} \langle y_1 | y_1 \rangle \ , \end{aligned} \tag{3.17}$$

to lowest order in ϵ. Integrating by parts gives, again to leading order,

$$\lambda^{(\epsilon)} = \frac{\left[\dot{y}_1^{(\epsilon)}(t) y_1(t) - \dot{y}_1(t) y_1^{(\epsilon)}(t)\right]_a^b}{\langle y_1 | y_1 \rangle} \tag{3.18}$$

This result is true for operators of the form (3.1) with arbitrary boundary conditions. As an example, suppose we impose the regularised boundary conditions (3.9). Then the eigenfunction $y_1^{(\epsilon)}(t)$ will satisfy them: $y_1^{(\epsilon)}(a) = 0$, $y_1^{(\epsilon)}(b) = \epsilon \dot{y}_1^{(\epsilon)}(b)$. In addition $y_1(a) = y_1(b) = 0$, so that to lowest order

$$\begin{aligned} \lambda^{(\epsilon)} &= -\frac{\dot{y}_1(b) y_1^{(\epsilon)}(b)}{\langle y_1 | y_1 \rangle} \\ &= -\epsilon \frac{\dot{y}_1(b) \dot{y}_1(b)}{\langle y_1 | y_1 \rangle} \end{aligned} \tag{3.19}$$

as given in Sec. 3.2. Note that the ϵ dependence simply came from the requirement that $y_1^{(\epsilon)}(b) = \epsilon \dot{y}_1(b)$, to lowest order.

Analogous results to eq. (3.18) hold for more general operators. For example, suppose that

$$L_{ij} = \delta_{ij} \frac{d^2}{dt^2} + P_{ij}(t) \ ; \quad i, j = 1, \ldots, r, \tag{3.20}$$

where $P(t)$ is a complex matrix, and suppose that the operator (3.20) has a single zero mode $y_{i,1}$, that is, $\sum_{j=1}^r L_{ij} y_{j,1} = 0$. In matrix notation, the zero mode is the column vector $\underline{y}_1 = (y_{1,1}, \ldots, y_{r,1})^T$. Let $\underline{y}_1^{(\epsilon)}(t)$ be the corresponding eigenfunction of the regularised problem with eigenvalue $\lambda^{(\epsilon)}$. Then to lowest order we have

$$\int_a^b dt \sum_{i,j} y_{i,1}^* L_{ij} y_{j,1}^{(\epsilon)} = \lambda^{(\epsilon)} \sum_i \langle y_{i,1} | y_{i,1} \rangle, \tag{3.21}$$

where now

$$\langle y_1 | y_1 \rangle \equiv \sum_i \langle y_{i,1} | y_{i,1} \rangle = \int_a^b dt \sum_i |y_{i,1}(t)|^2. \tag{3.22}$$

Integrating the left-hand-side of (3.21) by parts gives the leading order result

$$\lambda^{(\epsilon)} = \frac{\sum_{i=1}^{r} \left[y^*_{i,1}(t) \dot{y}^{(\epsilon)}_{i,1}(t) - \dot{y}^*_{i,1}(t) y^{(\epsilon)}_{i,1}(t) \right]_a^b}{\langle y_1 | y_1 \rangle} + \frac{\int_a^b dt \, \sum_{i,j} y^*_{i,1}(t) \{ P_{ij} - P^*_{ji} \} y^{(\epsilon)}_{j,1}(t)}{\langle y_1 | y_1 \rangle}. \quad (3.23)$$

In most cases of interest to us L will be formaliy self-adjoint, and so the second term in eq. (3.23) will vanish. The self-adjoint nature of L is expected from its origin as the second functional derivative of the action in the path integral with respect to the fields:

$$L(t,t')_{ij} = \frac{\delta^2 S}{\delta u^*_i(t) \delta u_j(t')}. \quad (3.24)$$

The most general operator that we shall study in this paper takes the form:

$$L_{ij} = [P_0(t)]_{ij} \frac{d^2}{dt^2} + [P_1(t)]_{ij} \frac{d}{dt} + [P_2(t)]_{ij}, \quad (3.25)$$

where $P_0(t)$, $P_1(t)$ and $P_2(t)$ are complex $r \times r$ matrices. We begin by making the transformation

$$p_{ij}(t) = \exp \left\{ \frac{1}{2} \int^t dt \, (P_0)^{-1} (P_1) \right\}_{ij}, \quad (3.26)$$

$$P_{ij}(t) = \left[p \, (P_0)^{-1} (P_2) \, (p)^{-1} \right]_{ij} - \left[\dot{p} \, (p)^{-1} \right]_{ij} \quad (3.27)$$

so that

$$L_{ij} = (P_0)_{ik} \, (p^{-1})_{kl} \mathcal{L}_{lm} \, (p)_{mj}, \quad (3.28)$$

where

$$\mathcal{L}_{ij} = \delta_{ij} \frac{d^2}{dt^2} + P_{ij}(t). \quad (3.29)$$

Now if $\hat{L}$ is such that $\hat{P}_0(t) = P_0(t)$, then

$$\frac{\det L}{\det \hat{L}} = \frac{\det \mathcal{L}}{\det \hat{\mathcal{L}}}, \quad (3.30)$$

where $\hat{\mathcal{L}}$ is as in eq. (3.29), but with P replaced by $\hat{P}$. Therefore the problem has been reduced to that considered earlier in this section (see eqs. (3.20) *et seq*). In fact, as regards determining the ratio of the determinants, Forman gives a general expression for the left-hand-side of eq. (3.30) (see next section), and so there is no

need to implement the transformation given in eqs. (3.26) and (3.27). To find the eigenvalue $\lambda^{(\epsilon)}$, however, this transformation is useful. It is easy to see that $\mathcal{L}$ has a zero mode if, and only if, L does, and that, in particular, if $y_i(t)$ is an eigenfunction of L_{ij} with zero eigenvalue, then $z_i(t) = \sum_j p_{ij}(t)y_j(t)$ is an eigenfunction of $\mathcal{L}_{ij}$ with zero eigenvalue. The results of eqs. (3.21)-(3.23) now hold, but with L and y replaced by $\mathcal{L}$ and z, respectively. As in all of the examples discussed in this section, a judicious choice for the boundary conditions on the regularised eigenfunction $\underline{y}_1^{(\epsilon)}$ will yield an explicit regularised form for $\lambda^{(\epsilon)}$ with the minimum of calculational effort.

3.4 General Procedure

There are two aspects to our approach to the calculation of $\det' L/\det \hat{L}$. One is the operation of finding $\lambda^{(\epsilon)}$ to leading order, which was explored for the general case in the last section. The other aspect concerns the application of Forman's method for the calculation of $\det L/\det \hat{L}$, but with the regularised boundary matrices $M^{(\epsilon)}$ and $N^{(\epsilon)}$. This was illustrated with a simple example in Sec. 3.2; in this section we discuss Forman's method in more detail and explain how to apply it to the general operator (3.25). We end the section with a summary of the general procedure that we have developed in this chapter.

We suppose, following Forman [4], that the boundary conditions on (3.25) may be expressed as

$$M \begin{bmatrix} \underline{u}(a) \\ \dot{\underline{u}}(a) \end{bmatrix} + N \begin{bmatrix} \underline{u}(b) \\ \dot{\underline{u}}(b) \end{bmatrix} = \begin{bmatrix} \underline{0} \\ \underline{0} \end{bmatrix}, \tag{3.31}$$

where M and N are $2r \times 2r$ matrices. This equation is simply the r-dimensional analogue of (3.2). So, for instance, if the boundary conditions are $\underline{u}(a) = \underline{u}(b) = 0$, then

$$M = \begin{bmatrix} I_r & 0 \\ 0 & 0 \end{bmatrix}, \quad N = \begin{bmatrix} 0 & 0 \\ I_r & 0 \end{bmatrix}, \tag{3.32}$$

where I_r is the $r \times r$ identity matrix.

Now suppose that $h_i(t); i = 1, \ldots, r$, is a solution of the homogeneous differential equation $\sum_j L_{ij} h_j = 0$, and define the $2r \times 2r$ matrix $Y(t)$, which describes the evolution of a solution and its first derivative with respect to t, by

$$\begin{bmatrix} \underline{h}(t) \\ \dot{\underline{h}}(t) \end{bmatrix} = Y(t) \begin{bmatrix} \underline{h}(a) \\ \dot{\underline{h}}(a) \end{bmatrix}. \tag{3.33}$$

If $\underline{y}_1(t), \underline{y}_2(t), \ldots, \underline{y}_{2r}(t)$, are $2r$ solutions of $Lh = 0$, then eq. (3.33) will apply to each solution separately, i.e., $H(t) = Y(t)H(a)$, where

$$H(t) = \begin{bmatrix} \underline{y}_1(t) & \underline{y}_2(t) & \cdots & \underline{y}_{2r}(t) \\ \dot{\underline{y}}_1(t) & \dot{\underline{y}}_2(t) & \cdots & \dot{\underline{y}}_{2r}(t) \end{bmatrix}. \tag{3.34}$$

So, in particular, $H(b) = Y(b)H(a)$, or, if the solutions are independent so that $\det H \neq 0$,

$$Y(b) = H(b)H^{-1}(a) \tag{3.35}$$

This explains the second construction [labelled (ii)] in Sec. 3.2.

The formula for the ratio of determinants for operators of the type given in eq. (3.25) is [4]

$$\frac{\det L}{\det \hat{L}} = \frac{\exp\left(\frac{1}{2}\int_a^b dt\, \mathrm{tr} P_1(t) P_0^{-1}(t)\right) \det(M + NY(b))}{\exp\left(\frac{1}{2}\int_a^b dt\, \mathrm{tr} \hat{P}_1(t) P_0^{-1}(t)\right) \det(M + N\hat{Y}(b))}. \tag{3.36}$$

For this result to be applicable, the matrices $P_1(t)$ and $\hat{P}_1(t)$, and also $P_2(t)$ and $\hat{P}_2(t)$ need not be equal, however the matrix $P_0(t)$, multiplying the second derivative, must be the same for both operators. In most applications L will be normalised by an $\hat{L}$, which has a different, and simpler, matrix P_2, but is otherwise the same. In these situations $\hat{P}_1 = P_1$, the exponential factors in (3.36) cancel out, and the simple formula given by (3.6) holds (except, of course, that M, N and $Y(b)$ are now $2r \times 2r$, not 2×2, matrices). We also note that, although the formula seems to be asymmetric with respect to the two points a and b, one could just as well define a matrix $\tilde{Y}(t)$ by

$$\begin{bmatrix} \underline{h}(t) \\ \dot{\underline{h}}(t) \end{bmatrix} = \tilde{Y}(t) \begin{bmatrix} \underline{h}(b) \\ \dot{\underline{h}}(b) \end{bmatrix} \tag{3.37}$$

so that $H(a) = \tilde{Y}(a)H(b)$. Then $\det(M + NY(b)) = \det(N + M\tilde{Y}(a))$. Therefore, alternative formulae to (3.6) and (3.36) exist, with M and N interchanged and $Y(b)$ replaced by $\tilde{Y}(a)$.

All of the formalism discussed so far in this section also applies to the problem with regularised boundary conditions — the only difference is that M and N are replaced by $M^{(\epsilon)}$ and $N^{(\epsilon)}$ respectively. We are now in a position to summarise the whole procedure:

1. Modify the boundary conditions of the original problem by a small amount (ϵ), so that $\underline{y}_1(t)$ is no longer a zero mode. Let $\underline{y}_1^{(\epsilon)}(t)$ be the eigenfunction of the new problem with an eigenvalue $\lambda^{(\epsilon)}$ which tends to zero as $\epsilon \to 0$. Express the modified boundary conditions in the form (3.31) so that they are characterised by two matrices $M^{(\epsilon)}$ and $N^{(\epsilon)}$.

2. Calculate $Y(b) = H(b)H^{-1}(a)$, where $H(t)$ is given by eq. (3.34).

3. Calculate $\det(M^{(\epsilon)} + N^{(\epsilon)}Y(b))$.

4. Calculate $\lambda^{(\epsilon)}$ from eq. (3.23).

5. Hence determine
$$\lim_{\epsilon \to 0} \frac{\det(M^{(\epsilon)} + N^{(\epsilon)}Y(b))}{\lambda^{(\epsilon)}}. \tag{3.38}$$

6. Calculate the denominator factor $\det(M + N\hat{Y}(b))$

7. The ratio of the results of the last two steps gives $\det' L / \det \hat{L}$.

We will now study various specific examples where this procedure is applied.

3.5 Specific Examples

The algorithm given at the end of the last section gives a method for determining the ratio $\det' L / \det \hat{L}$. In this section we will give explicit results for a few examples with commonly met boundary conditions and also discuss one example in some detail

to show how the method we have developed works in practice. We will only give results for the quantity given by (3.38), as the final result is found by normalising this by $\det \hat{L}$, which can be found from the formulae given in, for example, Forman's paper [4].

For simplicity we only consider the single component ($r = 1$) case where the operator has the form (3.1), for a variety of boundary conditions.

(a) With the boundary conditions $Au(a) + B\dot{u}(a) = 0$; $Cu(b) + D\dot{u}(b) = 0$,

$$\frac{\det' L}{\langle y_1|y_1\rangle} = \begin{cases} +AC/\dot{y}_1(a)\dot{y}_1(b), & \text{if } A, C \neq 0, \\ -BC/y_1(a)\dot{y}_1(b), & \text{if } B, C \neq 0, \\ -AD/\dot{y}_1(a)y_1(b), & \text{if } A, D \neq 0, \\ +BD/y_1(a)y_1(b), & \text{if } B, D \neq 0. \end{cases} \tag{3.39}$$

If all four constants A, B, C, D are non-zero it is easy to see that all four expressions are equivalent. Similarly, if only three of the constants are non-zero, then the two applicable expressions are equivalent. If only two constants are non-zero, one involved in the boundary condition at a, and the other at b, then only one of the above applies. The simple example given in section 2 falls into this class: the boundary conditions there correspond to $A = 1, B = 0, C = 1, D = 0$, and in this case eq. (3.39) reduces to eq. (3.14).

(b) With periodic boundary conditions $u(a) = u(b)$; $\dot{u}(a) = \dot{u}(b)$,

$$\frac{\det' L}{\langle y_1|y_1\rangle} = \frac{y_2(b) - y_2(a)}{y_1(a)\,\det H(a)}, \tag{3.40}$$

where $\det H(a) = \dot{y}_2(a)y_1(a) - \dot{y}_1(a)y_2(a)$ is the Wronskian.

(c) With anti-periodic boundary conditions $u(a) = -u(b)$; $\dot{u}(a) = -\dot{u}(b)$,

$$\frac{\det' L}{\langle y_1|y_1\rangle} = -\frac{y_2(b) + y_2(a)}{y_1(a)\,\det H(a)}. \tag{3.41}$$

As an example of the application of these results, we use one of the most well known situations in which instantons exist: imaginary time quantum mechanics with a potential $V(x) = \frac{1}{2}x^2 - \frac{1}{4}x^4$ [6]. As shown in App. E, this problem leads one to consider operators of the form

$$L = -\frac{d^2}{dt^2} + 1 - 3\beta^2 \mathrm{dn}^2(u|m), \tag{3.42}$$

where dn is an elliptic function [10], $u = \beta(t - t_0)/\sqrt{2}$ and $\beta = 2(1-m)/(2-m)$. The constants t_0 and m originate from the integration of the second order ordinary differential equation that is satisfied by the instanton. The parameter t_0 reflects the breaking of the time-translational invariance of the original theory and m is related to the energy of the classical particle in the mechanical analogy. The spectral properties of the system can be studied by imposing periodic boundary conditions on the path-integral [11], which dictates that we use eq. (3.40) to find the required functional determinant. A straightforward calculation, outlined in App. E, yields

$$\frac{\det' L}{\langle y_1|y_1\rangle} = -\frac{2(2-m)^{7/2}}{m^2}\left[\frac{K(m)}{2-m} - \frac{E(m)}{2(1-m)}\right] \tag{3.43}$$

where $K(m)$ and $E(m)$ are the complete elliptic integrals of the first and second kind respectively.

This result simplifies considerably in the limit where the energy of the particle in the mechanical analogy is zero and consequently the period of the instanton T becomes infinite. In App. E it is shown that the asymptotic forms of eq. (3.43), $\det(M + N\hat{Y}(b))$ and $\langle y_1|y_1\rangle$, for T large are, respectively, $e^T/16$, $-e^T$ and $\frac{4}{3}$. Combining all of these results gives

$$\lim_{T\to\infty} \frac{\det' L}{\det \hat{L}} = -\frac{1}{12} \tag{3.44}$$

This is in agreement with previous calculations (e.g., eq. (29) of Ref. [6]). It also illustrates the extra complication that may occur if the range (a, b) is infinite. In these cases the numerator (3.38) and the denominator $\det(M+N\hat{Y}(b))$ may separately diverge as $T \equiv (b-a) \to \infty$. One can avoid these divergences in various ways, but the

most obvious way to proceed in these cases is to use T as a regulator and to perform all calculations with T large, but finite, cancelling out the potential divergences between numerator and denominator before taking the $T \to \infty$ limit.

3.6 Conclusions

In this chapter we have developed a simple and effective way of regularising operators which have zero modes. The method allows the functional determinants for these kinds of operators, with the zero mode extracted, to be calculated. The main advantage of the method, and the reason for its power, is that it leaves much of the structure of the unregularised problem intact. This means that much of the formalism originally developed in this case can be taken over with very little change. The approach that we have adopted has not emphasised rigor; it would be very interesting to put this work on a rigorous footing and explore further possible generalisations.

References

[1] I. Gel'fand and A. Yaglom, J. Math. Phys. **1**, 48 (1960).

[2] S. Levit and U. Smilansky, Proc. Am. Math. Soc. **65** 299 (1977).

[3] T. Dreyfuss and H. Dym, Duke Math. J. **45**, 15 (1978).

[4] R. Forman, Invent. Math. **88**, 447 (1987).

[5] R. Rajaraman *Solitons and Instantons* (North Holland, Amsterdam, 1982).

[6] E. Brézin, J. C. Le Guillou and J. Zinn-Justin, Phys. Rev. D **15**, 1544 (1977).

[7] M. B. Tarlie, E. Shimshoni and P. M. Goldbart, Phys. Rev. B **49** 494 (1994).

[8] G. Barton, A. J. Bray and A. J. McKane, Am. J. Phys. **58** 751 (1990).

[9] I. H. Duru, H. Kleinert and N. Uñal J. Low Temp. Phys. **81** 121 (1980).

[10] M. Abramowitz and I. A. Stegun, *Handbook of Mathematical Functions* (Dover, New York, 1965).

[11] L. S. Schulman, *Techniques and Applications of Path Integration* (Wiley, New York, 1981).

[12] C. Fox, *An Introduction to the Calculus of Variations* (Dover, New York, 1987) Chapter 2.

Chapter 4

Supercurrent Dynamics Near the Critical Current

4.1 Introduction

In this chapter the dynamics of the supercurrent for currents close to the critical current will be discussed. As in Chap. 2, the physical system under consideration is a superconducting ring of circumference L threaded by a time-dependent solenoidal flux. In this chapter, we take the flux to be a linearly increasing function of time, so that by Faraday's law of induction, a time-independent electromotive force (emf) V will be induced in the ring.

According to the London theory [1, 2], a phenomenological theory of the electrodynamic behavior of superconductors, the electric field (of strength V/L) will accelerate the condensate. More specifically, the London theory assumes that there is a distinction between superconducting electrons and non-superconducting electrons. The phase transition from the normal state of a material to the superconducting state is viewed as a type of condensation of the superconducting electrons; the collection of superconducting electrons is therefore referred to as the condensate. The first London equation is simply Newton's first law of motion ($\mathbf{F} = m\mathbf{a}$) applied to the superconducting electrons, i.e.,

$$dI/dt \propto V, \tag{4.1}$$

where I is the supercurrent. (The normal electrons are assumed to obey Ohm's law: $I_n \propto V$, where I_n is the normal current.) Thus, according to eq. (4.1), the supercurrent increases without bound.

However, the existence of a critical current I_c is well established [3, 4]. Generally, the critical current is associated with the thermodynamic critical magnetic field H_c. In other words, I_c is understood as the value of the current that produces a magnetic field of strength H_c. This is known as Silsbee's rule [3]. Therefore, the unbounded growth of I predicted by eq. (4.1) is unphysical. Rather, we expect that the supercurrent will increase to the critical current. The question of what happens next is the focus of this chapter.

Clearly, the London theory is unable to shed light on the question of the supercurrent dynamics near the critical current. However, based on the success of the stochastic time-dependent Ginzburg-Landau (STDGL) theory (c.f. Sec. 2.3) as a basis for the understanding of the width of the resistive transition in quasi-one-dimensional wires [5], it is reasonable to use the STDGL theory to describe the behavior of a quasi-one-dimensional superconductor in the presence of a constant electric field. In the problem of the width of the resistive transition, the system is close to equilibrium, i.e., the supercurrent flowing in the wire is much smaller than the critical current. Here, however, the supercurrent is close to the critical current, i.e., the superconductor is far from equilibrium. Thus, the success of the TDGL theory in the near-equilibrium regime does not justify our use of the TDGL in the far-from-equilibrium regime, it simply makes our choice reasonable.

In the Ginzburg-Landau (GL) description of a superconducting ring of a finite length, there are a finite number of metastable current-carrying states of the superconductor, each of which is a local minimum of the GL free energy (see Chap. 2). At this stage it is useful to refer to Fig. 4.1 (c.f. Fig. 2.1), where the metastability of the free energy is illustrated schematically. This figure is a schematic plot of the free energy as a function of the supercurrent at a particular time. The important point is that there are a finite number of metastable states in which the system can reside. Suppose that the system occupies the metastable state labelled by the arrow. We assume that the electric field is strong enough, and that the noise is weak enough (i.e., T is sufficiently far from T_c) so that thermally activated processes have a van-

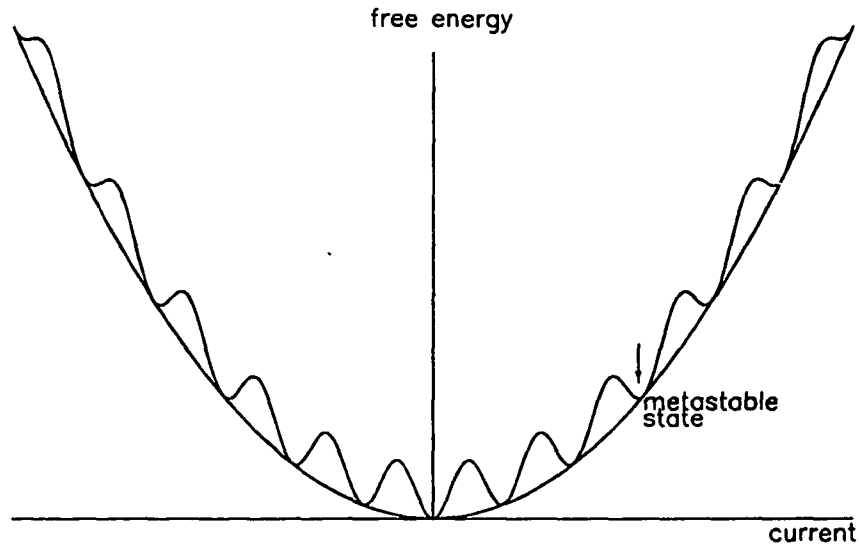

Figure 4.1: Schematic plot of the free energy as a function of current.

ishingly small probability of occuring on the time scale required to drive the current to the critical current [6]. Then, in the presence of an electric field, the current, and hence energy, of this state will increase. The system point will thus move along the envelope curve in Fig. 4.1. As this 'motion' takes place, the energy barrier protecting this state will decrease (c.f. Chap. 2, Sec. 2.6), i.e., the free energy schematically pictured in Fig. 4.1 will evolve in time. This process will continue until the energy barrier protecting this state vanishes. At this point the system becomes unstable; the instability is known as the Eckhaus instability [7]. What happens then? One reasonable hypothesis is that the system makes a transition to a metastable current-carrying state of lower current and energy. But, as pictured in Fig. 4.1, there can be a multiplicity of such states. Which one of these, if any, is the one selected?

In this chapter, we shall find that when the instability is reached, the system makes transitions to metastable current-carrying states of lower current and free en-

ergy. In addition, the particular state that is selected depends on the strength of the electric field V/L. For 'small' electric field strengths, transitions to the *nearest* metastable state predominate. In other words, one quantum of current is lost. These transitions correspond to the occurence of *single phase-slip* processes, which are described in detail in Chap. 2. However, as the field strength is increased, there is a crossover to a situation in which transitions to the *next-nearest* metastable state, with a lower current and free energy, predominate. In this case, two quanta of current are lost. These transitions correspond to the occurence of *double phase-slip* processes. Obtaining an understanding of this crossover phenomena is the focus of this chapter.

It should be emphasized that the transitions of concern in this chapter are from a point of *instability*, in contrast to the situation in Chap. 2, where the transitions are from a point of *metastability*. In other words, in the situation here, the important dynamical processes do not involve thermal activation over an energy barrier. Rather, the electric field drives the system to a point of local instability where there is no longer any energy barrier. The theoretical description of the decay from a metastable state is by now very well developed. By contrast, the theory of the decay from an unstable state, especially when multiple metastable states can compete for occupation, is not well developed.

Recently, the Eckhaus instability, the instability associated with the critical current, has been studied rather intensively [8, 9, 10, 11, 12]. The interest in this subject is part of the more general interest in the problem of pattern formation [13, 14]. In a paper that partially inspired the work to be presented in this chapter, Kramer *et al.* [9] studied the behavior of a system initially prepared in an unstable state far from the Eckhaus instability. They were motivated primarily by the problem of pattern selection in classical physical systems, such as Taylor-Couette systems, Rayleigh-Bénard convection cells, and the buckling instability of thin plates. In their work, they envisioned preparing the system in a state beyond the Eckhaus instability and analyzed the dependence of the final state on the initial state. This is in contrast to the situation here, where the system is driven through the Ekchaus instability. They

were unable to study systematically the behavior of the system close to the Eckhaus instability because their simulations became prohibitively computer-time consuming. They did note, however, the possibility of multiple phase-slip processes.

Previous work in the area of nonequilibrium superconductivity has focused on situations in which the superconducting wire is connected to a current source, i.e., the total current flowing in the wire is the independent variable. This is in contrast to the situation of interest in this chapter, where the system is driven by a voltage source. The basic problem is to understand the *current-induced* breakdown of superconductivity in narrow superconducting wires. In general the wires are assumed to be connected to external leads. The recent book by Tidecks [4] contains a comprehensive review of the vast experimental and theoretical work in this area. Here, I will briefly mention a few examples. One of the first theoretical attempts (1972) to study this problem was that of Rieger *et al.* [15]. They considered a weak (quasi–one-dimensional) superconductor, bounded at its two ends by two strong superconductors. The weak superconductor is defined by the condition that it have a lower transition temperature than the strong superconductors. Thus, for temperatures close to the transition temperature of the weak superconductor, phase-slip events will occur in the weak superconductor, but not in the strong superconductors. The main result of their work is that for applied currents that are larger than the critical current of the weak superconductor, the supercurrent is an oscillatory function of time, where the amplitude of the oscillations is constant in time, and the frequency of the oscillations is the Josephson frequency. The reason that the amplitude of the current oscillations is constant is due to the fact that the phase-slips were introduced into the calculation by hand. More specifically, as soon as the free energy of the current-carrying state exceeded the free energy of the nearest metastable state, the authors slipped the phase by 2π. The validity of this approach is questionable [16]. In a later work (ca. 1974), Likharev [17] showed, via a numerical integration of the TDGL equation, that for an applied current I_0 that is slightly smaller than the critical current, a normal-superconducting interface is stable. He therefore concluded that if the applied

current is smaller than I_0 then the interface propagates in the direction of the normal phase, whereas if the current is larger than I_0 then the superconducting state is unstable, and the interface propagates in the direction of the superconducting phase. In 1977, Kramer and Baratoff [16] found, using numerical techniques, locally stable solutions of the TDGL equation for applied currents slightly smaller than the value of I_0 found by Likharev. One of their conclusions was that the Langer-Ambegaokar-McCumber-Halperin (LAMH) theory must be modified for currents near the critical current. This conclusion should not be too surprising. The results derived in Chap. 2, which are an extension of the results of the LAMH theory, are only valid in the regime where $\ell\sqrt{1-3k_s^2} \gtrsim 1$ [c.f. eq. (2.47)]. However, near the critical current k_s is close to $1/\sqrt{3}$ and the above inequality can therefore not be satisfied.

This chapter consists of two main parts. Sections 4.2-4.5 comprise the first part of the chapter. In Sec. 4.2 the basic equations are introduced. Section 4.3 contains a discussion of what we expect to see based on our experience discussed in Chap. 2. In Section 4.4, the numerical results obtained by integrating the stochastic time-dependent Ginzburg-Landau equation will be presented. The main result of this section is that for small electric field strengths, single phase-slip processes dominate the dynamics, but as the field strength is increased, there is a crossover to double phase-slip domination. In Sec. 4.5 the Eckhaus instability will be studied using linear stability analysis. The results of such an analysis will allow us to understand the essential reason for the crossover phenomenon. Section 4.6 comprises the second part of this chapter, which is devoted to the search for a systematic approach to the problem of the decay from an unstable state when multiple metastable states can compete for occupation. In this section I will present a theoretical approach, based on a path-integral technique, aimed at this question. Finally, this chapter is summarized in Sec. 4.7.

4.2 Theoretical Description

Consider the situation in which an infinitely long solenoid, carrying a current that varies linearly with time, passes through the center of the superconducting ring. According to Faraday's law of induction, the solenoidal current, and hence flux, will produce a static electric field in the direction tangent to the ring. In order to incorporate the effect of this emf on the superconductivity, we need to determine the electromagnetic vector potential $\mathbf{A}$ (see Sec. 2.2). This is done in the following way. The solenoidal current will produce a linearly time-dependent magnetic field

$$\mathbf{B} = \nabla \times \mathbf{A} \tag{4.2}$$

that is completely confined to the interior of the solenoid. According to one of Maxwell's equations the time-dependent magnetic field induces an electric field $\mathbf{E}$, i.e.,

$$\begin{aligned} \nabla \times \mathbf{E} &= -c^{-1}\partial_t \mathbf{B} && (4.3) \\ &= -c^{-1}\partial_t(\nabla \times \mathbf{A}). && (4.4) \end{aligned}$$

If eqs. (4.3) and (4.4) are integrated over a surface which passes through the ring, then the right hand side of eq. (4.3) is given by $-c^{-1}\partial_t\hat{\Phi}$, where $\hat{\Phi}$ is the solenoidal flux. In addition, we can use Stokes' theorem to convert the surface integrals over $\nabla \times \mathbf{E}$ and $\partial_t(\nabla \times \hat{\mathbf{A}})$ to line integrals over $\mathbf{E}\cdot\mathbf{dx}$ and $\partial_t\mathbf{A}\cdot\mathbf{dx}$, respectively. Here, $\mathbf{dx}$ is the infinitesmal longitudinal line segment. By symmetry, the integrands of the line integrals are constant in x. If we denote the longitudinal component of the electric field by E_x and the longitudinal component of the vector potential by A_x then we get that, up to a time-independent constant,

$$A_x = -E_x ct = \frac{\hat{\Phi}}{L} \tag{4.5}$$

The electromotive force (emf) V is related to the tangential component of the electric field E_x via

$$V = E_x L. \tag{4.6}$$

As discussed in the Introduction, our description of the superconductor is based on the STDGL equation (2.33) for the space- and time-dependent order parameter $\tilde{\psi}(x,t)$. In this formulation, $\tilde{A}_x \equiv (2e\xi/\hbar c)A_x$ is the dimensionless longitudinal component of the vector potential (see Sec. 2.2). Using eqs. (4.5) and (4.6), $\tilde{A}_x$ can be expressed in terms of the emf V via

$$\tilde{A}_x = -\frac{2eV}{\hbar}\frac{\xi}{L}t. \tag{4.7}$$

At this stage it is convenient to define a dimensionless wavevector and a dimensionless frequency

$$k(t) \equiv k_o + \omega t/\ell, \tag{4.8}$$

$$\omega \equiv \tau_{GL}(2eV/\hbar). \tag{4.9}$$

so that $\tilde{A}_x = k_o - k(t)$, with k_o a constant. The parameter ω is a dimensionless measure of the electromotive force V. In terms of the wavevector $k(t)$, the STDGL equation (2.33) for $\tilde{\psi}$ can be written as

$$\partial_t\tilde{\psi} = \big(\partial_x + ik(t)\big)^2\tilde{\psi} + \tilde{\psi} - \tilde{\psi}|\tilde{\psi}|^2 + \tilde{\eta} \tag{4.10}$$

where $\tilde{\psi}$ satisfies the periodicity condition:

$$\tilde{\psi}(\ell + x, t) = \tilde{\psi}(x,t). \tag{4.11}$$

[See Sec. 2.2 for the definitions of the parameters that appear in eq. (4.10).]

For the purpose of estimating the values of certain important quantities, throughout this chapter we will use the following (typical) values for the various parameters: $T = 0.93T_c$, $T_c = 3K$, $H_c(0) = 300G$, $\xi(0) = 1000\mathring{A}$, and $\sqrt{\sigma} = 1000\mathring{A}$. With these parameters we have that $D = 0.001$, $\tau_{GL} \approx 1.4 \times 10^{-11}$s, $V \approx 23\omega\,\mu$V. (τ_{GL} and D are given in eqs. (2.31) and (2.32), respectively.) The relationship between the physical supercurrent I and the dimensionless supercurrent $\mathcal{J}$ is given in eq. (2.16), i.e., $I = (4ek_BT/\hbar D)\mathcal{J}$. For the above parameters this gives $I \approx 2.3 \times 10^{-4}\mathcal{J}$ A. Thus, for $\mathcal{J} = \mathcal{J}_c = 2/\sqrt{27}$, this corresponds to a critical current $I_c \approx 9.0 \times 10^{-5}$A.

In eq. (4.10), there are two dimensionless parameters: ω and D. The first, ω, is a dimensionless measure of the strength of the external field. Our aim is to understand the behavior of the system as ω is varied. Typically ω will lie between 10^{-4} and 10^{-2}; thus, we consider ω to be a small parameter. In order of magnitude, the range of values of ω correspond to emf's of between 2.3 nV and 0.23 μV . A voltage of 2.3 nV corresponds to roughly 10^6 flux quanta passing through the ring in one second. The second dimensionless parameter, D, is a measure of the noise strength. In this chapter, this parameter is fixed and for the parameters introduced in the preceding paragraph, $D = 0.001$; i.e., we are working in the small noise regime.

Intuitively, we expect that if we drive the system with a sufficiently strong electric field, and if the noise is sufficiently weak, then thermally activated processes will not have time to occur, and the system will find itself at the Eckhaus instability. This notion is made more precise in Sec. 4.3 where we find that for $D = 0.001$, the emf must be such that $\omega \gg \ell \times 10^{-25}$. Thus, for all practical values of ω the current will be driven to the critical current.

Two main approximations have been made in taking eq. (4.10) as the dynamical equation. First, the dynamics of the vector potential **A** have been ignored. More specifically, the solenoidal current produces an electric field that accelerates the superconducting electrons, and, in addition, produces a normal current, according to Ohm's law. These currents will, in turn, generate magnetic fields. It is these fields that are not taken into account when the dynamics of $\hat{\mathbf{A}}$ are ignored. Justification for this approximation is dependent on the geometric properties of the wire [18]: for wires in which the cross-sectional dimensions are much smaller than either the temperature-dependent correlation length or magnetic penetration depth, this approximation is reasonable.

The second approximation is the neglect of the electrochemical potential V_{ec} that enters into eq. (4.10) by replacing ∂_t with $\partial_t + i(2eV_{ec}/\hbar)\tau_{GL}$ [19]. Inclusion of this term allows the normal current generated by the electric field to be taken into account. This is done by invoking Ohm's law, so that $I_N = L\sigma_N \partial_x V_{ec}$, where I_N is the

normal current, σ_N is the normal-state conductance, and L is the circumference of the wire. Now, V_{ec} is determined by imposing the requirement that any change in the supercurrent be compensated for by a corresponding change in the normal current, so that $\partial_x(I_N + I_S) = 0$, where $I_S = (4ek_BT/\hbar D)\mathrm{Im}\tilde{\psi}(\partial_x + ik)\tilde{\psi}$ is the supercurrent [c.f. eq. (2.16)]. (Here, Im denotes the imaginary part.) This requirement leads to an equation for V_{ec}, of the form

$$\frac{\partial^2 V_{ec}}{\partial x^2} = -\frac{1}{L\sigma_N}\frac{\partial I_S}{\partial x}. \tag{4.12}$$

Thus, as can be seen from eq. (4.12), by neglecting V_{ec} we are assuming that the normal state conductivity σ_N is infinite. In other words, the quasi particles respond instantaneously to any changes in the condensate (i.e., order parameter); that is, we are making an adiabatic approximation. In a realistic situation, σ_N will be finite. Therefore, our neglect of V_{ec} cannot be well justified. Nevertheless, my hope is that the corrections that result from the inclusion of this term will not affect my qualitative conclusions.

The dynamical equation (4.10) can be put into a different form, more convenient for numerical computation, by making the transformation $\tilde{\psi} \to e^{ik(t)x}\psi$, so that ψ satisfies the equation

$$\dot{\psi} = \psi'' + \psi - \psi|\psi|^2 + i\ell^{-1}\omega x\psi + \eta \tag{4.13}$$

where the overdot denotes partial differentiation with respect to time, and ψ satisfies the (twisted) periodicity condition:

$$\psi(\ell + x, t) = e^{ik(t)\ell}\psi(x, t). \tag{4.14}$$

This formulation makes it apparent that the effect of the electric field is to 'wind up' the order parameter, i.e., the total phase difference $k(t)\ell$ (modulo 2π) increases linearly with time.

In order that eq. (4.13) can be integrated numerically, this equation is converted to a discrete map by first constructing a space-time lattice of points, spatial points

being separated by a distance h_x, and temporal points separated by a time h_t. The function $\psi(x,t)$, defined on the space-time continuum, is then approximated by its values $\psi_{i,j} \equiv \psi(x_i,t_j)$ at the nodes $(x_i,t_j) = (ih_x, jh_t)$ of the lattice. In addition, the noise term $\eta(x,t)$ becomes $\eta_{i,j}/\sqrt{h_x h_t}$, where $\eta_{i,j}$ is Kronecker-delta correlated in i and j, the discrete spatial and temporal coordinates, respectively. The square-root factor is introduced to account for the difference in units between the Kronecker-delta, and the Dirac-delta. On the discrete lattice, the second-order spatial derivative ψ'' is approximated by a space-centered finite-difference $(\psi_{i+1,j} + \psi_{i-1,j} - 2\psi_{i,j})/h_x^2$, and the first-order time derivative $\dot{\psi}$ is approximated by a forward difference $(\psi_{i,j+1} - \psi_{i,j})/h_t$. Finally, there is an ambiguity as to how to integrate the noise term. I will follow the Itô interpretation, in which eq. (4.13) is causal [20]. Thus, the discrete map is of the form

$$\frac{\psi_{i,j+1} - \psi_{i,j}}{h_t} = \frac{\psi_{i+1,j} + \psi_{i-1,j} - 2\psi_{i,j}}{h_x^2} + \psi_{i,j} - \psi_{i,j}|\psi_{i,j}|^2 + i\ell^{-1}\omega x \psi_{i,j} + \frac{\eta_{i,j}}{\sqrt{h_x h_t}}. \tag{4.15}$$

There are five parameters that enter into (4.15): $\omega, D, \ell, h_x, h_t$. The first two, ω and D, have already been discussed. A useful way to parametrize the length ℓ is in terms of a parameter n_ℓ, such that $2\pi n_\ell = \ell/\sqrt{3}$. Then, n_ℓ is interpreted as the winding number of $\tilde{\psi}$ at which the instability is encountered (see the following paragraph). In this chapter, n_ℓ will always be taken as 2.5. This corresponds to $\ell = 27.2$, which, if we use the parameters listed at the end of Sec. 4.2, corresponds to $L = 10.3\mu$m. This value of n_ℓ allows enough complexity, in that the winding number can change by 1 or by 2 without becoming negative (i.e., without the current having to change sign), yet it is small enough so that the numerical calculations are feasible in a reasonable amount of time. I have performed numerical calculations using values of n_ℓ larger than 2.5. Although I have not systematically analyzed these other cases, in all cases the the crossover phenomena was exhibited.

The parameters h_x and h_t are chosen so that eq. (4.15) is numerically stable. We

are not focusing on high numerical accuracy. Rather, our goal is to understand the general phenomena contained in the time-dependent Ginzburg-Landau equation so that we may obtain a caricature of the behavior in the presence of an electric field. This is the reason that a simple Euler differencing scheme, rather than a more accurate scheme, such as Runge-Kutta, is sufficient. Typically, we would like to represent one wavelength by at least 8 points. This means that we should have $h_x < n_\ell/8$, or if N_x denotes the number of spatial points, we should take $N_x > 8n_\ell = 20$. For the standard diffusion equation, in order for the Euler differencing scheme to be stable, $h_t < h_x^2$, up to some constants of order unity. This is a reasonable rule of thumb. The philosophy here is to use values for h_x and h_t that are numerically efficient, and then to change these values, comparing the qualitative results to ensure that the numerical results are not a numerical artifact. It should be kept in mind that the quantitative results will depend on the choices of h_x and h_t. This can be seen most easily by studying the linear stability properties of eq. (4.15). The growth rates depend quantitatively on h_x and h_t, but the qualitative feautures that are important for the results of this chapter are not sensitive to these values.

4.3 Expectations

Before proceeding with the results of the numerical integration, it is useful to take a moment to discuss a certain class of fixed points of eq. (4.10). In the Introduction to this chapter I discussed the results we might expect based on the notion of metastability (see Fig. 4.1). The discussion in this section more precisely quantifies these ideas. Here, a state $\tilde{\psi}$ is called a fixed point of eq. (4.10) if the right hand side, evaluated at $\tilde{\psi}$, vanishes. For our purposes, the important class of fixed points of eq. (4.10), denoted by $\tilde{\psi}_n$, are given by

$$\tilde{\psi}_n(x,t) = \sqrt{1 - Q_n(t)^2}\, \exp(iq_n x), \tag{4.16}$$

where

$$q_n \equiv 2\pi n/\ell, \tag{4.17}$$

$$Q_n(t) \equiv k(t) + q_n. \tag{4.18}$$

The states $\tilde{\psi}_n$ are nothing but the metastable current-carrying states ψ_m that were discussed in Chap. 2. The states $\tilde{\psi}_n$ have (dimensionless) free energy

$$\mathcal{F}_n(t) = -(\ell/2)(1 - Q_n^2)^2, \tag{4.19}$$

and (dimensionless) current

$$\mathcal{J}_n(t) = Q_n(1 - Q_n^2). \tag{4.20}$$

(Notice that $\mathcal{J}_n = \ell^{-1}\partial\mathcal{F}_n/\partial Q_n$.) For $\omega > 0$, both the free energy $\mathcal{F}_n$ and the current $\mathcal{J}_n$ are increasing functions of time, $\mathcal{J}_n$ achieving a maximum value $\mathcal{J}_c \equiv 2/\sqrt{27}$, at $Q_n = k_c \equiv 1/\sqrt{3}$, the same point at which $\mathcal{F}_n$ has a point of inflection. For $|Q_n| < k_c$, the curvature of $\mathcal{F}$ is positive, and for $|Q_n| > k_c$, the curvature is negative. This implies that those states $\tilde{\psi}_n$ for which $|Q_n| > k_c$ are unstable. In other words, this simple analysis indicates that in the presence of an electric field, the supercurrent will increase to $\mathcal{J}_c$, at which point the system becomes unstable. What happens then? Does the system end up in a state $\tilde{\psi}_{n'}$ for which $|Q_{n'}| < k_c$, and if so, which value of n' is selected? Furthermore, how does the value that is selected depend on the rate ω at which the system is driven? As we will see in the following sections, the above analysis is not quite accurate. Nevertheless, it captures the essence of the problem in a simple manner.

What we shall find is that after encountering the instability, the system indeed ends up in a state $\tilde{\psi}_{n'}$ for which $|Q_{n'}| < k_c$. For 'small' electric field strengths (i.e., small values of ω) $n' = n - 1$. This corresponds to the occurence of a single phase-slip process. However, as the strength of the field is increased, it becomes more and more likely that states $\tilde{\psi}_{n'}$ for which $n' = n - 2$ will be selected. Thus, we shall find that there is a crossover from single phase-slip domination to double phase-slip domination, as the strength of the field is increased. The main purpose of this chapter is to understand this crossover in a comprehensive and systematic way.

At this stage we are in a position to estimate how strong the electric field must be in order that the system reach the Eckhaus instability before the occurence of a thermally activated phase-slip. In Chap. 2 we determined the transition rates $\ell\Gamma_{\pm}$ out of a metastable state ψ_m [c.f. eq. (2.35)]. We will use these rates to estimate, for a given D, how large ω must be. Now, in the presence of an electric field, the wavevector $k_m \equiv k$ that characterizes state ψ_m will be time dependent, according to eq. (4.8). Thus, $\ell\Gamma_{\pm}$, will depend on time. We now ask: If the system is initially in a metastable state $\sqrt{1-k(0)^2}e^{ik(0)x}$, what is the probability $P(t_c)$ that at time $t_c = (k_c - k(0))/\omega$ the system is in state $\sqrt{1-k_c^2}e^{ik_c x}$? Then, the condition that the system be likely to reach the instability is: $1 - P(t_c) \ll 1$.

We determine $P(t_c)$ as follows. First, we denote by $P(t)$ the probability that at time t the system is in state $\psi_k(t) \equiv \sqrt{1-k(t)^2}e^{ik(t)x}$. Next, if we define

$$\gamma(t) \equiv \ell(\Gamma_+ + \Gamma_-), \tag{4.21}$$

then $\gamma(t)dt$ is the probability that between time t and time $t + dt$ a single phase-slip process occurs. (For the purposes of this estimate, we do not consider double, or higher, phase-slip processes, as we expect these to be be less likely.) With these definitions we have that

$$P(t + dt) = P(t)[1 - \gamma dt]. \tag{4.22}$$

If we take $dt \ll 1$, then we can write $P(t+dt) \approx P(t) + \partial_t P(t)dt$, which when inserted into eq. (4.22) gives a differential equation for $P(t)$ of the form $\partial_t P(t) = -\gamma P(t)$. This equation is elementary to solve, with the result that

$$P(t_c) = e^{-\int_0^{t_c} dt\,\gamma(t)}, \tag{4.23}$$

The condition (i.e., $1 - P(t_c) \ll 1$) that the system reach the Eckhaus instability is satisfied if the exponent in eq. (4.23) is much smaller than unity, i.e., if

$$\int_0^{t_c} dt\,\gamma(t) \ll 1. \tag{4.24}$$

If $\omega \ll 1$ then we can make the quasi-static approximation (see Sec. 2.9), and we have that

$$\gamma = \ell(\Gamma_+(k(t)) + \Gamma_-(k(t))), \tag{4.25}$$

$$= (\Omega_+ e^{-D^{-1}\Delta\mathcal{F}_+} + \Omega_- e^{-D^{-1}\Delta\mathcal{F}_-}). \tag{4.26}$$

If we change the variable of integration in eq. (4.24) from t to k, where $dk/dt = \omega/\ell\tau_{GL}$, the condition (4.24) that the system reach the Eckhaus instability can be written as

$$\frac{\omega}{\ell} \gg \tau_{GL} \int_{k(0)}^{k_c} dk\, (\Omega_+ e^{-D^{-1}\Delta\mathcal{F}_+} + \Omega_- e^{-D^{-1}\Delta\mathcal{F}_-}), \tag{4.27}$$

where we have used eq. (4.26) for γ. For $D \ll 1$, the right-hand-side (rhs) of (4.27) will be very small, due to the factors of $e^{-D^{-1}\Delta\mathcal{F}_\pm}$. We can use the expressions for $\Delta\mathcal{F}_\pm$ [see eq. (2.58)] and $\Omega_\pm$ [see eq. (2.67)] that were obtained in Chap. 2 to compute the numerical value of the rhs of (4.27). Strictly speaking, this is not valid, as these results were derived based on the assumption that $e^{-\ell\sqrt{\Delta(k)}} \ll 1$ [see eq. (2.47)]. Near the Eckhaus instability however, $\Delta = 1 - 3k^2 \to 0$. Nevertheless, for the purposes of this estimation these forms for Ω and $\Delta\mathcal{F}$ should be sufficient. Taking $D = 0.001$ and $k(0) = 0.55$ ($k_c = 0.57735$), the rhs of (4.27) is $\approx \ell \times 10^{-25}$. [As $D \ll 1$ this integral is only weakly sensitive to $k(0)$.] Thus, for this value of D (0.001) a very small value of ω is sufficient to ensure that the system survive to the Eckhaus instability. Finally, it should be noticed that the right hand side of eq. (4.27) is extremely sensitive to D. For example, if $D = 0.01$ then the rhs of (4.27) is $\approx 4\ell \times 10^{-14}$, and for $D = 0.1$ it is $\approx 6\ell \times 10^{-8}$.

Finally, I should remark that I have not systematically addressed the question of what happens for stronger electric fields. In my preliminary investigations of this issue, I have seen evidence of triple, and higher, phase-slips. However, as the field strength is increased, the dynamics becomes more complicated. For example, the phase-slips cease to be localized in time, instead they tend to overlap. It is possible that in regions of parameter space I have not explored, there is other interesting dynamical behavior. For example, in the context of pattern forming systems, Riecke and

Paap [11] found evidence for spatio-temporal chaos by applying what they described as 'smooth spatial ramps' to pattern forming systems that exhibit the Eckhaus instability. In their language, the term $\omega(x/\ell)$ that appears in eq. (4.15) is a smooth spatial ramp. Although the dynamical system studied by Riecke and Paap is not identical to that considered here, their results are suggestive of potentially interesting effects in systems that can be described by time-dependent Ginzburg-Landau equations.

4.4 Numerical Results

The numerical integration of eq. (4.15) proceeds as follows. For a given initial condition $\psi_{i,0}$, a particular emf (i.e., a particular value of ω), and $D = 0.001$, eq. (4.15) is iterated forward in time, generating $\psi_{i,j}$. In order to understand the dynamical behavior of the system, the space-average current $\bar{\mathcal{J}}(t)$, and the winding number $\bar{n}(t)$, are computed as a function of time (i.e., j). The former quantity, in the continuum notation, is given by

$$\bar{\mathcal{J}}(t) = (2\ell)^{-1} \int_0^\ell dx \, \mathrm{Im}(\psi^*(x,t)\partial_x\psi(x,t)), \tag{4.28}$$

and the latter by

$$\bar{n}(t) = (2\pi)^{-1} \int_0^\ell dx \, \partial_x \arg(\psi(x,t)). \tag{4.29}$$

For $\omega = 10^{-4}$, eq. (4.15) is iterated for a given realization of the noise, and $\bar{n}(t)$ and $\bar{\mathcal{J}}(t)$ are plotted in Figs. 4.2 (a) and (b), respectively. Using values for the parameters as described in Sec. 4.2, this particular value of ω corresponds to an emf V of approximately 2 nV. As expected, the current increases to the critical current, at which point the Eckhaus instability (see Sec. 4.5) is encountered, and a *single* phase-slip process occurs, resulting in a decrease of *one* quantum of current [21]. The supercurrent then continues to increase, and the phase-slip process is repeated. The important point is that in this case, it is only single phase-slip processes that occur. In other words, the winding number only changes by one, and not by two or more. The time between phase-slips is approximately $\tau_{GL} 2\pi/\omega$. Using $\tau_{GL} \sim 1.4 \times 10^{-11}$s (see Sec. 4.2), we can estimate that the phase slips are separated in time by $\approx 0.9 \times 10^{-6}$s.

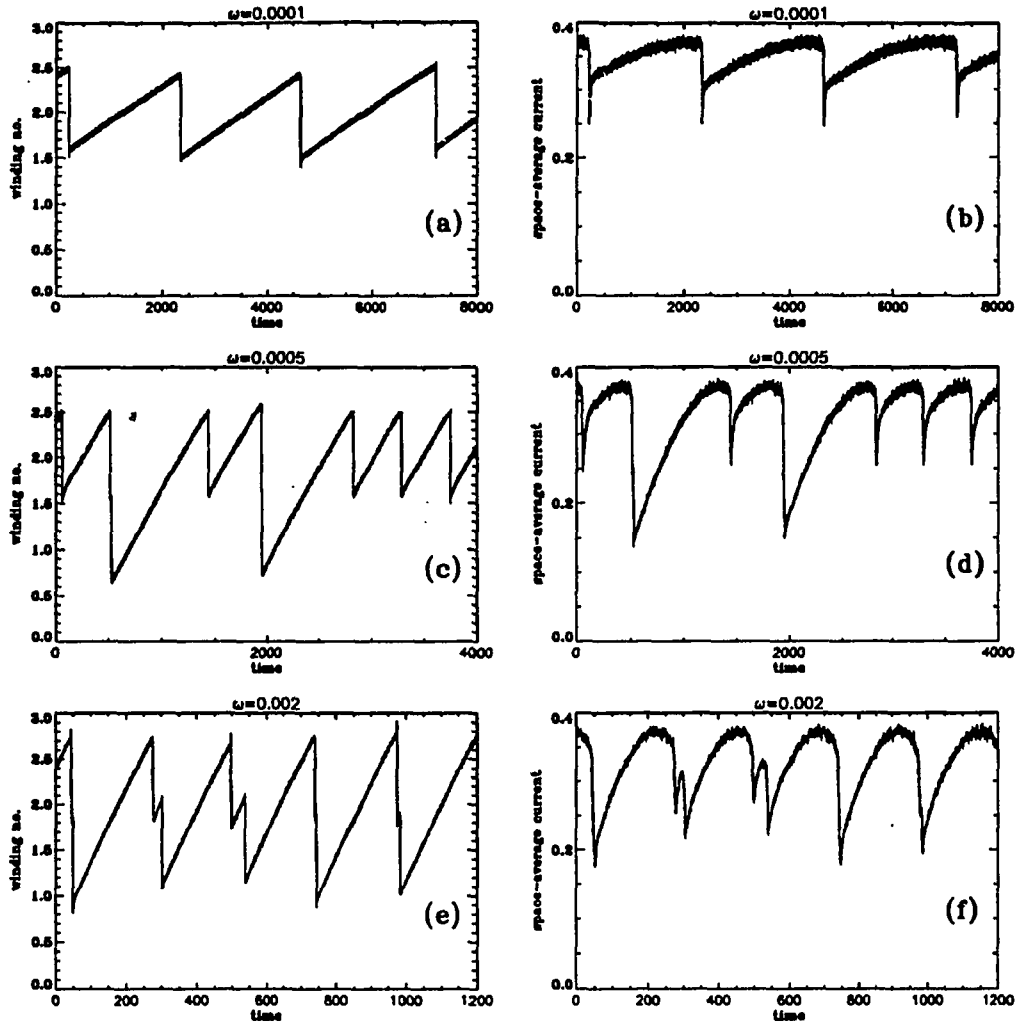

Figure 4.2: Winding number (left column) and current (right column) as a function of time. Parameters used: $N_x = 32$, $h_t = 0.2$ (and $n_\ell = 2.5$).

Now, we increase ω to 5×10^{-4} ($V \sim 10\,\mathrm{nV}$). The winding number $\bar{n}(t)$ and the space-average current $\bar{\mathcal{J}}(t)$ are plotted in Figs. 4.2 (c) and (d), respectively. Again, due to the presence of the electric field, the current increases to the critical current, but now we observe that the current sometimes changes by one quantum, and at other times by two. In this plot [as well as that of Fig. 4.2 (f)], we can plainly see

the growth of the fluctuations of the current as the Eckhaus instability is approached. This growth is an indication that the free-energy landscape about the metastable states is flattening out. This will be discussed in considerable detail in the following sections, especially Sec. 4.5.

We now increase ω even further, to $\omega = 2 \times 10^{-3}$ ($V \sim 400\,\mathrm{nV}$). As can be seen in Figs. 4.2 (e) and (f), for this field strength, only double phase-slip processes occur. Using $\tau_{GL} \sim 1.4 \times 10^{-11}\mathrm{s}$, we can estimate that the double phase slips are separated in time by $\tau_{GL} 2\pi/\omega \approx 4.4 \times 10^{-8}\mathrm{s}$. Notice that in some cases a double phase-slip process appears to occur via a sequence of single phase-slips. This is not in fact the case; the noise strength $D = 10^{-3}$ is so small that after entering a metastable state, there is essentially zero probability of a thermally activated process. This then precludes the possibility of a double phase-slip occuring via a sequence of single phase-slips. What is actually causing the step-like features will be discussed below.

Thus, what we have found is that for small values of ω, single phase-slip processes dominate. As the field strength is increased, it becomes more and more likely that double phase-slip processes will occur. In other words, as the strength of the electric field is increased, there is a crossover from single phase-slip domination to double phase-slip domination.

This crossover phenomena can be illustrated in a more quantitative way, as follows. For a given electric field, eq. (4.15) is integrated N times, each time the integration is stopped the first time a particular event (i.e., either a single or a double phase-slip) occurs. The number N_1 (N_2) of single (double) phase-slips is then counted, yielding the probability $P_1(\omega) = N_1/N$ ($P_2(\omega) = N_2/N$) of a single (double) phase-slip, as a function of electric field. The results for P_1 (with $N = 100$ and $D = 10^{-3}$) are shown in Fig. 4.3.

Before proceeding with the details of the analysis that will explain this crossover phenomena, it is useful to investigate in detail the dynamics of the order parameter

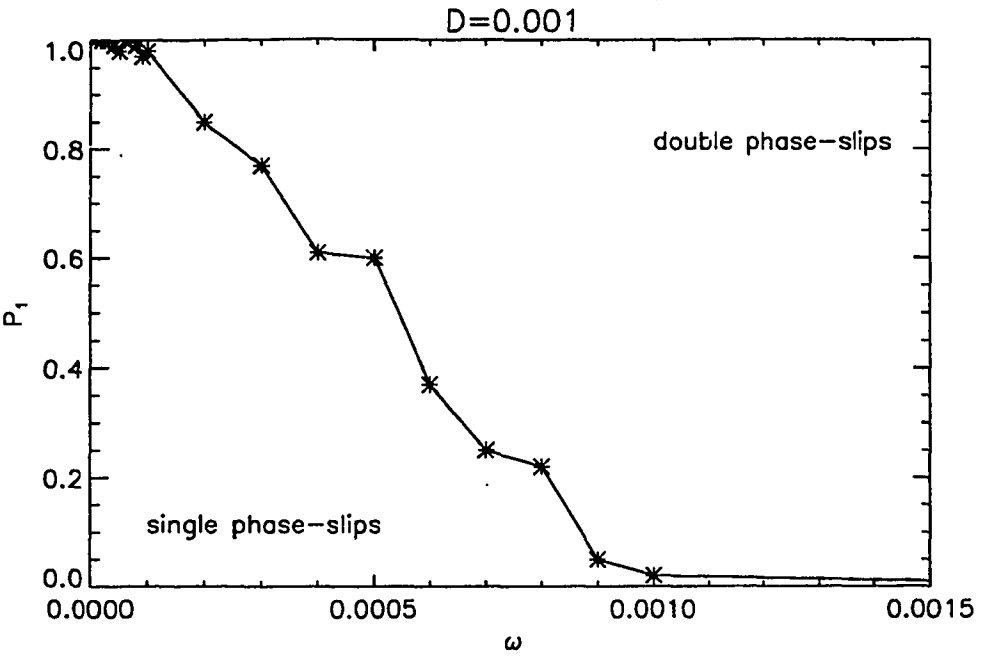

Figure 4.3: Probability of a single phase slip vs. ω. Parameters used: $N_x = 32$, $h_t = 0.2$ (and $n_\ell = 2.5$).

during a phase-slip event. This is done via a mode expansion:

$$\psi(x,t) = \sum_n a_n(t) \exp(iQ_{-n}(t)x), \tag{4.30}$$

in which the $a_n(t)$ are complex, time-dependent expansion coefficients, and q_n and Q_n are given in eqs. (4.17) and (4.18), respectively. Notice that explicit temporal dependence of $\psi(x,t)$ appears via both $a_n(t)$ and $k(t)$. Initially, $a_0(0) = \sqrt{1-k(0)^2}$, and all other $a_n(0) = 0$. The value of $k(0)$ is chosen so that the initial state is metastable. (The results do not depend on the specific value of $k(0)$, as long as it is such that the initial state is locally stable.) In this representation, a single phase-slip process corresponds to $|a_1(t)| \neq 0$ at some time $t > 0$, with all other $|a_n(t)| \ll 1$. Likewise, a double phase-slip process corresponds to $|a_2(t)| \neq 0$ at some time $t > 0$, with all other $|a_n(t)| \ll 1$. More precisely, after a type-n process (e.g., type-1 refers

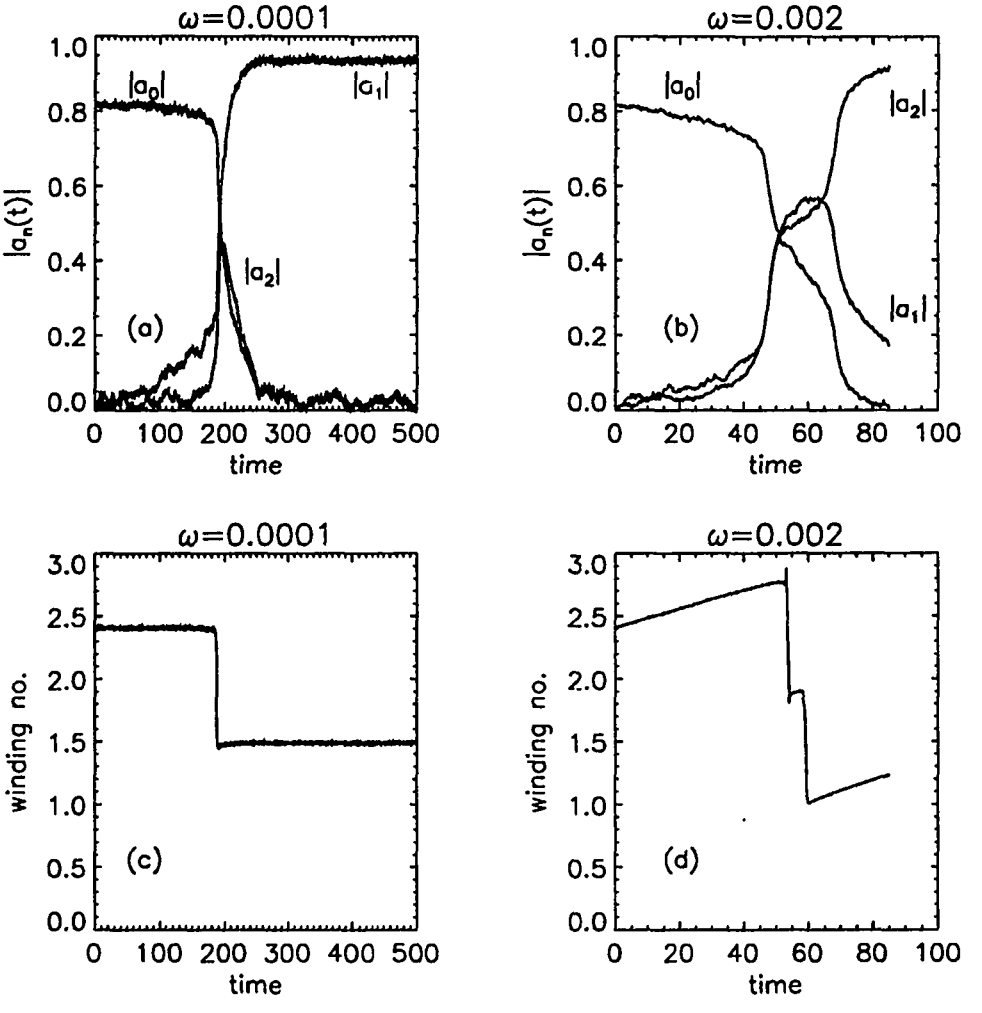

Figure 4.4: Mode amplitudes for a single phase-slip process (a) and a double phase-slip process (b). Parameters used: $k_o = 0.58$, $N_x = 32$, $h_t = 0.2$ (and $n_\ell = 2.5$).

to a single phase-slip) has occured, we find that $a_n(t) \approx \sqrt{1 - Q_{-n}(t)^2}$, and all other amplitudes are $\ll 1$. These other amplitudes are not identically zero because of the presence of the noise.

As a first example, plotted in Fig. 4.4 (a) are the absolute values $|a_0(t)|, |a_1(t)|$ and $|a_2(t)|$ for a case in which a single phase-slip has occured. That is, after the

event $|a_1(t)| \approx \sqrt{1 - Q_{-1}^2(t)}$, and both $|a_0(t)|$ and $|a_2(t)|$ are $\ll 1$. Note that there is essentially no coexistence of the various modes, i.e., the transition is fairly sharp, as can be seen in Fig. 4.4 (c), where the winding number is plotted. A second example is given in Fig. 4.4 (b), where the $n = 0$, 1 and 2 mode amplitudes are plotted. In this case, a double phase-slip has occured, and, in addition, the winding number, plotted in Fig. 4.4 (d), changes in a step-like way [as in Fig. 4.2 (e)]. The reason for the step-like change in the winding number is that in the this case there is some coexistence of the various amplitudes, i.e., the transition is not sharp. Also note, that even though $|a_1| > |a_2|$ for a certain period of time, a_2 ends up dominating. For the times in which $|a_1| > |a_2|$, neither of these amplitudes is small, in fact they are both ≈ 0.5. This implies that nonlinearities appear to play a role in determining which state is selected. We will come back to this issue in Sec. 4.5.

An understanding of the dynamics of the a_n is central to understanding the crossover effect. In fact, the qualitative features can be understood by examining the nature of the Eckhaus instability (the instability associated with the critical current) using linear stability analysis (LSA). This will be done in Sec. 4.5. We will learn from the LSA that the system first becomes unstable with respect to fluctuations with wavevector $k \pm q_1$, and later on, the system becomes unstable with respect to fluctuations with wavevector $k \pm q_2$. However, the q_2-type fluctuations, once they start growing, grow more rapidly than the q_1-type. So, although the q_1 fluctuations start growing earlier than the q_2 fluctuations, it is possible for the q_2 fluctuations to dominate the dynamics, as we have seen.

Before proceeding with the linear stability analysis of the Eckhaus instability, we first turn our attention to whether or not it might be possible to observe experimentally the crossover effect. The natural quantity to measure is the time-dependence of the magnetic moment of the ring. There are three important issues. First, there is the issue of the sensitivity of the magnetometer to the magnitude of the current. For a type-n process, the current changes by an amount $\Delta I_n = (4ek_BT/\hbar D)(\mathcal{J}(k_c) - \mathcal{J}(k_c - q_n))$. For the parameters given in Sec. 4.2,

i.e., $T_c = 3\text{K}$, $T = 0.93T_c$, and $D = 0.001$, we have that $\Delta I_1 \approx 1.9 \times 10^{-5}\text{A}$ and $\Delta I_2 \approx 6.4 \times 10^{-5}\text{A}$. Thus the magnetometer must be sensitive enough to detect current changes of this magnitude. The second issue is the time sensitivity of the magnetometer. For the single phase-slips pictured in Figs. 4.2 (a) and (b), the time between phase-slips is $0.9 \times 10^{-6}\text{s}$. If time is measured in units of $2\pi\tau_{GL}/\omega$, then the period is unity. On the other hand, for the double phase-slips pictured in Figs. 4.2 (e) and (f), the time between phase-slips is $4.4 \times 10^{-8}\text{s}$. If time is measured in units of $2\pi\tau_{GL}/\omega$, then in this case the period is two. If the magnetometer has the temporal resolution to resolve double phase-slip events, then these can be distinguished from the single phase-slip events by the periodicity of the time-dependence of the magnetic moment if time is scaled in the appropriate way, i.e., in units of $2\pi\tau_{GL}/\omega$. The third issue is the time rate of change of magnetic flux that corresponds to the values of ω considered here. As discussed in Sec. 4.2, a value of $\omega = 10^{-4}$ corresponds to 10^6 flux quanta passing through the ring per second, which correspnds to $\approx 0.207\,\text{Gcm}^2\text{s}^{-1}$. Thus, if $L = 10\,\mu\text{m}$, the magnetic field must change at a rate of $\approx 10^8\,\text{Gs}^{-1}$. If the field is applied for $10^{-4}\,\text{s}$, then the final value of the field is $10^4\,\text{G}$. These rather large values are due to the small cross-sectional area $L^2/4\pi$. If the ring is made longer, then the field values will be reduced. However, for longer rings, the magnitude of the current changes will be be made smaller.

4.5 Eckhaus Instability

The essential understanding of the crossover effect can be obtained by examining the linear stability properties of the fixed points $\tilde{\psi}_m(x,t) = \sqrt{1 - Q_m^2(t)}\exp(iq_m x)$ of eq. (4.10); see Refs. [8, 9, 10]. At this stage, it is convenient to make an adiabatic approximation in which we set $\omega = 0$, so that $k(t)$ is constant in time. This assumption considerably simplifies the linear stability analysis, and is justified because $\omega \ll 1$. The basic idea is to understand the circumstances under which the (metastable current-carrying) states $\tilde{\psi}_m$ become unstable with respect to very small

fluctuations $\delta\tilde{\psi}_m$; if $\tilde{\psi}_m$ is locally stable, then $\delta\tilde{\psi}_m$ will decay with time, whereas, if $\tilde{\psi}_m$ is locally unstable, then $\delta\tilde{\psi}_m$ will grow with time. Since $\delta\tilde{\psi}_m$ is assumed to be very small, the TDGL can be linearized around $\tilde{\psi}_m$. The solution to the resulting linear equation can be written in the form

$$\begin{aligned}\delta\tilde{\psi}_m &= \sum_{n\geq 0} a_n(0)e^{iq_m x}[\{e^{-iq_n x} + f_{m,n}e^{iq_n x}\}e^{\lambda^+_{m,n}t} \\ &\quad + \{e^{-iq_n x} - f_{m,-n}e^{iq_n x}\}e^{\lambda^-_{m,n}t}] \end{aligned} \tag{4.31}$$

where

$$f_{m,n} = \frac{2Q_m q_n - \sqrt{(1-Q_m^2)^2 + 4Q_m^2 q_n^2}}{1-Q_m^2}, \tag{4.32}$$

and

$$\lambda^{\pm}_{m,n} \equiv \lambda^{\pm}(Q_m, q_n) = -1 + Q_m^2 - q_n^2 \pm \sqrt{(1-Q_m^2)^2 + 4Q_m^2 q_n^2}\,. \tag{4.33}$$

The $a_n(0)$ are determined from the initial condition $\delta\tilde{\psi}_m(x,0)$. At this point, we would like to imagine that $\omega \neq 0$. Although the growth rates were derived assuming no external field, as $\omega \ll 1$, we are justified in taking the effect of the field into account by simply re-endowing $k(t)$, and hence $Q_m \equiv k(t) + q_m$, with the appropriate time dependence, via $k(t) = k_o + \omega t/\ell$.

The quantities $\lambda^{\pm}_{m,n}$ are the growth rates: $\lambda^+_{m,1}$ and $\lambda^+_{m,2}$ are plotted in Fig. 4.5. Their sign determines whether or not the state $\tilde{\psi}_m$ is stable (negative) or unstable (positive) with respect to fluctuations characterized by a wavevector q_n. The growth rates $\lambda^-_{m,n}$ are negative-definite, and hence will be ignored. On the other hand, $\lambda^+_{m,n}$ can sometimes be positive. More specifically, for a given n, $\lambda^+_{m,n}$ is a nondecreasing function of Q_m, being negative for $|Q_m| < \kappa_n$, and changing sign at $Q_m = \pm\kappa_n$, where

$$\kappa_n = \frac{1}{\sqrt{3}}[1 + q_n^2/2]^{1/2}. \tag{4.34}$$

(For $n_\ell = 2.5$, $\kappa_1 = 0.585$ and $\kappa_2 = 0.607$.) The points $\pm\kappa_1$ locate the so-called Eckhaus boundary. It is interesting to notice that for ℓ finite, $\kappa_1 > k_c \equiv 1/\sqrt{3}$, where k_c is the location of the Eckhaus boundary for $\ell = \infty$. Thus, the finite length has

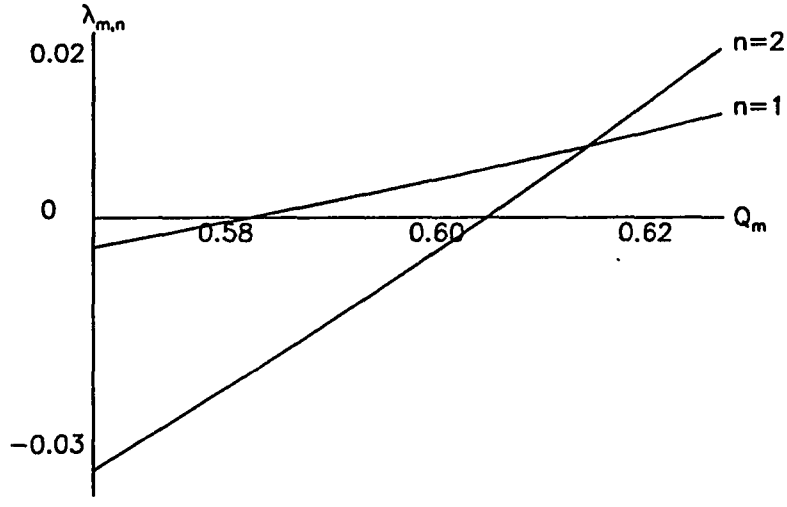

Figure 4.5: Growth rates for $n = 1$ and $n = 2$ ($n_\ell = 2.5$).

a stabilizing effect [8], expanding the domain of stable wavevectors by an amount $\kappa_1 - k_c$.

For present purposes, the growth rates $\lambda^+_{m,n}$ have two important features (see Fig. 4.5). First, the κ_n have the property that $\kappa_1 < \kappa_2 < \kappa_3 \ldots$. Thus, $\tilde{\psi}_m$ is locally stable (i.e., metastable) as long as $Q_m < \kappa_1$. For Q_m between κ_1 and κ_2, $\tilde{\psi}_m$ is unstable with respect to fluctuations of wavevector $k \pm q_1$. (As it is the q_1-type fluctuations that grow first, it is sometimes said that the Eckhaus instabiity is characterized by the instability with respect to long wavelength fluctuations.) As Q_m increases beyond κ_2, state $\tilde{\psi}_m$ now becomes unstable with respect to fluctuations of wavevector q_1 *and* q_2. It is in this situation that the competition between single and double phase-slip processes may arise. In general, if Q_m lies between κ_n and κ_{n+1}, then $\tilde{\psi}_m$ is unstable with respect to all wavevectors $q_{n'} < q_n$. The possibility thus exists for competitition between many different modes.

The second important feature of the growth rates is that $\lambda'_n < \lambda'_{n+1}$, where $\lambda'_n \equiv \partial\lambda^+(\kappa_n, q_n)/\partial Q$. (For $n_\ell = 2.5$, $\lambda'_1 = 0.263$ and $\lambda'_2 = 0.921$.) In other words, the growth rates for the higher n modes increase more rapidly with Q_m, after the onset of the respective instability, than do the lower n modes. This means that, although the system becomes unstable with respect to the $n = 1$ mode first, if this mode does not have sufficient time to grow to dominance, it is possible, by virtue of the fact that $\lambda'_2 > \lambda'_1$, for the second mode to actually win, corresponding to a double phase-slip process.

The situation is (loosely) analogous to a race of a tortoise and a hare, if we take $|a_1|$ to represent the position of the tortoise, and $|a_2|$ to represent the position of the hare. In this case, the tortoise starts the race earlier than the hare, by an amount of time $(\kappa_2 - \kappa_1)/\omega$, but the hare is the faster runner (i.e., $\lambda'_2 > \lambda'_1$) so that it is possible for the hare to overtake the tortoise.

To make the discussion in the above paragraph more precise, consider the time-dependent Ornstein-Uhlenbeck process [22] for two modes, a_1 and a_2:

$$\frac{da_n(t)}{dt} = \lambda^+(k(t), q_n)a_n(t) + \tilde{\eta}_n(t), \tag{4.35}$$

where $\tilde{\eta}_n$ is a Gaussian random variable with mean zero, and variance $2D/\ell$. (This renormalization of the noise strength by the factor ℓ^{-1} can be obtained by considering eq. (4.35) to be derived from a linearized version of eq. (4.10), by multiplying (4.10) by $e^{iq_n x}$, and integrating from 0 to ℓ.) By integrating eq. (4.35), we find that

$$\langle |a_n(t)|^2 \rangle = \frac{2D}{\ell} e^{2\sigma_n(t)} \int_0^t dt'\, e^{-2\sigma_n(t')}, \tag{4.36}$$

where $\sigma_n(t) \equiv \int_0^t dt\, \lambda^+(k(t), q_n)$, and angular brackets denote a noise average. To evaluate the right-hand-side of eq. (4.36), first notice that $\sigma_n(t)$ is non-positive (at least for the times of interest to us here), being zero at $t = 0$, and achieving a local minimum at $t_n = \ell(\kappa_n - k_o)/\omega$. Thus, the integral on the right hand side of eq. (4.36) is bounded from above, and so is of secondary importance for the growth of $\langle |a_n(t)|^2 \rangle$. Of primary importance is the factor $e^{2\sigma_n(t)}$.

For t near t_n, we can expand $\sigma_n(t)$ to second order in $t - t_n$, i.e.

$$\sigma_n(t) \approx \sigma_n(t_n) + \frac{1}{2}\frac{\lambda_n'\omega}{\ell}(t - t_n)^2.$$

Then, inserting this expansion into eq. (4.36), we get

$$\langle |a_n(t)|^2 \rangle = \frac{2D\tau_n}{\ell} e^{z_n(t)^2} \int_{-t_n/\tau_n}^{z_n(t)} dz' e^{-(z_n')^2}, \tag{4.37}$$

where we have defined $z_n(t) \equiv (t - t_n)/\tau_n$ and

$$\tau_n \equiv \sqrt{\ell/\lambda_n'\omega}. \tag{4.38}$$

Thus, we can identify a characteristic time

$$t_n^* \sim \tau_n \sqrt{\ln(\ell/2D\tau_n)} \tag{4.39}$$

as the time, after the onset of the instability with respect to mode n, at which $\langle |a_n|^2 \rangle \sim \mathcal{O}(1)$. The characteristic time t_n^* depends weakly (i.e., logarithmically) on the noise. More interesting, however, is the fact that τ_n, and hence t_n^*, is inversely proportional to the geometric mean of λ_n' and ω/ℓ; the former factor being a reflection of the intrinsic dynamics, and the latter a reflection of the strength of the external field. From eq. (4.39) a characteristic wavevector

$$k_n^* \equiv \kappa_n + \omega t_n^* \tag{4.40}$$

can be defined for each mode, where t_n^* is given in eq. (4.39). The crossover field $\omega_c^{1,2}$ separating the regimes of single and double phase-slip domination is then defined by the solution to the equation $k_1^* = k_2^*$. For $\omega < \omega_c^{1,2}$, single phase-slip processes should dominate, whereas for $\omega > \omega_c^{1,2}$, double phase-slip processes should dominate. For $D = 0.001$ and $\ell = 2\pi n_\ell \sqrt{3}$, where $n_\ell = 2.5$ (i.e., the same parameters as those used in obtaining the results of Fig. 4.3), the condition $k_1^* = k_2^*$ yields a value for $\omega_c^{1,2} \approx 1.9 \times 10^{-5}$. Comparing this value with that obtained from the simulation (i.e., that of Fig. 4.3), it is seen that this estimate is too small by an order of magnitude. This should not be unexpected, as our estimate is based on the results from the linear

stability analysis. As was exhibited explicitly in Fig. 4.4, the state-selection can occur in the nonlinear regime. Thus, any analysis that is restricted to the linear properties is undoubtedly inadequate. Nevertheless, this analysis is useful in that we are able to understand in a qualitative way the essential reason for the crossover phenomenon.

The above analysis can be used to deduce what we might expect to see for an arbitrary value of n_ℓ. Let us denote by $\omega_c^{n,n+1}$ the value of ω for which $k_n^* = k_{n+1}^*$, where k_n^* is given in eq. (4.40). Then for ω between $\omega_c^{n-1,n}$ and $\omega_c^{n,n+1}$ we expect that type-n processes (e.g., type-2 corresponds to a double phase-slip) will dominate. As mentioned previously in Sec. 4.3, I have not investigated the behavior for values of $\omega > \omega_c^{n_{max}-1,n_{max}}$ where n_{max} is the smallest integer nearest to n_ℓ. In this regime, the phase-slips begin to overlap in time, and the dynamics becomes complicated.

Finally, before proceeding further, it is useful to notice in eq. (4.31) that the term multiplying $e^{\lambda_{m,n}^+ t}$ is a sum of $e^{iq_n x}$ and $e^{-iq_n x}$. The modes that have wavevector $-q_n$ have the possibility of achieving occupation, whereas those modes with wavevector $+q_n$ do not. To see this, suppose that state $\tilde{\psi}_m$ is unstable, i.e., $Q_m > \kappa_n$ for some $n > 0$. Now, according to eq. (4.31), the amplitudes for both q_n and $-q_n$ grow, initially at a rate $\lambda_{m,n}^+$. However, the component of $\delta\tilde{\psi}_m$ that has a wavevector $q_m + q_n$ has an associated $Q_{m+n} > Q_m$, and thus has no chance of becoming a stable fixed point, as this would require a Q value, such as Q_{m-n}, in the stable range. It is the nonlinearities, not included in the present analysis, that will cause the amplitude of this mode eventually to decay to zero. Although the modes with positive q_n cannot compete for occupation, they are nevertheless extremely important. In fact, they act as 'catalysts'. That is, as can be seen from eq. (4.31), in the linear regime they are vital to the growth of the negative q_n modes. Thus, any approximation in which a mode expansion of $\tilde{\psi}_n$ is truncated, must include these positive q_n modes, otherwise the resulting dynamical system will not have the same linear-stability properties as the original dynamical system. In App. F I will present the construction of a two-mode dynamical system that exhibits the crossover effect. The positive q_n modes play an important role in the construction of the two-mode system.

4.6 Path Integral Approach to the Decay From an Unstable State

In the first part of this chapter, we saw that the effect of the externally applied electric field is to drive the system to a point of instability. When the system reaches this point, there are multiple metastable states that can compete for occupation. The question is: how can we understand the resulting state-selection? In other words, we seek a theory for the decay from an unstable state when multiple metastable states compete for occupation. A succesful theory should be able to predict the relative number of single versus double phase-slips as a function of electric field.

In this section I will present a possible approach to this problem, in the limit where the noise strength $D \ll 1$. The path integral approach, to be presented below, allows the derivation of a closed form expression for the probability of a single phase-slip, relative to that of a double phase-slip. This expression, which involves only the ratio of determinants of fluctuation operators, is analogous to the Arrhenius-type expression for the decay rate *when there is no barrier*. This is appealing because here we are dealing with the decay from an unstable state, i.e., *there is no energy barrier*.

The derivation is based on the following hypothetical picture of the dynamics of the probability density functional $P[\tilde{\psi}]$. In principle, the dynamics of $P[\tilde{\psi}]$ can be determined from the functional Fokker-Planck equation associated with the stochastic eq. (4.10). However, the functional nature of this equation renders this procedure intractable. The general picture of the dynamics of P is as follows. We imagine that at some time, say $t = 0$, we have an ensemble of systems, all of which reside in the same metastable state, say $\tilde{\psi}_n(0)$. Thus, all of the weight of $P[\tilde{\psi}]$ is located at a single point in function space. In the presence of an electric field, and as long as the ensemble of systems have not encountered the Eckhaus instability, the peak value of $P[\tilde{\psi}]$ will follow the point $\tilde{\psi}_n(t)$ in function space. The noise will cause P to spread out, but as long as the state $\tilde{\psi}_n(t)$ remains locally stable, the probability will remain localized about this state. (We are assuming that the noise strength D is small enough so that thermally activated processes do not occur.) The situation will change dramatically

when the systems encounter the Eckhaus instability. When this occurs, the probability will flow away from the state $\tilde{\psi}_n$. Based on the results of the first part of this chapter, if the electric field is such that single phase-slip processes are dominant, we expect that most of the probability will flow to the neighborhood of state $\tilde{\psi}_{n-1}$, i.e., most of the members of the ensemble will experience single phase-slips. On the other hand, if the electric field is such that double phase-slip processes dominate the dynamics, we expect that most of the probability will flow to the neighborhood of state $\tilde{\psi}_{n-2}$, i.e., most of the members of the ensemble will experience double phase-slips. For an electric field of intermediate strength, we expect that some of the probability will flow to state $\tilde{\psi}_{n-1}$ and some to state $\tilde{\psi}_{n-2}$, the amount of probability that flows to each state will depend on the relative number of single versus double phase-slips that occured. Subsequent to the transitions, we expect that $P[\tilde{\psi}]$ will remain localized about states $\tilde{\psi}_{n-1}$ and $\tilde{\psi}_{n-2}$, and that the relative number of single versus double phase-slips will be given by the ratio of $P[\tilde{\psi}_{n-1}]$ to $P[\tilde{\psi}_{n-2}]$. In the rest of this section I will present a derivation of this ratio. The results contained here should be regarded as speculative. In addition, due to the complexity of the STDGL equations, it is difficult to verify explicitly the ideas contained in this section. In App. F a two-mode dynamical system that exhibits the crossover effect is constructed. For this system of reduced dimensionality we can (numerically) solve the Fokker-Planck equation, and this enables to visualize the probability flow in a two-dimensional plane. The results (see Fig. F.2) are consistent with the picture described above.

Suppose that at time $t = 0$, the system is in the state $\tilde{\psi}(x,0) \equiv \tilde{\psi}_0 = \sqrt{1-k(0)^2}$, where $k(0) < \kappa_1$, so that $\tilde{\psi}(x,0)$ is a stable fixed point. We then ask, for a given value of ω, what is the (conditional) probability that at a later time τ, the system will be in the metastable state $\tilde{\psi}_n(x,\tau) = \sqrt{1-Q_n(\tau)^2}e^{-iq_n x}$. That is, we will only consider those states $\tilde{\psi}_n$ for which $Q_n(\tau) < \kappa_1$. Denoting this conditional probability by $P_\omega(n,\tau|0,0) = P_\omega(n,\tau)$, a definition of this quantity is [23]

$$P_\omega(n,\tau) = \langle \delta(\tilde{\psi}(x,\tau) - \tilde{\psi}_n(x,\tau)) \rangle, \tag{4.41}$$

where $\delta(\cdot)$ is a functional delta-function, the angular brackets denote an average over the noise, and $\tilde{\psi}(x,\tau)$ satisfies eq. (4.10). From an operational point of view, the interpretation of eq. (4.41) is as follows. Suppose we have an ensemble of systems, each governed by the dynamical equation (4.10), and characterized by a particular realization of the noise $\tilde{\eta}$. At $t = 0$ each member of the ensemble is in state $\tilde{\psi}_0$. The systems then evolve according to eq. (4.10), and at time τ we observe each member of the ensemble, and count the fraction that are in state $\tilde{\psi}_n(x,\tau)$. This number is $P_\omega(n,\tau)$.

Strictly speaking, we should ask not for the probability that the system is *in* state $\tilde{\psi}_n(\tau)$, but for the probability that the system is *in the neighborhood of* state $\tilde{\psi}_n(\tau)$, where the size of the neighborhood is proportional to D. Then the functional delta-function in eq. (4.41) should be replaced by a sharply peaked functional with a width proportional to D. For simplicity of presentation, we will continue with the form of $P_\omega(n,\tau)$ given in eq. (4.41), although it is straightforward to modify the following discussion.

The key idea is that the probability distribution for the noise, denoted here by $P[\tilde{\eta}]$, is known. Thus, $P_\omega(n,\tau)$ can be written as

$$P_\omega(n,\tau) = \int \mathcal{D}\tilde{\eta}\, P_{0,\tau}[\tilde{\eta}]\, \delta(\tilde{\psi}(x,\tau) - \tilde{\psi}_n(x,\tau)), \tag{4.42}$$

where

$$P_{0,\tau}[\tilde{\eta}] \propto \exp\Big(-\int_0^\tau dt \int_0^\ell dx |\tilde{\eta}(x,t)|^2/2D\Big). \tag{4.43}$$

The noise distribution is only required for $t \in [0,\tau]$ because of our causal interpretation of the stochastic equation (see Sec. 4.2). In eq. (4.42), the functional integral should be interpreted as the integral over the real and imaginary parts of the complex variables $\tilde{\eta}_{i,j} \equiv \tilde{\eta}(x_i,t_j)$ defined on the nodes of the lattice described in Sec. 4.2, in the limit that the lattice spacings h_x and h_t go to zero. Then, $\mathcal{D}\tilde{\eta}$ is to be interpreted as

$$\lim_{\substack{h_x\to 0\\ h_t\to 0}} \prod_{i,j} d\tilde{\eta}^{(1)}_{i,j} d\tilde{\eta}^{(2)}_{i,j},$$

where $\tilde{\eta}_{i,j}^{(1)}$ is the real part of $\tilde{\eta}_{i,j}$, and $\tilde{\eta}_{i,j}^{(2)}$ the imaginary part. By regarding eq. (4.10) as a mapping from η-space to ψ-space, $P_\omega(n,\tau)$ can be written as a path integral over $\tilde{\psi}$ by a simple change of variables. As our interpretation of the stochastic equation is causal, the Jacobian, $|\delta\tilde{\eta}(x,t)/\delta\tilde{\psi}(x',t')|$, is a constant, which we can ignore as it will only affect the normalization. In addition, the functional delta function can be accounted for by imposing the boundary condition $\tilde{\psi}(x,\tau) = \tilde{\psi}_n(\tau)$ on the functional integral. Thus, $P_\omega(n,\tau)$ can be written as

$$P_\omega(n,\tau) = \int_{\tilde{\psi}(x,0)=\tilde{\psi}_0}^{\tilde{\psi}(x,\tau)=\tilde{\psi}_n(\tau)} \mathcal{D}\tilde{\psi}\, e^{-\tilde{S}[\tilde{\psi}]/2D} \tag{4.44}$$

where

$$\tilde{S}[\tilde{\psi}] = \int_0^\tau d\tau \int_0^\ell dx \left|\partial_t\tilde{\psi} - (\partial_x + ik(t))^2\tilde{\psi} - \tilde{\psi} + \tilde{\psi}|\tilde{\psi}|^2\right|^2. \tag{4.45}$$

Thus, the conditional probability is given by a sum over all possible configurations consistent with the boundary conditions, each term in the sum being weighted by a factor $e^{-\tilde{S}[\tilde{\psi}]/2D}$. This is analogous to the (imaginary-time) Feynman path integral for the probability amplitude in quantum mechanics. The term in the exponent, $\tilde{S}[\tilde{\psi}]$, is referred to as the generalized Onsager-Machlup functional, or the thermodynamic action [24, 25, 26, 27, 28, 23].

The normalization of $P_\omega(n,\tau)$ is determined by the requirement that at any given time the system must occupy some state. That is, from eq. (4.44) we see that the probability $P_\omega[\tilde{\psi}_f](\tau)$ that a state $\tilde{\psi}_f$ is occupied at time τ is given by

$$\int_{\tilde{\psi}(x,0)=\tilde{\psi}_0}^{\tilde{\psi}(x,\tau)=\tilde{\psi}_f} \mathcal{D}\tilde{\psi} e^{-\tilde{S}[\tilde{\psi}]/2D}. \tag{4.46}$$

The normalization condition is then given by

$$\int \mathcal{D}\tilde{\psi}_f P_\omega[\tilde{\psi}_f](\tau) = 1. \tag{4.47}$$

As we are working in the small noise regime, the path integral in eq. (4.44) will be dominated by the paths of least action, denoted by $\tilde{\zeta}_n$. These paths are determined by the condition that they make $\tilde{S}[\tilde{\psi}]$ stationary, i.e., $\delta\tilde{S}/\delta\tilde{\psi}|_{\tilde{\zeta}} = 0$. In the steepest

descent approximation, $P_\omega(n,\tau)$ will be given by

$$P_\omega(n,\tau) \approx \frac{\mathcal{V}_n}{\sqrt{\det' L_n}} e^{-\tilde{S}_n(\tau)/2D} \tag{4.48}$$

where

$$\tilde{S}_n(\tau) \equiv \tilde{S}[\tilde{\zeta}_n], \tag{4.49}$$

and L_n is the fluctuation operator (in this case a matrix partial differential operator) associated with the second variation,

$$\delta^{(2)}\tilde{S} = \int dt \int dx \delta\tilde{\Psi}^\dagger L_n[\tilde{\zeta}]\delta\tilde{\Psi}\,,$$

of $\tilde{S}$. $\tilde{\Psi}$ is the two component vector $[\tilde{\psi}(x,t), \tilde{\psi}^*(x,t)]^T$. The prime on det indicates that any zero modes must not be included in the determinant of L_n. The factor $\mathcal{V}_n$ is a consequence of the integration over the collective coordinates associated with the zero modes.

Let us first consider the behavior of $\tilde{S}_n(\tau)$, the minimum value of $\tilde{S}$, as a function of τ. We can distinguish two regimes: the early-time regime and the late-time regime. In the early-time regime, the paths of least action $\tilde{\zeta}$ are essentially ballistic trajectories connecting $\tilde{\psi}_0$ with $\tilde{\psi}_n(\tau)$. More specifically, if $\tau \ll 1$, then $\tilde{\zeta}_n \approx (1 - t/\tau)\tilde{\psi}_0 + (t/\tau)\tilde{\psi}_n(\tau)$. In other words, in order for a path to propagate from the initial state to the final state in a short amount of time, the trajectory must be ballistic. This means that for these configurations, $\tilde{S}_n(\tau)$ is dominated by the kinetic energy of the $\tilde{\zeta}$ trajectories, and thus $\tilde{S}_n(\tau) \sim \tau^{-1}$. Thus, in the early-time regime $\tilde{S}_n(\tau) \gg D$. This means that for these times the states $\tilde{\psi}_n(\tau)$ are not appreciably occupied. Rather, the probability distribution has spread into regions of function space that do not include the initial and final states. As time progresses, however, we expect that the probability distribution will begin to accumulate about the states $\tilde{\psi}_n$. This will begin to occur in the late-time regime, characterized by those times for which $\tilde{S}_n(\tau) \ll D$. Because the system is continuously being driven, we should only consider those times τ that are smaller than $\tau_{n,\text{upper}} \equiv 2\pi n/\omega$, the time required for the phase-difference to change by $2\pi n$. The characteristic time $t_n^* \sim (\omega/\ell)^{-1/2}$ [see eq. (4.39)] provides an

estimate of the time separating the early- and late-time regimes. Notice that since $t_n^* \sim 1/\sqrt{\omega}$ and $\tau_{n,upper} \sim 1/\omega$, we have that $t_n^* \lesssim \tau_{n,upper}$. This condition implies that if a type-n process occurs, the time required for the system to make the transition is shorter than the time required for the external field to drive the system back to the Eckhaus instability.

The existence of configurations $\tilde{\zeta}_n$ for which $\tilde{S}_n[\tilde{\zeta}_n] \ll D$, can be motivated in the following way. The first ingredient in the motivation is that the dynamics of $\tilde{\psi}$ is relaxational, i.e., in the abscence of noise $\tilde{\psi}$ obeys

$$\frac{\partial \tilde{\psi}}{\partial t} = -2\frac{\delta \mathcal{F}}{\delta \tilde{\psi}^*} \tag{4.50}$$

[see eq. (4.10)]. In other words, the dynamical equation (4.50) can only take the system 'downhill' in energy. The second ingredient is the prescence of the Eckhaus instability. That is, after encountering this instability (i.e., if $Q(t) > \kappa_n$), there are unstable directions in function space with a component $e^{-iq_n x}$ (see Sec. 4.5). Thus, the dynamical equation (4.50), in spite of the abscence of a stochastic noise source, can carry the system from the unstable state, $\tilde{\psi}_0 = \sqrt{1 - Q_0(t)^2}$, to the stable state, $\tilde{\psi}_n = \sqrt{1 - Q_{-n}(t)^2}e^{-iq_n x}$. Therefore, in principle, a zero-action path can be constructed by integrating eq. (4.50) with the initial condition $\tilde{\psi}(x,0) = \tilde{\psi}_0(x)$. In practice, however, the initial condition must have a component in the unstable direction, so that $\tilde{\psi}(x,0) = \tilde{\psi}_0(x) + \epsilon\tilde{\psi}_n(x)$. The configuration $\tilde{\psi}_{n,\epsilon}(x,t)$ generated from this initial condition will not, in general, make $\tilde{S}$ stationary. However, if $\epsilon \ll 1$, then $\tilde{S}[\tilde{\psi}_{n,\epsilon}] \ll 1$, and, as $\tilde{S} \geq 0$, the configuration $\tilde{\psi}_{n,\epsilon}$ will be almost stationary. Then, if ϵ can be made small enough, $\tilde{S}[\tilde{\psi}_{n,\epsilon}]$ can be made much less than D.

The above discussion is neither rigorous, nor a proof, that in the late-time regime $\tilde{S}[\tilde{\zeta}_n] \ll D$. Rather, it is intended to simply make this notion plausible. In App. F, where a two-mode dynamical system that exhibits the crossover effect is constructed, numerical evidence is presented (see Tables F.2 and F.3) that shows that in the late-time regime the minimum value of the thermodynamic action (for the two-mode dynamical system) is much smaller than D. This result adds weight to the above

discussion.

If we accept the above arguments that in the late-time regime $\tilde{S}[\tilde{\zeta}_n] \ll D$, then we are led to the conclusion that in the late time regime $P_\omega(n,\tau) \equiv \tilde{P}_\omega(n)$ is determined entirely by the pre-exponential factor. In other words, the probability of a type-n phase slip relative to a type-m phase-slip is given by

$$\frac{\tilde{P}_\omega(n,\tau)}{\tilde{P}_\omega(m,\tau)} = \frac{\mathcal{V}_n}{\mathcal{V}_m}\sqrt{\frac{\det' L_m}{\det' L_n}}. \tag{4.51}$$

In this late time regime, we also expect that $\tilde{\psi}_n(\tau)$ are the only states which may be appreciably occupied (since $D \ll 1$), so that the normalization condition becomes

$$\sum_n \tilde{P}_\omega(n) = 1, \tag{4.52}$$

where the sum extends over those integers n for which $|Q_n(\tau)| < \kappa_1$. Equations (4.51) and (4.52) provide a complete prescription for the theoretical determination of the probability of a type-n process, as a function of the external field.

From equation (4.51) we see that the relative probability of a type-n process versus a type-m process is determined by the relative curvature of the thermodynamic action about the entire space-time paths ζ_n and ζ_m. The implication of eq. (4.51) is that if the curvature of the thermodynamic action about the entire space-time path $\tilde{\zeta}_n$ is smaller than the curvature about the path $\tilde{\zeta}_m$, i.e., $\det' L_n < \det' L_m$, then the probability of a type-n process is greater than that of a type-m process. A smaller curvature implies larger fluctuations. Thus, those paths $\tilde{\zeta}_n$ that allow fluctuations more freedom are associated with the more likely processes.

In the problem of the decay rate from a metastable state, the attempt frequency prefactor depends on the relative curvature of the free energy about the metastable state and its associated saddle-point state (see Chap. 2). In other words, it is the fluctuations about particular points in *configuration space* that are important. By contrast, in the problem of the decay from an unstable state it is the fluctuations about the *entire space-time paths* (denoted here by $\tilde{\zeta}_n$) that minimize the thermodynamic action that are important. Thus, the result for the decay from an unstable state is

analogous to the Arrhenius expression for the decay rate from a metastable if we take the barrier height in the Arrhenius expression to be zero. This is appealing because in the decay from an unstable state there is no energy barrier.

The calculation of the ratio of determinants $\det' L_m / \det' L_n$ is a formidable problem. The operators L are matrix *partial* differential operators. For such operators we know of no expression, analogous to eq. (2.66), that allows the ratio of determinants to be expressed in terms of solutions to the corresponding homogeneous equations. Therefore, I have not been able to compute the ratio of determinants that is required for the computation of eq. (4.51).

4.7 Summary

In this chapter we have investigated the dynamics of the supercurrent in a quasi-one-dimensional ring of circumference L under the influence of a static electromotive force. The electric field (associated with the emf) causes the supercurrent to increase to the critical current, at which point the system becomes locally unstable. By numerically integrating the stochastic time-dependent Ginzburg-Landau equation, we found that there is a crossover from a situation in which single phase-slip processes dominate the dynamics to a situation in which double phase-slip processes dominate.

In Sec. 4.5 we analyzed the linear stability properties of the Eckhaus instability, paying particular attention to the growth rates λ_1 and λ_2 for the mode amplitudes a_1 and a_2 that correspond to the occurence of single and double phase-slips, respectively. We found that, although the system becomes unstable with respect to fluctuations of a_1 first, λ_2 increases more rapidly with time than does λ_1. Thus, if the field is 'weak' then a_1 can grow to dominance before a_2 ever has a chance to grow. But if the field is stronger, then a_1 has less of a head start, and the fact that λ_2 increases more rapidly with time than λ_1 means that it is possible for a_2 to dominate.

The results contained in the first part of the chapter motivated us to search for a systematic approach to the problem of the decay from an unstable state when mul-

tiple metastable states compete for occupation. Using a path integral approach, we obtained a formula for the relative probability of a single phase-slip process versus a double phase-slip process. In this formula the relative probability is determined entirely by the pre-exponential factor, i.e., the ratio of determinants of fluctuation operators (which in this case are matrix *partial* differential operators). The interpretation is that it is the relative size of the fluctuations about the entire space-time paths of least action that are important.

References

[1] F. London, *Superfluids*, Vol. 1 (J. Wiley, New York, 1950).

[2] J. R. Schrieffer, *Theory of Superconductivity* (Benjamin/Cummings, Reading, MA, 1983).

[3] M. Tinkham, *Introduction to Superconductivity* (Krieger, Malabar, FL, 1980).

[4] R. Tidecks, *Current Induced Nonequilibrium Phenomena in Quasi-One-Dimensional Superconductors*, (Springer-Verlag, Berlin, 1990).

[5] See Chap. 7 of Ref. [3].

[6] In Sec. 4.3 the relationship between the field strength necessary to drive the current to the critical current and the noise strength is estimated.

[7] W. Eckhaus, *Studies in Nonlinear Stability Theory* (Springer, New York, 1965).

[8] L. Kramer and W. Zimmerman, Physica **16D**, 221 (1985).

[9] L. Kramer, H. R. Schober and W. Zimmerman, Physica D **31**, 212 (1988).

[10] L. S. Tuckerman and D. Barkley, Physica D **46**, 57 (1990).

[11] H. Riecke and H. Paap, Europhys. Lett. **14** (5), 433 (1991).

[12] E. Hernández-García, J. Viñals, R. Toral, and M. San Miguel, Phys. Rev. Lett. **70**, 3576 (1993).

[13] M. C. Cross and P. C. Hohenberg, Rev. Mod. Phys. **65**, 851 (1993).

[14] P. E. Cladis and P. Palffy-Muhoray (eds.) *Spatio-Temporal Patterns in Nonequilibrium Complex Systems* (Addison-Wesley, Reading, MA, 1995).

[15] T. J. Rieger, D. J. Scalapino, and J. E. Mercereau, Phys. Rev. B **6**, 1734 (1972).

[16] L. Kramer and A. Baratoff, Phys. Rev. Lett. **38**, 518, (1977).

[17] K. K. Likharev, JETP Lett. **20**, 338 (1974).

[18] J. S. Langer and V. Ambegaokar, Phys. Rev. **164**, 498, (1967).

[19] D. E. McCumber and B. I. Halperin, Phys. Rev. B **1**, 1054 (1970).

[20] N. G. van Kampen, *Stochastic Processes in Physics and Chemistry* (North Holland, Amsterdam, 1992).

[21] The requirement that the order parameter be single-valued results in the quantization of the supercurrent, in a manner entirely analogous to the quantization of angular momentum in quantum mechanics.

[22] C. W. Gardiner, *Handbook of Stochastic Methods for Physics, Chemistry and the Natural Sciences* (Springer-Verlag, Berlin, 1990).

[23] A. J. McKane, H. C. Luckock and A. J. Bray, Phys. Rev. A **41**, 644 (1990).

[24] L. Onsager and S. Machlup, Phys. Rev. **91**, 1505 ; *ibid.*, **91**, 1512 (1953).

[25] R. Graham, Quantum Statistics in Optics and Solid-State Physics (G. Höhler, ed.), Springer Tracts in Modern Physics, Vol. **66** (1973) 1-97.

[26] R. Graham in *Order and Fluctuations in Equilibrium and Nonequilibrium Statistical Mechanics* (G. Nicolis, G. Dewel and J. W. Turner, eds.), XVIIth International Solvay Conference on Physics (Wiley, New York, 1981).

[27] R. L. Stratonovich, Selected Translations in Mathematical Statistics and Probability, Providence, RI: Am. Math. Soc. (1972) 273.

[28] F. Moss and P. V. E. McClintock, *Noise in Nonlinear Dynamical Systems* (Cambridge University Press, 1989).

Appendix A

Overview of Superconductivity

For completeness, in this appendix a brief overview of superconductivity will be given, with an emphasis on those aspects that are relevant in this thesis. Particularly useful general references are [1, 2, 3]. In 1911, H. K. Onnes discovered that mercury, when cooled below 4.2K, loses all measurable resistance to the flow of electrical current [4]. Although the vanishing of the electrical resistance is at first sight the most striking signature of a superconductor, it is not a characteristic feature. In 1911, when Onnes discovered superconductivity, he also observed that the superconducting state could be destroyed by a sufficiently strong magnetic field, usually denoted by H_c. However, the details of the response of the superconductor to fields smaller than the critical field H_c were elusive. In 1933, W. Meissner and R. Ochsenfeld (MO) made a very important discovery [5]. They observed that if they cooled a mono-crystal of tin, immersed in a magnetic field smaller than H_c, to a temperature lower than the superconducting transition temperature, the magnetic field was expelled from the interior of the crystal. This experimental result was a clear indication that a superconductor is more than just a perfect conductor (i.e., a metal with no resistance). This can be seen by first considering the theory of electrodynamics, in which the curl of the electric field is related to the time rate of change of the magnetic field. Now, for a perfect conductor that carries no current, the electric field in the specimen must be zero, (otherwise, according to Ohm's law, an infinite current would flow). This implies that for a perfect conductor, it is only the *change* in magnetic field that is zero. But the MO

experiment showed that the magnetic field itself is zero.

The Meisser-Ochsenfeld effect goes further. It also implies that the superconducting state is a state of thermodynamic equilibrium. More specifically, if the material is first cooled below the superconducting transition temperature in the abscence of a magnetic field, and then the field is turned on, the magnetic field will be screened from the interior, as in the case of a perfect conductor. On the other hand, the same final state is achieved if the magnetic is first turned on, and then the material is cooled, in contrast to the case of a perfect conductor. This implies that regardless of the manner in which the temperature and magnetic field are changed, the final state of the system depends only on the final values of temperature and magnetic field. As we shall see, the notion that the superconducting state is a state of thermodynamic equilibrium has profound implications.

In order to explain the Meissner-Ochsenfeld effect, F. London and H. London, in 1935, developed a phenomenological theory of the electrodynamics of superconductors [6, 7]. The London's utilized the notion of two fluids (an idea originally introduced by C. Gorter and H. Casimir [8]): a 'normal-fluid' that is dissipative, i.e., it requires a constant input of energy from an external source in order to flow, and a 'superfluid' that is not dissipative, i.e., it can flow freely. According to the London theory, the perfect diamagnetism (i.e., the expulsion of the magnetic field) observed by Meissner and Ochsenfeld is a consequence of screening supercurrents that flow in a thin layer bounded by the surface of the material. As a consequence, the magnetic field penetrates only a small distance into the material. The distance of this penetration is known as the magnetic penetration depth, usually denoted by λ, the temperature dependence of which is measurable. The Londons showed that the number density n_s of the (postulated) superelectrons is inversely proportional to the magnetic penetration depth. Thus, from the measured temperature dependence of the penetration depth, they were able to deduce the temperature dependence of the superelectron density. For temperatures at, and above, the superconducting transition temperature, the density is zero, but as the temperature is reduced below the

transition temperature the number density increases continuously. We will return to this idea shortly.

In 1950, V. Ginzburg and L. Landau [9] developed a phenomenological theory of superconductivity based on Landau's general theory of continuous phase transtions [10], which was developed in 1937. The concept of an order parameter—a quantity that is zero in the disordered phase, and becomes nonzero in a continuous manner as the system orders—is central in Landau's general theory. In the ordered phase, it is sometimes useful to view the order parameter as a thermodynamic variable. Thus, from this viewpoint, the number density of superelectrons introduced in the London theory seems like a natural order parameter. However, the order parameter introduced by Ginzburg and Landau is a complex-valued function, usually denoted by Ψ, so that the *modulus squared* of the order parameter is proportional to the number density of superconducting electrons, i.e., $n_s \propto |\Psi|^2$. The idea of Ginzburg and Landau was to consider the order parameter Ψ to be an 'effective wavefunction' of the superconducting electrons, so that by analogy with quantum mechanics, it is taken to be a complex-valued function.

The theory of Ginzburg and Landau is based on an expansion of the free energy of the superconductor in powers of the square of the modulus, and the square of the gradients of the modulus, of Ψ. (The mathematical details are provided in Sec. 2.2.) The idea is that for temperatures close to the transition temperature, the number density of superconducting electrons is small compared to the number of normal electrons, so that a truncation of the power series expansion is valid. Thus, a description based on the GL theory is valid only for temperatures that are not too far below the transition temperature. In addition, if the temperature is too close to the transition, then the root-mean-square value of the fluctuations of the order parameter become of the same size as the average value of the order parameter, and the concept of a well-defined order parameter is no longer valid. The temperature that defines this upper limit is given by the Ginzburg criterion [11].

The Ginzburg-Landau theory introduces a a new characteristic length, in addition

to the magnetic penetration depth. This length, the fluctuation correlation length (also known as the temperature-dependent coherence length), usually denoted by ξ, represents the length-scale over which the order parameter can vary without an undue cost in energy. In addition, the correlation of the order parameter between two points in space decreases exponentially with the separation, with the scale of the decrease set by the correlation length. (This is the reason for the nomenclature.) Thus, ξ sets the scale of a statistically independent subunit of the system.

Using the Ginzburg-Landau theory, A. Abrikosov [12], in 1957, showed that there is an important distinction between systems for which the magnetic penetration depth is smaller than the temperature-dependent coherence length, (these are known as type-I superconductors), and systems for which the inequality is reversed (these are known as type-II superconductors). Prior to Abrikosov's work, all superconductors were believed to be of type-I. In fact, it is only for type-II superconductors ($\lambda \ll \xi$) that the London theory, which assumes a local relationship between the current and vector potential, is valid. A non-local generalization of the London theory, motivated by experimental evidence, was introduced in 1953 by A. Pippard [13]. In 1967, the flux lattice predicted by Abrikosov for type-II superconductors was observed experimentally. Abrikosov's result is important not only because of the specific insight that it provides to our understanding of the physical behaviour of superconductors, but the result also illustrates the predictive power of the GL theory, one of the pillars in the theory of superconductivity.

In the same year (1957) that Abrikosov predicted the existence of type-II superconductors, J. Bardeen, L. Cooper, and J. R. Schrieffer developed the so-called BCS theory of superconductivity [14]. The groundwork for their theory was laid by Cooper in 1956, when he showed that if two electrons, in the presence of a filled Fermi sea of electrons, interact attractively, then no matter how weak this attraction, the two electrons will form a bound state [15]. This bound state is known as a Cooper pair. Ordinarily, by virtue of their like electric charge, two electrons repel one another. However, lattice vibrations (the quanta of which are phonons) can mediate an at-

tractive interaction. The isotope effect, discovered in 1950, was used as evidence for phonon-mediated attraction. The BCS theory is based on a model Hamiltonian in which two electrons that are within roughly a Debye energy of the Fermi surface attract one another. Using the pairing concept as a guide, Schrieffer constructed a variational ground state wavefunction for this model Hamiltonian.

The BCS theory has proved remarkably successful. Not only did the theory explain known facts, but the theory also made new predictions. For example, the ratio of the energy gap (essentially the binding energy of a Cooper pair) to the transition temperature is predicted to be a universal constant, at least for the so-called weak coupling superconductors for which this ratio is not too large. This prediction was subsequently verified experimentally. Thus, the BCS theory stands as a second pillar of the theory of superconductivity.

In 1959, L. Gor'kov bridged the gap between the Ginzburg-Landau and BCS theories [16]. For temperatures close to the transition temperature, Gor'kov derived the GL theory from the BCS theory. In this thesis, our description will be based on the GL theory as it is more suited to the particular problems that we shall consider.

References

[1] J. R. Schrieffer, *Theory of Superconductivity* (Benjamin/Cummings, Reading, MA, 1983).

[2] P. G. de Gennes, *Superconductivity of Metals and Alloys* (Addison-Wesley, Redwood City, CA, 1989).

[3] M. Tinkham, *Introduction to Superconductivity* (Krieger, Malabar, FL, 1980).

[4] H. K. Onnes, Leiden Comm. **122b, 124c** (1911).

[5] W. Meissner and R. Ochsenfeld, Naturwissenschaften **21**, 787 (1933).

[6] F. London and H. London, Physica **2**, 341 (1935).

[7] F. London, *Superfluids*, Vol. I (Wiley, New York, 1950).

[8] C. J. Gorter and H. B. G. Casimir, Physica **1**, 305 (1934).

[9] V. L. Ginzburg and L. D. Landau, Sov. Phys. JETP **20**, 1064 (1950).

[10] L. D. Landau, Sov. Phys. JETP **7**, 19 (1937); *ibid.* **7**, 627 (1937).

[11] A. P. Levanyuk, Sov. Phys. JETP **36**, 571 (1959); V. L. Ginzburg, Sov. Phys. Sol. State **2** 1824 (1960); N. Goldenfeld, *Lectures on Phase Transitions and the Renormalization Group* (Addison-Wesley, Reading, MA, 1992).

[12] A. A. Abrikosov, Sov. Phys. JETP **32**, 1442 (1957).

[13] A. B. Pippard, Proc. Roy. Soc. (London) **A216**, 547 (1953).

[14] J. Bardeen, L. N. Cooper, and J. R. Schrieffer, Phys. Rev. **108**, 1175 (1957).

[15] L. N. Cooper, Phys. Rev. **104**, 1189 (1956).

[16] L. P. Gor'kov, Soviet Phys. JETP **9**, 1364 (1959).

Appendix B

Derivation of Saddle-Point Solution

In this appendix we derive the saddle-point solution ψ_s. The most straightforward approach is to begin with the expression for E given in (2.27), but with ϕ' replaced by J/f^2, so that

$$E = (f')^2 + f^2 - \frac{1}{2}f^4 + f^{-2}J^2 = 0. \tag{B.1}$$

Rearranging this expression, and defining x_0 to be the point at which f vanishes, we find that f is given by

$$\int_{f(x_0)}^{f(x)} \frac{df}{\sqrt{E - 2V(f;J)}} = x - x_0, \tag{B.2}$$

where $V(f;J) \equiv f^2/2 - f^4/4 + J^2/2f^2$. Defining $u(f) \equiv f^2$, eq. (B.2) can be written as

$$\int_{f(x_0)^2}^{f(x)^2} \frac{du}{\sqrt{u^3 - 2u^2 + 2Eu - 2J^2}} = \frac{x - x_0}{\sqrt{2}}. \tag{B.3}$$

As it now stands, f apparently depends on the four constants $J, E, x_0, f(x_0)$. Notice, however, that $f(x_0)$ and x_0 are not independent; the freedom to choose one of these will be useful in what follows. We are with the situation in which $V(f_1;J) < E < V(f_0;J)$, so that the denominator of eq. (B.3) can be written as $\sqrt{(u-a^2)(u-b^2)(u-c^2)}$, where the constants a, b, and c (see Fig. 2.2) satisfy

$$a^2 + b^2 + c^2 = 2, \tag{B.4}$$

$$a^2b^2 + a^2c^2 + b^2c^2 = 2E, \tag{B.5}$$

$$a^2b^2c^2 = 2J^2. \tag{B.6}$$

Thus, a, b, and c are completely determined by E and J. If we use our freedom to choose $f(x_0) = c$, then eq. (B.3) may be integrated to give $u(x) = f_s^2(x)$ [1]:

$$f_s^2(x) = c^2 + (b^2 - c^2)\mathrm{sn}\Big(\sqrt{\frac{a^2 - c^2}{2}}(x - x_0)|m\Big) \tag{B.7}$$

where $m \equiv (b^2 - c^2)/(a^2 - c^2)$. Thus, the parameter m, which appears naturally, can be used instead of E to characterize f. In addition, k_s, which will turn out to be the effective wavevector of ψ_s, can be used instead of J provided we make the definitions

$$a^2 \equiv u(k_s) + \frac{1}{3}m_1\Delta(k_s), \tag{B.8}$$

$$b^2 \equiv u(k_s) - \frac{2}{3}m_1\Delta(k_s), \tag{B.9}$$

$$c^2 \equiv 2k_s^2 + \frac{1}{3}m_1\Delta(k_s), \tag{B.10}$$

in which $u(q) \equiv 1 - q^2$ and $\Delta(q) \equiv 1 - 3q^2$. Combining eqs. (B.7), (B.8)-(B.10) yields the desired result, eq. (2.41), for ψ_s.

References

[1] M. Abramowitz and I. Stegun, *Handbook of Mathematical Functions* (Dover, New York, 1970), Chaps. 16 and 17.

Appendix C

Derivation of Fluctuation Rate Formula

In this appendix we discuss the derivation of the formula for the fluctuation rate. The following discussion follows the derivation given reference [1]. Other useful references are [2, 3, 4, 5]. We start by assuming that the system is described by an energy $F[\tilde{\psi}]$ [see eq. (2.13)] and exhibits metastability, i.e., F possesses both local minima and saddle-points. Furthermore, we assume that the barrier heights U (see Sec. 2.3) are much larger than the thermal energy $k_B T$, i.e., the kinetics is governed by the behavior of the metastable states. Although we present the derivation for the specific case of a superconductor, the situation is rather generic, and the following discussion also applies to many problems that exhibit metastability.

The starting point in the derivation of the general expresion for the fluctuation rates is the stochastic time-dependent Ginzburg-Landau (STDGL) equation given in eq. (2.33), which for completeness is reproduced here:

$$\frac{\partial \tilde{\psi}(x,t)}{\partial t} = -\frac{\delta \mathcal{F}[\tilde{\psi}]}{\delta \psi^*(x,t)} + \tilde{\eta}(x,t), \tag{C.1}$$

where $\mathcal{F}$ is given in Sec. 2.2. (Throughout this appendix, the notation of Chap. 2 will be used.) The topography of the free-energy is such that $\mathcal{F}$ possesses two types of stationary points: (i) metastable points, i.e., locally stable; and (ii) saddle-points, i.e., unstable in one direction in function space, (a direction that is sometimes referred to as the reaction coordinate). The system spends most of the time in the neighborhood of of a metastable state. However, as a consequence of the interaction with the thermal bath, (improbable) fluctuations occur that carry the system into another

metastable state. The most probable route for such a transition passes through the saddle-point. Consequently, if one considers a nonequilibrium steady-state ensemble of systems, the fluctuation rate can be computed by calculating the probability flux through the saddle-point. The flux is computed by (functionally) integrating the probability current, in the direction of the reaction coordinate, over all directions in function space perpendicular to the reaction coordinate.

The first step in determining the probability flux through the saddle-point is to convert from the Langevin description of eq. (C.1), to the Fokker-Planck equation for $P[\tilde{\psi}]$:

$$\frac{\partial P}{\partial t} = \frac{\delta}{\delta \tilde{\psi}}\left[\frac{\delta \mathcal{F}}{\delta \tilde{\psi}} P + D\frac{\delta P}{\delta \tilde{\psi}}\right]. \tag{C.2}$$

This equation is in the form of a continuity equation for P, thus the bracketed term on the right-hand-side is interpreted as the probability current. We are interested in the probability flux which flows through the saddle-point. It is therefore convenient to make a coordinate transformation from $\tilde{\psi}$ to principal-axis coordinates (denoted by c_n) having their origin at the saddle-point state $\tilde{\psi}_s$. Thus, we can write

$$\tilde{\psi} = \tilde{\psi}_s + \sum_{n\geq 0} c_n(t)\zeta_{sn}(x), \tag{C.3}$$

where the normal modes ζ_{sn} are the eigenfunctions (with associated eigenvalues $\{\lambda_{sn}\}$ arranged in increasing order) of the fluctuation operator L_s, associated with the second variation of $\mathcal{F}$ about state $\tilde{\psi}_s$ [see eq. (2.62)]. As L_s is Hermitian, the ζ_{sn} form a complete set of orthogonal functions. Due to the fact that $\tilde{\psi}_s$ is a saddle-point, λ_{s0} is negative, i.e., ζ_0 is the reaction coordinate. In addition, due to the translational and global phase symmetries of the free energy, there are two zero-modes, ζ_1 and ζ_2, i.e., $\lambda_{s1} = \lambda_{s2} = 0$.

As the transformation from the $\tilde{\psi}$ coordinates to the c_n coordinates is orthogonal (see previous paragraph), the component of the probability current in the c_n direction is given by

$$\mathcal{J}_n = \frac{\partial \mathcal{F}}{\partial c_n} P + D\frac{\partial P}{\partial c_n};\ n \geq 0, \tag{C.4}$$

where D is the strength of the noise source [see eq. (2.32)]. We now assume that the probability current only flows in the c_0 (i.e., unstable) direction, so that $\mathcal{J}_1 \neq 0$, while all other components vanish. (Our convention is that moving in the negative c_0 direction will return the system to the original metastable state, i.e., $\mathcal{J}_0$ is positive.) We can therefore determine P in terms of $\mathcal{J}_0$ by solving eq. (C.4) with $n = 0$, with the result that

$$P = -D^{-1}\mathcal{J}_0 e^{-\mathcal{F}/D}\int_0^{c_0} dc\, e^{\mathcal{F}/D}, \tag{C.5}$$

$$= -D^{-1}\mathcal{J}_0 e^{-\mathcal{F}/D}\int_0^{c_0} dc\, \exp\left[(\mathcal{F}_s + \frac{1}{2}\sum_{n\geq 0}\lambda_{sn}c_n^2)/D\right], \tag{C.6}$$

where in obtaining the second line in eq. (C.6) we have expanded the free energy appearing in the integrand, viz., $\mathcal{F} \approx \mathcal{F}_s + (1/2)\sum_{n\geq 0} c_n\lambda_{sn}^2$, where $\mathcal{F}_s$ is the dimensionless free energy of the saddle-point state. This expansion is justified because $D \ll 1$. Our expression for P given in eq. (C.6) must also satisfy eq. (C.4) for values of n other than zero. Therefore, we must have that

$$\mathcal{J}_0 = \mathcal{N}\exp\left[(\mathcal{F}_s + \frac{1}{2}\sum_{n\geq 1}\lambda_{sn}c_n^2)/D\right], \tag{C.7}$$

where $\mathcal{N}$ is a normalization constant which will be determined by the requirement that the probability P be normalized to unity. Notice that in the exponent of eq. (C.7), the sum does not include $n = 0$; this is a consequence of our steady state assumption $\partial P/\partial t = -\partial\mathcal{J}_0/\partial c_0 = 0$, i.e., $\mathcal{J}_0$ must be independent of c_0. Inserting eq. (C.7) into eq. (C.6), we see that P can be written as

$$P = -D^{-1}\mathcal{N}e^{-\mathcal{F}/D}\int_0^{c_0} dc\, \exp[(2D)^{-1}\lambda_{s0}c_0^2] \tag{C.8}$$

The dominant contribution to the normalization will come from the neighborhood of the metastable state (since $D \ll 1$). Thus, for the purposes of computing $\mathcal{N}$, we can expand $\mathcal{F}$ appearing in eq. (C.8) about the metastable state, i.e., $\mathcal{F} \approx \mathcal{F}_m + (1/2)\sum_{n\geq 1}\lambda_{mn}b_n^2$, where λ_{mn}; $n \geq 1$ are the eigenvalues of L_m, b_m are the principal-axis coordinates, and $\mathcal{F}_m$ is the free energy of the saddle-point state. Then setting

$c_0 = -\infty$, we get

$$\int \prod_{n\geq 1} db_n \, P \approx D^{-1}\mathcal{N}\mathcal{V}_m^1 \left[\frac{D\pi}{2\lambda_{s0}}\right]^{1/2} \prod_{n\geq 1} \left[\frac{2D\pi}{\lambda_{mn}}\right]^{1/2}, \tag{C.9}$$

where the 'volume factor'

$$\mathcal{V}_m^1 \equiv \int db_1. \tag{C.10}$$

is a consequence of the integration over b_1, the coordinate associated with the zero eigenvalue λ_{m1}. (The calculation of this quantity will be discussed below.) Equating (C.9) to unity gives $\mathcal{N}$. The probability current given in eq. (C.7) is thus completely determined, allowing us to calculate the fluctuation rate $\ell\Gamma$, given by the flux of probability in the direction of the reaction coordinate, i.e.,

$$\ell\Gamma = \int \prod_{n>0} dc_n \, \mathcal{J}_0. \tag{C.11}$$

Utilizing the results of eqs. (C.7) and (C.9), the integrals in eq. (C.11) can be performed, giving

$$\ell\Gamma = \frac{\mathcal{V}_s^1 \mathcal{V}_s^2}{\mathcal{V}_m^1} |\lambda_{s0}| \frac{\det' L_m}{\det' L_s} e^{-(\mathcal{F}_s - \mathcal{F}_m)/D}, \tag{C.12}$$

where

$$\frac{\det' L_m}{\det' L_s} \equiv \frac{\prod_{n=2}^{\infty} \lambda_{mn}}{\prod_{n=3}^{\infty} \lambda_{sn}}, \tag{C.13}$$

and

$$\mathcal{V}_s^n \equiv \int dc_n; \; n = 1, 2 \tag{C.14}$$

are the 'volume' factors associated with the translational and global phase symmetries of $\mathcal{F}$. Finally, due to the fact that t is measured in units of τ_{GL}, eq. (C.12) must be multiplied by τ_{GL}^{-1}. Equation (C.12) is the same as eq. (2.36) of Ref. [5].

The volume factors given in eqs. (C.10) and (C.14) are computed in the following way. As the computation of the $\mathcal{V}_s^n$ factors proceeds along precisely the same lines as that of the $\mathcal{V}_m^1$ factor, it is sufficient to focus on $\mathcal{V}_m^1$. The zero mode responsible for this factor is a consequence of the global phase symmetry of $\mathcal{F}$, which is manifested by the fact that $\partial\psi_m/\partial\phi_{m,0}$ is an eigenvector of L_m with zero eigenvalue. We therefore

expect that the variations in the coordinate b_1 are related to variations in $\phi_{m,0}$. To establish this relationship, we first expand ψ about ψ_m:

$$\psi = \psi_m + \sum_{n\geq 1} b_n \zeta_{mn}, \tag{C.15}$$

where ζ_{mn} are the normalized eigenvectors of L_m, and ψ_m is given in eq. (2.35). Thus, a variation of ψ in the b_1 direction can be written as

$$\delta\psi_1 = db_1 \zeta_{m1}. \tag{C.16}$$

On the other hand, the variation $\delta\psi_\phi$, a consequence of altering $\phi_{m,0}$ by $\Delta\phi_{m,0}$, is given by

$$\delta\psi_\phi = \Delta\phi_{m,0} \frac{\partial\psi_m}{\partial\phi_{m,0}}. \tag{C.17}$$

If we equate eq. (C.16) and eq. (C.17), and use the fact that $\zeta_{m1} = \partial\psi_m/\partial\phi_{m,0}/\mathcal{N}_m$, where $\mathcal{N}_m \equiv \int dx\, |\partial\psi_m/\partial\phi_{m,0}|^2$, we get

$$db_1 = \mathcal{N}_m \Delta\phi_{m,0}. \tag{C.18}$$

The integration over b_1 in eq. (C.10) can thus be converted to an integration over $\phi_{m,0}$, which extends from 0 to 2π, thus giving

$$\mathcal{V}_m^1 = \mathcal{N}_m 2\pi. \tag{C.19}$$

The factors $\mathcal{V}_s^1$ and $\mathcal{V}_s^2$ can be computed in a similar manner, with the results that

$$\mathcal{V}_s^1 = \mathcal{N}_s^1 2\pi, \tag{C.20}$$

$$\mathcal{V}_s^2 = \mathcal{N}_s^1 \ell, \tag{C.21}$$

where $\mathcal{N}_s^1 \equiv \int dx\, |\partial\psi_s/\partial\phi_{s,0}|^2$, and $\mathcal{N}_s^2 \equiv \int dx\, |\partial\psi_s/\partial x_0|^2$, and ψ_s is given in eq. (2.41).

References

[1] J. S. Langer, *Phys. Rev. Lett.* **21**, 973 (1968).

[2] R. Landauer and J. A. Swanson, *Phys. Rev.* **121**, 1668 (1961);

[3] J. S. Langer, *Ann. Phys.* (NY), **41** 108 (1967).

[4] J. S. Langer, *Ann. Phys.* (NY) **54**, 258 (1969).

[5] D. McCumber and B. Halperin, *Phys. Rev.* B1, 1054 (1970).

Appendix D

Regularization via Operator Perturbation

In this appendix I will describe the perturbation procedure devised in order to compute the ratio $R' \equiv \det' L_s / \det' L_m$, which arises in the computation of the fluctuation rate [see eqs. (2.34), (2.62), and (2.61)]. The primes indicate that zero modes are not included in the determinant. The computation uses, as its basis, Forman's equation [1]:

$$R \equiv \frac{\det L_s}{\det L_m} = \frac{\det\left[M + NY_s(\ell/2)\right]}{\det\left[M + NY_m(\ell/2)\right]}, \tag{D.1}$$

for the quotient of determinants R, including *all* eigenvalues. In eq. (D.1), the M and N matrices encode the twisted periodic boundary conditions for ψ and ψ' given in (2.22) and (2.25). These matrices are not unique, but a convenient choice is

$$-M = \begin{bmatrix} e^{i\Phi} & 0 & 0 & 0 \\ 0 & e^{-i\Phi} & 0 & 0 \\ 0 & 0 & e^{i\Phi} & 0 \\ 0 & 0 & 0 & e^{-i\Phi} \end{bmatrix}, \quad N = \begin{bmatrix} 1 & 0 & 0 & 0 \\ 0 & 1 & 0 & 0 \\ 0 & 0 & 1 & 0 \\ 0 & 0 & 0 & 1 \end{bmatrix}. \tag{D.2}$$

In Forman's notation the boundary conditions given in eqs. (2.22) and (2.25) are written in the form

$$M \begin{bmatrix} \Psi(-\ell/2) \\ \Psi'(-\ell/2) \end{bmatrix} + N \begin{bmatrix} \Psi(\ell/2) \\ \Psi'(\ell/2) \end{bmatrix} = \begin{bmatrix} \underline{0} \\ \underline{0} \end{bmatrix}, \tag{D.3}$$

where $\Psi(x) \equiv [\psi(x), \psi^*(x)]^T$, and $\underline{0} \equiv [0,0]^T$. The Y_e matrix is the so-called fundamental matrix, and is defined to have the property that, for any (complex two-component) solution $\zeta_e(x)$ of the so-called Jacobi accessory equation (i.e., the homo-

geneous equation $L_e\,\zeta_e = 0$), one has

$$\begin{bmatrix} \zeta_e(x) \\ \zeta_e'(x) \end{bmatrix} = Y_e(x) \begin{bmatrix} \zeta_e(-\ell/2) \\ \zeta_e'(-\ell/2) \end{bmatrix}, \tag{D.4}$$

where the prime denotes differentiation with respect to x. Notice that, by definition, $Y_e(-\ell/2)$ is the (4×4) identity matrix. The computation of Y_e is at the heart of the calculation of R, and hence R'. The prescription for constructing Y_e is as follows. First construct an auxiliary matrix $H_e(x)$, in which the ith column of H_e is the vector $[\eta_{e,i}, \partial_x \eta_{e,i}]^T$, where $\{\eta_{e,i}\}_{i=1}^4$ is a set of linearly independent solutions to the Jacobi accessory equation. Then Y_e is given by

$$Y_e(x) = H_e(x) H_e^{-1}(-\ell/2). \tag{D.5}$$

Thus, the computation of R has been reduced to the problem of finding the sets $\{\eta_{e,i}\}_{i=1}^4$ of linearly independent solutions of the accessory equation.

The source of the difficulty in computing the fluctuation rate $\ell\Gamma$ (see eq. (2.64)), is that, due to the presence of zero modes, we cannot directly apply Forman's equation (D.1) (see Sec. 2.7). More specifically, one or more of the $\eta_{e,i}$ satisfies the boundary conditions defined by M and N; these solutions are therefore eigenvectors of L_e with an eigenvalue of zero. It is these solutions that are responsible for the vanishing of $\det L_e$. A regularization procedure is therefore required in order that we may compute $R' \equiv \det' L_s / \det' L_m$. The procedure to be presented in this appendix uses Forman's equation (D.1) as its basis.

The regularization procedure consists of perturbing the operators $L_e(k_e)$ by transforming the wavevector $k_e \to \tilde{k}_e \equiv k_e + \delta k_e$, but leaving the boundary conditions fixed. Thus, under this transformation, $L_e(k_e) \to L_e(\tilde{k}_e) \equiv \tilde{L}_e$. The homogenous solutions will then be characterized by $\tilde{k}_e$, but the boundary conditions, not having been altered by the regularization, will still only depend on k_e. Thus, the culprit homogenous solution (i.e., the zero mode) will no longer satisfy the boundary conditions, and hence will no longer be an eigenfunction. Therefore, what were once zero eigenvalues, will now become nonzero with a size proportional to the strength δk_e of the perturbation.

If $\delta k_e \ll 1$, these pseudo-zero eigenvalues can be calculated using standard first-order perturbation theory.

If we denote by d_e ($d_m = 1$, and $d_s = 2$) the degeneracy of the zero modes of L_e then we expect that for $\delta k_e \ll 1$ we shall find $\det\tilde{L}_e \propto (\delta k_e)^{d_e}$. At the same time, the pseudo-zero eigenvalues, denoted by $\tilde{\lambda}_{e,i}$; $i = 1, d_e$, will each be proportional to δk_e. In this notation, R' is given by

$$R' = \lim_{\delta k_e \to 0} \frac{\prod_{i=1}^{d_m} \tilde{\lambda}_{m,i}}{\det \tilde{L}_m} \frac{\det \tilde{L}_s}{\prod_{j=1}^{d_s} \tilde{\lambda}_{s,j}}. \tag{D.6}$$

We can now use Forman's equation (D.1) to compute $\det \tilde{L}_s / \det \tilde{L}_m$, so that

$$R' = \lim_{\delta k_e \to 0} \frac{\prod_{i=1}^{d_m} \lambda_{m,i}}{\prod_{j=1}^{d_s} \tilde{\lambda}_{s,j}} \frac{\det\left[M + N\tilde{Y}_s(\ell/2)\right]}{\det\left[M + N\tilde{Y}_m(\ell/2)\right]}. \tag{D.7}$$

The computation of R' using eq. (D.7) requires that we construct the fundamental matrix $\tilde{Y}_e$ for the perturbed operators $\tilde{L}_e$. However, as will be shown explicitly, since the analytic dependence of the $\eta_{e,i}$ on k_e is known, construction of $\tilde{Y}_e$ is trivial once Y_e has been determined. Thus, the utility of this regularization scheme depends on knowing the explicit form for the $\eta_{e,i}$. In the following two subsections I will show how the above strategy is implemented, first for L_m, which is the simpler (and hence more transparent) of the two cases, and then for L_s.

D.1 $\det' L_m$

The first step is to construct the auxiliary matrix $H_m(x)$ from a set of four linearly independent solutions (denoted by $\{\eta_{m,i}\}_{i=1}^4$), and their derivatives with respect to x, of the accessory equation $L_m\eta = 0$. In this case it is straightforward to solve the accessory equation, with the result that

$$\eta_{m,1}(x) = \begin{bmatrix} i\exp(ikx) \\ -i\exp(-ikx) \end{bmatrix}, \tag{D.8}$$

$$\eta_{m,2}(x) = \begin{bmatrix} (-k+iu(k)x)\exp(ikx) \\ (-k-iu(k)x)\exp(-ikx) \end{bmatrix}, \tag{D.9}$$

$$\eta_{m,3}(x) = \begin{bmatrix} (2\omega\cosh(2\omega x) - i2k\sinh(2\omega x))\exp(ikx) \\ (2\omega\cosh(2\omega x) + i2k\sinh(\omega x))\exp(-ikx) \end{bmatrix}, \tag{D.10}$$

$$\eta_{m,4}(x) = \begin{bmatrix} (2\omega\sinh(2\omega x) - i2k\cosh(2\omega x))\exp(ikx) \\ (2\omega\sinh(2\omega x) + i2k\cosh(2\omega x))\exp(-ikx) \end{bmatrix}, \tag{D.11}$$

where $u(q) \equiv 1-q^2$, $\omega = \omega(k) \equiv \sqrt{\Delta(k)/2}$, and for notational convenience $k = k_m$. Notice that $\eta_{m,i}$ depends only on the constant k; the constant $\phi_{m,0}$ has been set to 0. Also, $[\eta_{m,1}, \eta'_{m,1}]^T$ is the only solution that satisfies the boundary condition (D.3). Thus, as expected, L_m has a single zero mode $\eta_{m,1}$, so that d_m is indeed unity.

The choice of the $\eta_{m,i}$ is not unique. The above form is particulary convenient in that the factors which multiply the exponentials can be written as the sum of symmetric functions ($\sigma_{m,i}(x)$ and $\sigma'_{m,i}(x)$) and antisymmetric functions ($\alpha_{m,i}(x)$ and $\alpha'_{m,i}(x)$), so that

$$\eta_{m,i}(x) = \begin{bmatrix} (\alpha_{m,i}(x)+\sigma_{m,i}(x))\exp(ikx) \\ (\alpha^*_{m,i}(x)+\sigma^*_{m,i}(x))\exp(-ikx) \end{bmatrix}, \tag{D.12}$$

$$\eta'_{m,i}(x) = \begin{bmatrix} (\alpha'_{m,i}(x)+\sigma'_{m,i}(x))\exp(ikx) \\ (\alpha'^*_{m,i}(x)+\sigma'^*_{m,i}(x))\exp(-ikx) \end{bmatrix}. \tag{D.13}$$

Using the symmetry/antisymmetry properties of $\eta_{m,i}$, and eq. (D.5), we can write $Y_m(\ell/2)$ as

$$Y_{m,1j}(\ell/2) = \delta_{1j}e^{ik\ell} + 2e^{ik\ell/2}\sum_{i=1}^{4}\alpha_{m,i}(\ell/2)H^{-1}_{m,ij}(-\ell/2), \tag{D.14}$$

$$Y_{m,2j}(\ell/2) = \delta_{2j}e^{-ik\ell} + 2e^{-ik\ell/2}\sum_{i=1}^{4}\alpha^*_{m,i}(\ell/2)H^{-1}_{m,ij}(-\ell/2), \tag{D.15}$$

$$Y_{m,3j}(\ell/2) = \delta_{3j}e^{ik\ell} + 2e^{ik\ell/2}\sum_{i=1}^{4}\alpha'_{m,i}(\ell/2)H^{-1}_{m,ij}(-\ell/2), \tag{D.16}$$

$$Y_{m,4j}(\ell/2) = \delta_{4j}e^{-ik\ell} + 2e^{-ik\ell/2}\sum_{i=1}^{4}\alpha'^*_{m,i}(\ell/2)H^{-1}_{m,ij}(-\ell/2), \tag{D.17}$$

where δ_{ij} is the Kronecker symbol, and $Y_{m,ij}$ is the (i,j) element of Y_m. This form for $Y_m(\ell/2)$ is useful because it is readily seen that the first term in each of the above expressions yields $-M$. Thus, $\det[M + NY_m(\ell/2)]$ is given by the determinant of the matrix formed from the second terms in eq. (D.14); that this determinant is zero can be readily deduced by inserting the explicit forms for the $\alpha_{m,i}$ and $\alpha'_{m,i}$ into (D.14), and performing elementary row additions, which preserve the determinant.

We now turn to the issue of regularization, which, as we have just seen, is borne out of necessity. As described above, the regularization consists of transforming $k \to \tilde{k} \equiv k + \delta k$ in Y_m but keeping the matrix $M = diag\{e^{ik\ell}, e^{-ik\ell}, e^{ik\ell}, e^{-ik\ell}\}$ fixed. In other words, we are regularizing the *operator* keeping the ***boundary conditions*** fixed. Replacing k by $\tilde{k}$ in eq. (D.14), and expanding to $\mathcal{O}(\delta k)$, we find:

$$\left[M + N\tilde{Y}_m(\ell/2)\right]_{1j} = \epsilon_{m,1j} + 2e^{ik\ell/2}\sum_{i=1}^{4}\alpha_{m,i}(\ell/2)H^{-1}_{m,ij}(-\ell/2), \qquad \text{(D.18)}$$

$$\left[M + N\tilde{Y}_m(\ell/2)\right]_{2j} = \epsilon_{m,2j} + 2e^{-ik\ell/2}\sum_{i=1}^{4}\alpha^{*}_{m,i}(\ell/2)H^{-1}_{m,ij}(-\ell/2), \qquad \text{(D.19)}$$

$$[M + N\tilde{Y}_m(\ell/2)]_{3j} = \epsilon_{m,3j} + 2e^{ik\ell/2}\sum_{i=1}^{4}\alpha'_{m,i}(\ell/2)H^{-1}_{m,ij}(-\ell/2), \qquad \text{(D.20)}$$

$$[M + N\tilde{Y}_m(\ell/2)]_{4j} = \epsilon_{m,4j} + 2e^{-ik\ell/2}\sum_{i=1}^{4}\alpha'^{*}_{m,i}(\ell/2)H^{-1}_{m,ij}(-\ell/2), \qquad \text{(D.21)}$$

where $\epsilon_{m,ij} = \delta k\,\delta_{ij}[\exp i(k\ell/2 + \pi)]^{i+1}$. In eqs. (D.18)-(D.21), the second terms in the right-hand-sides can be evaluated at k, rather than $\tilde{k}$; evaluating these terms at $\tilde{k}$ will introduce corrections to $\det[M + N\tilde{Y}_m(\ell/2)]$ which are of order δk^2, and will not contribute when we take the limit $\delta k \to 0$. Using eqs. (D.18)-(D.21), and undertaking some algebra, it is found, to leading order in δk, that

$$\det[M + NY'_m(\ell/2)] = -8\,\delta k\,k\,u(k)\,\Delta^{-1}(k)\,[\ell\sinh(\omega(k)\ell)]^2. \qquad \text{(D.22)}$$

The next task is to calculate the formerly-zero eigenvalue $\tilde{\lambda}_{m,1}$. As $\delta k \ll 1$ we have that $\tilde{L}_m \approx L_m(k) + \delta k(\partial L_m(k)/\partial k)$, and so $\tilde{\lambda}_{m,1}$ can be calculated using standard first-order perturbation theory, i.e.,

$$\langle 1|1\rangle\tilde{\lambda}_{m,1} = \delta k\,\langle 1|\partial L_m/\partial k|1\rangle,$$

$$= -\delta k\, 4k\ell, \tag{D.23}$$

where $\langle x|1\rangle \equiv \eta_{m,i}(x)$, and $\langle\cdot|\cdot\rangle$ denotes inner product, e.g.

$$\langle 1|1\rangle = \int_{-\ell/2}^{\ell/2} dx\, \eta_{m,1}^{\dagger}(x)\, \eta_{m,1}(x), \tag{D.24}$$

with $\eta_{m,1}^{\dagger} \equiv [\eta_{m,1}^{*}, \eta_{m,1}]$. Dividing eq. (D.22) by eq. (D.23) we finally obtain

$$\lim_{\delta k \to 0} \frac{\det[M + NY_m'(\ell/2)]}{\lambda_{m,1}} = 2\langle 1|1\rangle u(k)\Delta^{-1}(k)\ell \sinh^2(\omega(k)\ell). \tag{D.25}$$

To complete the calculation we must compute $\mathcal{V}_m^1$, the factor that results from integrating over the collective coordinate associated with the gauge symmetry. In appendix C it is shown that

$$\mathcal{V}_m^1 = 2\pi\langle 1|1\rangle. \tag{D.26}$$

Combining eqs. (D.25) and (D.26) we finally obtain the result that

$$\frac{|\det' L_m|^{1/2}}{\mathcal{V}_m^{(1)}} = \pi^{-1} u(k)\Delta^{-1}(k)\ell \sinh^2(\omega(k)\ell). \tag{D.27}$$

We must now turn our attention to the computation of $\det' L_s$.

D.2 $\det' L_s$

As for the metastable states, the first step is to find a linearly independent set of solutions $\{\eta_{s,i}\}_{i=1}^{4}$ to the homogeneous equation $L_s\eta = 0$. Then the i^{th} column of the auxiliary matrix is given by the (four-component) vector $[\eta_{s,i}, \eta_{s,i}']^T$, the prime as usual denoting differentation with respect to x. Whereas it was straightforward to find a set $\{\eta_{m,i}\}$, the same is not true for $\{\eta_{s,i}\}$. However, this problem is greatly facilitated, in fact becoming algorithmic, by Jacobi's theorem [2]. (See also Chap. 3 for a specific example). This theorem states that a linearly independent set of solutions to the homogeneous equation $L_s[\psi_s]\eta = 0$ can be obtained by computing the derivatives of ψ_s [c.f. eq. [2.41)] with respect to the constants of integration $(k_s, m, x_0, \phi_{s,0})$. Hereafter, for notational simplicity, $k_s \equiv k$. Rather than differentiate with respect

to k, it is more convenient to differentiate with respect to $\omega(k) \equiv \omega$. The linearly independent set of solutions is taken to be: $\eta_{s,1} \equiv -\partial_{x_0}\psi_s$, $\eta_{s,2} \equiv \partial_{\phi_{s,0}}\psi_s$, $\eta_{s,3} \equiv \partial_m\psi_s$, and $\eta_{s,4} \equiv \partial_\omega\psi_s$. As the final result is independent of the quantities $x_{s,0}$ and $\phi_{s,0}$, they can be set to zero once the corresponding η's have been computed. With these definitions, $\eta_{s,1}$ and $\eta_{s,2}$ are the zero modes (i.e., $d_s = 2$). This can be checked explicitly, or else it can be deduced from the fact that $\mathcal{F}[\psi_s]$ is independent of both x_0 and $\phi_{s,0}$; this independence represents the symmetries of translation and gauge-invariance. Although it is possible to write down the explicit forms for the $\eta_{s,i}$, it is more efficient to proceed by defining, as in the case of $\eta_{m,i}$, symmetric functions ($\sigma_{s,i}(x)$ and $\sigma'_{s,i}(x)$) and antisymmetric functions ($\alpha_{s,i}(x)$ and $\alpha'_{s,i}(x)$) so that

$$\eta_{s,i}(x) = \begin{bmatrix} (\alpha_{s,i}(x) + \sigma_{s,i}(x)) \exp i\phi_s(x) \\ (\alpha^*_{s,i}(x) + \sigma^*_{s,i}(x)) \exp -i\phi_s(x) \end{bmatrix}, \tag{D.28}$$

$$\eta'_{s,i}(x) = \begin{bmatrix} (\alpha'_{s,i}(x) + \sigma'_{s,i}(x)) \exp i\phi_s(x) \\ (\alpha'^*_{s,i}(x) + \sigma'^*_{s,i}(x)) \exp -i\phi_s(x) \end{bmatrix}. \tag{D.29}$$

The symmetric and antisymmetric functions can be identified from the fact that $f_s, f_s^m, f_s^\omega, \phi'_s, \phi_s^\omega, \phi_s'^m$ are symmetric, and $f'_s, f_s'^m, f_s'^\omega, \phi_s, \phi_s^m, \phi_s^\omega$ are antisymmetric. In this notation, the superscript denotes partial differential, e.g., $f_s^m \equiv \partial f_s/\partial_m$.

By exploiting the symmetry and antisymmetry properties of the $\eta_{s,i}$, and using eq. (D.5), the fundamental matrix $Y_s((\ell/2)$ can be written in the form

$$Y_{s,1j}(\ell/2) = \delta_{1j}e^{i\Delta\phi_s} + 2e^{i\phi_s(\ell/2)}\sum_{i=1}^{4}\alpha_{s,i}(\ell/2)H^{-1}_{s,ij}(-\ell/2), \tag{D.30}$$

$$Y_{s,2j}(\ell/2) = \delta_{2j}e^{-i\Delta\phi_s} + 2e^{-i\phi_s(\ell/2)}\sum_{i=1}^{4}\alpha^*_{s,i}(\ell/2)H^{-1}_{s,ij}(-\ell/2), \tag{D.31}$$

$$Y_{s,3j}(\ell/2) = \delta_{3j}e^{i\Delta\phi_s} + 2e^{i\phi_s(\ell/2)}\sum_{i=1}^{4}\alpha'_{s,i}(\ell/2)H^{-1}_{s,ij}(-\ell/2), \tag{D.32}$$

$$Y_{s,4j}(\ell/2) = \delta_{4j}e^{-i\Delta\phi_s} + 2e^{-i\phi_s(\ell/2)}\sum_{i=1}^{4}\alpha'^*_{s,i}(\ell/2)H^{-1}_{s,ij}(-\ell/2), \tag{D.33}$$

where $\Delta\phi_s \equiv \phi_s(\ell/2) - \phi_s(-\ell/2)$. Notice, that as was the case for $Y_m(\ell/2)$, it is only the antisymmetric functions $\alpha_{s,i}$ and $\alpha'_{s,i}$ that enter into the expression for $Y_s(\ell/2)$.

In addition, the first term in each of the four above expressions is seen to equal to $-M$. Thus, $\det[M + NY_s(\ell/2)]$ is given by the determinant of the second terms of eqs. (D.30)-(D.33); that this determinant is zero can be readily deduced by performing elementary row additions, which preserve the determinant.

We now turn to the regularization, which is carried out by transforming $\omega \to \omega + \delta\omega \equiv \tilde{\omega}$ in Y_s (but not in M). In the introductory section of this appendix, the regularization was described as consisting of transforming k_s; the transformation of ω is equivalent because ω depends only on k_s, and not on any of the other three constants m, x_0, or $\phi_{s,0}$ Transforming $\omega \to \tilde{\omega}$, and retaining terms to leading order in $\delta\omega$, we find

$$[M + NY_s'(\ell/2)]_{1j} = \epsilon_{1j} + 2e^{i\phi_s(\ell/2)} \sum_{i=1}^{4} \alpha_{s,i}(\ell/2) H^{-1}_{s,ij}(-\ell/2), \qquad \text{(D.34)}$$

$$[M + NY_s'(\ell/2)]_{2j} = \epsilon_{2j} + 2e^{-i\phi_s(\ell/2)} \sum_{i=1}^{4} \alpha^*_{s,i}(\ell/2) H^{-1}_{s,ij}(-\ell/2), \qquad \text{(D.35)}$$

$$[M + NY_s'(\ell/2)]_{3j} = \epsilon_{3j} + 2e^{i\phi_s(\ell/2)} \sum_{i=1}^{4} \alpha'_{s,i}(\ell/2) H^{-1}_{s,ij}(-\ell/2), \qquad \text{(D.36)}$$

$$[M + NY_s'(\ell/2)]_{4j} = \epsilon_{4j} + 2e^{-i\phi_s(\ell/2)} \sum_{i=1}^{4} \alpha'^*_{s,i}(\ell/2) H^{-1}_{s,ij}(-\ell/2), \qquad \text{(D.37)}$$

where $\epsilon_{s,ij} = \delta_{ij}\delta\omega\Delta\phi_s^\omega[\exp\sqrt{-1}(\phi_s(\ell/2)+\pi)]^{i+1}$ and $\Delta\phi_s^\omega \equiv \partial_\omega(\phi_s(\ell/2) - \phi_s(-\ell/2))$. Using eqs. (D.34)-(D.37) and certain properties of elliptic functions we find

$$\begin{aligned}\det[M + NY_s'(\ell/2)] &= 4\delta\omega^2 \left\{ \frac{4f_s'^2 f_s^2 - (\Delta\phi_s^\omega)^2(f_s^4 - f_s^6 - J_s^2) - 4f_s'\Delta\phi_s^\omega f_s J_s}{f_s^4 - f_s^6 - J_s^2} \right\}\Bigg|_{\ell/2} \\ &\quad \times \frac{(f_s'^\omega \phi_s^m - f_s'^m \phi_s^\omega)}{(\phi_s'^\omega f_s^m - \phi_s'^m f_s^\omega)}\Bigg|_{\ell/2} \\ &= -\delta\omega^2 \frac{128}{9} \frac{[1 - u(k)K(m)]^2[\Delta(k) - (1+3k^2)u(k)K(m)]}{[k\,u(k)\,\Delta(k)]^2} \qquad \text{(D.38)}\end{aligned}$$

where $J_s = k\,u(k)$ is the (dimensionless) space independent supercurrent of the saddle-point state, and $K(m)$ is the complete elliptic integral of the first kind. The first line of eq. (D.38) is generally valid, and the second line is obtained by ignoring terms of order m_1 in all terms except $K(m)$, which diverges logarithmically as $m_1 \to 0$.

The next step is to compute the product of the eigenvalues $\tilde{\lambda}_{s,1}$ and $\tilde{\lambda}_{s,2}$. In this case, as we have a two-fold degeneracy ($d_s = 2$) we must use first order degenerate perturbation theory, so that

$$\tilde{\lambda}_{s,1}\tilde{\lambda}_{s,2} = \delta\omega^2 \frac{L^1_{s,11}L^1_{s,22} - (L^1_{s,12})^2}{\langle 1|1\rangle\langle 2|2\rangle} \tag{D.39}$$

where $\langle x|i\rangle \equiv \eta_{s,i}$, and $L^1_{s,ij} \equiv \langle i|\partial L_s/\partial\omega|j\rangle$. The computation of the product $\tilde{\lambda}_{s,1}\tilde{\lambda}_{s,2}$ given in eq. (D.39) is rather tedious, and after a significant amount of algebraic manipulation it is found, to leading order in m_1, that

$$\prod_{i=1}^{2}\langle i|i\rangle\tilde{\lambda}_{s,i} = -\delta\omega^2 m_1^2 \frac{16}{9}\frac{\Delta(k)^3}{J(k)^2}[1 - u(k)K(m)][\Delta(k) - (1+3k^2)u(k)K(m)]. \tag{D.40}$$

Combining eqs. (D.38) and (D.40) we finally obtain

$$\lim_{\delta\omega\to 0}\frac{\det[M + NY'_s(\ell/2)]}{\tilde{\lambda}_{s,1}\tilde{\lambda}_{s,2}} = -8\langle 1|1\rangle\langle 2|2\rangle\frac{(u(k)K(m)-1)}{m_1^2\Delta(k)^5}. \tag{D.41}$$

The right hand side of eq. (D.41) can be expressed completely in terms of ℓ and k by using the fact that when $m_1 \ll 1$, we have that $16m_1 \approx \exp(-\ell\sqrt{\Delta(k)/2})$ [c.f. eq (2.47)]. Notice that eq. (D.41) has the opposite sign to that of eq. (D.25). This sign difference is a signature of the instability of state ψ_s, and a consequence of the fact that the spectrum of L_s has one negative eigenvalue (i.e., ψ_s is a saddle-point).

The remaining task is to include the product $\mathcal{V}_s^1\mathcal{V}_s^2$ of volume factors. As shown in appendix C, $\mathcal{V}_s^1 = \ell\mathcal{N}_1$ and $\mathcal{V}_s^2 = 2\pi\mathcal{N}_2$ so that when these are combined with eq. (D.41) the normalization factors cancel out, as in the case of the metastable state, and we finally obtain

$$\frac{|\det' L_s|^{1/2}}{\mathcal{V}_s^{(1)}\mathcal{V}_s^{(2)}} = -\frac{4}{\pi}\frac{(u(k)K(m)-1)}{m_1^2\Delta(k)^5}. \tag{D.42}$$

References

[1] R. Forman, *Invent. Math.* **88**, 447 (1987).

[2] C. G. J. Jacobi, *Journal für Mathematik*, Vol. XVII, 68 (1837); see, e.g., O. Bolza, *Lectures on the Calculus of Variations* (Stechert, NY, 1931); and C. Fox, *An Introduction to the Calculus of Variations* (Dover, NY, 1987), Chap. 2, Sec. 8.

Appendix E

Functional Determinant for x^4 Potential

In this appendix we give details of the calculation of the functional determinant of eq. (3.42). The motivation for studying an operator of this type is that it arises in the investigation of fluctuations about the instanton in one-dimensional quantum mechanics with the potential $V(x) = \frac{1}{2}x^2 - \frac{1}{4}x^4$ [1]. The instanton satisfies the equation $-\ddot{x} + V'(x) = 0$, which may be integrated once to give $\frac{1}{2}\dot{x}^2 - V(x) = E$, where E is a constant. Solutions to this equation are those of a classical particle of unit mass and energy E moving in the potential $-V(x)$. Bounded motion is allowed for $E < 0$, corresponding to the existence of real instantons.

Let the values of x at which the particle in this mechanical analogy has zero velocity be denoted by α and β $(0 < \alpha < \beta)$. Then $-V(\alpha) = -V(\beta) = E$, which implies $\alpha^2 + \beta^2 = 2$ and $E = -\alpha^2\beta^2/4$. The once-integrated equation of motion now reads

$$\left(\frac{dx}{dt}\right)^2 = \frac{1}{2}(x^2 - \alpha^2)(\beta^2 - x^2) \tag{E.1}$$

which implies that

$$\int_\beta^x \frac{dx}{\sqrt{(x^2 - \alpha^2)(\beta^2 - x^2)}} = -\frac{1}{\sqrt{2}}(t - t_0) \tag{E.2}$$

where t_0 is the time at which the particle was at $x = \beta$. This may be integrated in terms of elliptic functions [2]:

$$x_c(t; t_0, m) = \beta\,\mathrm{dn}(u|m), \tag{E.3}$$

where $u = \beta(t-t_0)/\sqrt{2}$ and $m = 1-(\alpha^2/\beta^2)$. The subscript 'c' denotes "classical" and simply indicates that this is a solution of the classical equation of motion $\delta S/\delta x(t) = 0$, where $S[x] = \int_a^b dt \left[\frac{1}{2}\dot{x}^2 + V(x)\right]$ is the action. The physical significance of the integration constant t_0 is clear: because the particle can start at any x ($\alpha \leq x \leq \beta$), the time at which it reaches β (defined to be t_0) is arbitrary. The constant m, on the other hand, is directly related to the energy of the particle, since $E = -(1-m)/2(2-m)^2$. An alternative to m, which also specifies the energy of the particle, is the period T defined by

$$\frac{T}{2}\frac{1}{\sqrt{2}} = \int_\alpha^\beta \frac{dx}{\sqrt{(x^2-\alpha^2)(\beta^2-x^2)}} \tag{E.4}$$

$$= \beta^{-1}\int_0^{\pi/2} \frac{d\theta}{\sqrt{1-m\sin^2\theta}} \tag{E.5}$$

$$= \left(\frac{2-m}{2}\right)^{1/2} K(m), \tag{E.6}$$

where $K(m)$ is the complete elliptic integral of the first kind [2].

We are interested in evaluating the expression (3.40), and therefore need to determine the values of the functions y_1 and y_2 at the endpoints a and b. These two functions are solutions of the homogeneous differential equation $Lh = 0$, where

$$L\delta(t-t') = \frac{\delta^2 S}{\delta x(t)\delta x(t')}\bigg|_{x=x_c} = \left[-\frac{d^2}{dt^2} + 1 - 3x_c^2(t;t_0,m)\right]\delta(t-t') \tag{E.7}$$

Using the explicit form for x_c given by eq. (E.3) we obtain eq. (3.42). But two independent solutions of $Lh = 0$ can be found by differentiating x_c with respect to t_0 and m [3], so we define y_1 and y_2 by:

$$y_1(t;t_0,m) \equiv \frac{\partial x_c(t;t_0,m)}{\partial t_0} \tag{E.8}$$

$$y_2(t;t_0,m) \equiv \frac{\partial x_c(t;t_0,m)}{\partial m} \tag{E.9}$$

It is a straightforward exercise in elliptic functions to find from eq. (E.3) that:

$$y_1(t;t_0,m) = \frac{m\beta^2}{\sqrt{2}}\,\mathrm{sn}(u|m)\,\mathrm{cn}(u|m), \tag{E.10}$$

$$\dot{y}_1(t;t_0,m) = \frac{m\beta^3}{2}\,\mathrm{dn}(u|m)\left\{\mathrm{cn}^2(u|m) - \mathrm{sn}^2(u|m)\right\}. \tag{E.11}$$

One can now check using (E.6) that $y_1(a) = y_1(b)$ and that $\dot{y}_1(a) = \dot{y}_1(b)$ for any initial and final times satisfying $b - a = T$. Therefore, since y_1 is a solution of $Lh = 0$ satisfying the correct boundary conditions, it is the zero mode for this problem, as expected.

A slightly longer calculation of the same type gives

$$\begin{aligned} y_2(t;t_0,m) &= \frac{d\beta}{dm}\,\mathrm{dn}(u|m) - \left\{um\frac{d\beta}{dm} - \frac{\beta\,E(u|m)}{2(1-m)} + \frac{\beta u}{2}\right\}\mathrm{sn}(u|m)\mathrm{cn}(u|m) \\ &\quad - \frac{\beta\mathrm{sn}^2(u|m)\,\mathrm{dn}(u|m)}{2(1-m)}, \end{aligned} \tag{E.12}$$

where $E(u|m)$ is the elliptic integral of the second kind. Using the periodicity of the elliptic functions

$$\begin{aligned} \frac{y_2(b) - y_2(a)}{y_1(a)} &= -2\left\{K(m)m\frac{d\beta}{dm} - \frac{\beta E(m)}{2(1-m)} + \frac{\beta}{2}K(m)\right\}\left\{\frac{\beta^2 m}{\sqrt{2}}\right\}^{-1} \\ &= -2\frac{(2-m)^{1/2}}{m}\left\{\frac{K(m)}{2-m} - \frac{E(m)}{2(1-m)}\right\}, \end{aligned} \tag{E.13}$$

as $\beta^2 = 2(2-m)^{-1}$. Here $E(m)$ is the complete elliptic integral of the second kind.

The Wronskian $\det H(t)$ is a constant, and so can be calculated for any convenient t. Choosing $t = t_0$, which implies $u = 0$ and so $y_1(t_0) = 0$, we have

$$\begin{aligned} \det H(t) &= \dot{y}_2(t_0)\,y_1(t_0) - \dot{y}_1(t_0)\,y_2(t_0) \\ &= -\left(\frac{\beta^3 m}{2}\right)\left(\frac{d\beta}{dm}\right) \\ &= -\frac{m}{(2-m)^3}. \end{aligned} \tag{E.14}$$

Substituting eqs. (E.13) and (E.14) into eq. (3.40), and taking into account the extra minus sign which comes about because the operator (3.42) is *minus* the definition of operators as given in the text, gives eq. (3.43).

Following the discussion of the most natural form for $\hat{L}$ given in Sec. 3.2, we take it to be the second functional derivative of the action for the harmonic oscillator with the potential $\hat{V}(x) = \frac{1}{2}x^2$. Then

$$\hat{L} = -\frac{d^2}{dt^2} + 1 \tag{E.15}$$

Choosing $\hat{y}_1(t) = e^t$ and $\hat{y}_2(t) = e^{-t}$ to be the two independent solutions of the homogeneous equation $\hat{L}h = 0$,

$$\hat{Y}(b) = \begin{bmatrix} \cosh(b-a) & \sinh(b-a) \\ \sinh(b-a) & \cosh(b-a) \end{bmatrix}. \tag{E.16}$$

Using the same periodic boundary conditions which gave (3.40),

$$\begin{aligned} \det(M + N\hat{Y}(b)) &= 2 - \hat{Y}_{11}(b) - \hat{Y}_{22}(b) \\ &= 2(1 - \cosh T) \qquad (E.17) \\ &= -4\sinh^2([2-m]^{1/2}K(m)). \qquad (E.18) \end{aligned}$$

Dividing (3.43) by (E.18) gives the required expression for

$$\frac{1}{\langle y_1|y_1\rangle}\frac{\det' L}{\det \hat{L}}. \tag{E.19}$$

As a check on the results let us look at the limit $E \to 0_-$, i.e., $m \to 1$ or $T \to \infty$. In this case $K(m) \sim \frac{1}{2}\ln(1-m)$, which from eq. (E.6) gives $m \sim 1 - 16\,e^{-T}$. Using $E(m) \to 1$ as $m \to 1$, we have

$$\frac{\det' L}{\langle y_1|y_1\rangle} \sim \frac{e^T}{16}, \quad \text{as } T \to \infty. \tag{E.20}$$

Since from (E.17), $\det \hat{L} \sim -e^T$ as $T \to \infty$,

$$\lim_{T\to\infty} \frac{1}{\langle y_1|y_1\rangle}\frac{\det' L}{\det \hat{L}} = -\frac{1}{16}. \tag{E.21}$$

The sign is the expected one: the zero mode that has been extracted, y_1, has a single node, which leads us to deduce that L has only one eigenfunction with a negative eigenvalue; all the other eigenvalues are non-negative. The signs of eqs. (E.18) and (E.20) are not those that we might naively expect, but these signs have no meaning separately — both the magnitude and sign of these terms can be changed at will by the replacement $M \to \lambda M, N \to \lambda N$, where λ is any real number.

The ratio (E.21) agrees with the calculation of Ref. [1]. To see this we note that $\alpha \to 0, \beta \to \sqrt{2}$ as $m \to 1$, hence the instanton becomes

$$x_c(t; t_0, m = 1) = \sqrt{2}\,\mathrm{sech}(t - t_0) \tag{E.22}$$

which implies that

$$y_1(t; t_0, m = 1) = \sqrt{2}\,\mathrm{sech}(t - t_0)\tanh(t - t_0), \tag{E.23}$$

$$\lim_{T\to\infty}\langle y_1|y_1\rangle = \frac{4}{3}. \tag{E.24}$$

Combining eqs. (E.21) and (E.24) gives eq. (3.44), as required.

References

[1] Brézin E, Le Guillou J C and Zinn-Justin J 1977 Phys. Rev. **D15** 1544.

[2] Abramowitz M and Stegun I A 1965 *Handbook of Mathematical Functions* (Dover, New York).

[3] Fox, C 1987 *An Introduction to the Calculus of Variations* (Dover, New York) Chapter 2.

Appendix F

Two-Mode Dynamical System

Our aim is to construct a two-mode dynamical system (DS) that exhibits the crossover-effect. The primary motivation for constructing the reduced DS is that the ideas presented in the Sec. 4.6 are more easily tested in this simpler system. In particular, by solving the Fokker-Planck equation for the reduced DS, we will be able to visualize the flow of probability away from the unstable state and accumulate around the neighboring metastable states. In addition, for the two-mode system it is computationally feasible to minimize the thermodynamic action. We shall provide numerical evidence to support the conjecture in Sec. 4.6 that in the late-time regime the minimum value of the action is much smaller than D. Finally, the notion that the thermodynamic action is not relevant to determining the relative final occupation probabilities of the competing metastable states leads to the conclusion that the important quantity is the ratio of fluctuation determinants (see eq. (4.51)). In other words, in order to compute the relative probability of a single phase-slip versus a double phase-slip, it is necessary to compute the ratio of fluctuation determinants. For the full dynamical system, i.e., the STDGL, the fluctuation operators are matrix *partial* differential operators. Computing the determinants of these operators is a formidable problem. As the fluctuation operators for the reduced DS are matrix *ordinary* differential operators, the hope is that the ratio of the determinants for these operators can be computed. Although the calculation for the reduced DS is simpler than the corresponding calculation for the full DS, it is still a difficult problem, and one that is not

yet solved.

We now proceed with the construction of the reduced dynamical system. The two-mode DS must satisfy two main requirements. First, the fixed-point structure, and the linear stability properties of the fixed points, must be the same as that of the original DS given in eq. (4.10). Second, the two-mode DS must exhibit the crossover effect. These two requirements are independent of one another. For example, one might be able to construct a DS for which the fixed-point structure and linear stability properties are the same as the STDGL, yet does not exhibit the crossover effect.

The construction of the two-mode DS proceeds in two stages. First, as we are interested in reproducing the crossover from single phase-slip domination to double, we truncate the expansion of eq. (4.30) at $n = 2$, so that

$$\tilde{\psi}(x,t) = \sum_{n=-2}^{2} \tilde{a}_n(t)\exp(-iq_n x). \tag{F.1}$$

As discussed in Sec. 4.5, the modes with a positive wavevector, in this case labelled by $n < 0$, are necessary in order that the approximate system have the same linear stability properties as the original TDGL. In general, the $\tilde{a}_n(t)$ are complex-valued time-dependent functions. However, as our goal is the construction of the simplest possible system, we will take the $\tilde{a}_n$ to be real. This Ansatz cannot be justified rigorously. However, if we consider the time-dependent Ginzburg-Landau equation *in the abscence of noise*, then if the mode amplitudes $a_n(0)$ are real, then at a later time they will remain so, i.e., $a_n(t)$ will be real. This is discussed in Ref. [1], and I have also checked this numerically. Now, the noise in the stochastic time-dependent GL equation *will* cause the complex components of the $a_n(t)$ to be nonzero; it is for this reason that we are not rigorously justified in making this Ansatz.

At this stage we have a system with five real degrees of freedom. The second step is to reduce this five-dimensional system to a two-dimensional DS. This is accomplished by introducing the following Ansatz:

$$\tilde{a}_0 \;=\; A_0 \prod_{n=1}^{2} (1 - a_n^2/A_n^2) \tag{F.2}$$

$$\tilde{a}_{-1} = (f_{0,1}a_1 - f_{0,2}a_2^2)\tilde{a}_0/A_0 \quad \text{(F.3)}$$

$$\tilde{a}_{-2} = (f_{0,2}a_2 - f_{0,1}a_1^2)\tilde{a}_0/A_0, \quad \text{(F.4)}$$

where $A_n = A_n(t) \equiv \sqrt{1 - Q_n(t)^2}$ and $f_{0,n}$ is given in eq. (4.32). The two-mode DS, with a_1 and a_2 as the dynamical variables, is generated by inserting eqs. (F.1) and (F.2) - (F.4) into eq. (4.10), multiplying by $\ell^{-1}e^{iq_m x}$ (where $m = 1$ or 2), and integrating from 0 to ℓ. The resulting DS can be written in the form

$$da_n/dt = g_n(\mathbf{a}(t), k(t)) + \eta_n(t) \ (n = 1, 2), \quad \text{(F.5)}$$

where $\eta_n(t)$ is a Gaussian random variable, Dirac-delta correlated in time, Kronecker-delta correlated in n, with mean zero, and variance D/ℓ. The variance of $\eta_n(t)$ is half of the variance of $\tilde{\eta}(t)$ because we are taking the a_n to be real. Hereafter, boldface quantities will denote two-component real vectors; e.g. $\mathbf{a}(t) = [a_1(t), a_2(t)]^T$.

The Ansatz given in eqs. (F.2)-(F.4) can be motivated in the following way. First, it was specifically chosen so that the two-mode DS would have the same fixed-point structure and linear stability properties as the original equation. The solution of the linearized TDGL, given in eq. (4.31), was used to determine the form of the Ansatz for a_1 and $a_2 \ll 1$; i.e. to first order in a_n (where $n = 1$ or 2), $a_0 = A_0$, and $a_{-n} = f_{0,n}a_n$. In addition to this, we require that when $a_n = \pm A_n$, the mode amplitudes a_0, a_{-1}, and a_{-2} vanish. The proportionality of a_0 to $1 - a_n^2/A_n^2$, and the fact that $a_{-n} \propto a_0$, ensures that this requirement is satisfied. There are still two terms, those of the form $-f_{0,n}a_n^2$, that have not been explained. If these terms are absent, the two-mode DS does not exhibit the crossover effect, even though this DS has the appropriate fixed point structure and linear stability properties. These terms are therefore required if the two-mode DS is to exhibit the crossover effect.

Further justification for this Ansatz, based on numerical evidence, can be given. In particular, we can numerically integrate the STDGL equation (4.10), thereby generating a time-dependent configuration $\tilde{\psi}(x,t)$. Using eq. (4.30), we can compute the mode amplitudes $a_n(t)$. The numerically computed amplitudes $a_n(t)$; $n = 0, -1, -2$ can then be compared with the $\tilde{a}_n(t)$ that are given in eqs. (F.2)-(F.4), and which are

completely determined from the two modes a_1 and a_2. In this way it can be verified that the $\tilde{a}_n(t)$ have the same qualitative features as the amplitudes $a_n(t)$ that were obtained from the original STDGL.

The vector $\mathbf{g}$, the components of which are polynomials in a_1 and a_2, and which defines the two-mode DS, has the following properties. First, $\mathbf{g}$ vanishes at the points

$$\mathbf{a}^{(\pm n)}(t) \equiv \pm A_n(t) \begin{bmatrix} \delta_{n,1} \\ \delta_{n,2} \end{bmatrix} \quad (n = 0, 1, 2), \tag{F.6}$$

where, as in the previous section, $A_n(t) = \sqrt{1 - Q_n(t)^2}$. Thus, the states $\mathbf{a}^{(n)}(t)$ are fixed points of the two-mode system, and are associated with the fixed points $\tilde{\psi}_n$. In addition, $\partial g_n/\partial a_n|_{\mathbf{a}^{(0)}(t)} = \lambda^+_{0,n}$, so that for $a_n \ll 1$, we have $a_n(t) \propto e^{\lambda^+_{0,n} t}$. Thus, for $\kappa_2 > Q_0(t) > \kappa_1$, state $\mathbf{a}^{(0)}(t)$ is unstable with respect to fluctuations of a_1, and for $Q_0(t) > \kappa_2$, $\mathbf{a}^{(0)}(t)$ is unstable with respect to fluctuations of both a_1 and a_2. Furthermore, $\partial g_n/\partial a_n|_{\mathbf{a}^{(\pm m)}(t)} < 0$ (where $m = 1$ or 2) and so states $\mathbf{a}^{(\pm 1)}(t)$ and $\mathbf{a}^{(\pm m)}(t)$ are metastable. In other words, the two-mode DS has the same fixed point structure as the original STDGL given in eq. (4.10), and the linear stability properties of state $\mathbf{a}^{(0)}(t)$, defined by the growth rates $\lambda^+_{0,n}$, are also the same.

To see that the DS given in eq. (F.5) exhibits the crossover effect, we numerically integrate eq. (F.5) using a simple Euler differencing scheme. That is, time is discretized into units of size h_t, and the continuous variables $a_n(t)$ are approximated by their values $a_{n,j} = a_n(t_j)$ at the discrete points $t_j = j h_t$. The evolution equation (F.5) then becomes

$$\frac{a_{n,j+1} - a_{n,,j}}{h_t} = g_n(\mathbf{a}_j, k_j) + \frac{\eta_{n,j}}{\sqrt{h_t}}; \tag{F.7}$$

where $k_j = k_o + j\omega h_t/\ell$, and $\eta_{n,j}$ is a Gaussian random variable with mean zero, Kronecker-delta correlated in n and j, and with variance D/ℓ. As in Sec. 4.2, the factor of $h_t^{-1/2}$ is introduced so that $\eta_{n,j}$ and $\eta_n(t)$ have the same dimensions. Armed with this numerical algorithm, we now proceed in the same way as in Sec. 4.4. That is, for a given ω, we integrate (F.5) N times, with an initial condition $\mathbf{a}(0) = \mathbf{a}^0(0)$, and $k(0) < \kappa_1$. We then count the number of times, N_n, that the system ends up in

ω	P_{-1}	P_1	P_{-2}	P_2
0.00001	0.58	0.42	0	0
0.00005	0.60	0.39	0	0.01
0.0001	0.63	0.33	0	0.04
0.0005	0.46	0.30	0	0.24
0.001	0.41	0.30	0	0.29
0.003	0.26	0.14	0.13	0.47
0.005	0.14	0.02	0.40	0.44
0.007	0.02	0	0.56	0.42
0.01	0	0	0.58	0.42

Table F.1: Probabilities P_n that the system ends up in state $\mathbf{a}^{(n)}$. Parameters: $N = 100$, $D = 0.001$, $k_o = 0.58$, and $h_t = 0.2$

state $\mathbf{a}^{(n)}(t)$. For $N = 100$ and $D = 10^{-3}$, the probabilities $P_n = N_n/N$ are given in Table F.1 as a function of ω. A comparison of these results with those of Fig. 4.3 shows that indeed that the approximate two mode DS exhibits the same qualitative behavior as the original STDGL. One interesting feature of the results of Table F.1 is the asymettry between $\mathbf{a}^{(n)}(t)$ and $\mathbf{a}^{(-n)}(t)$.

A useful way to visualize the dynamics is to construct a two-dimensional parametric (in time) plot, with $|a_1(t)|$ as the ordinate and $|a_2(t)|$ as the abscissa. Plotted in Fig. F.1 are 10 such graphs. In this case $\omega = 0.001$, so that a mixture of single and double phase-slips occur (see Table F.1).

We can now develop a picture of the time development of the probability density $P(a_1, a_2, t)$, where $P(a_1, a_2, t)da_1da_2$ is the probability that at time t the system is in (to within da_1 and da_2) state (a_1, a_2). To do so, consider an ensemble of systems, the dynamics of which are governed by eq. (F.5), and for which all of the members of the ensemble are initially in state $\mathbf{a}^{(0)}(t)$. Thus, at $t = 0$, the initial condition is

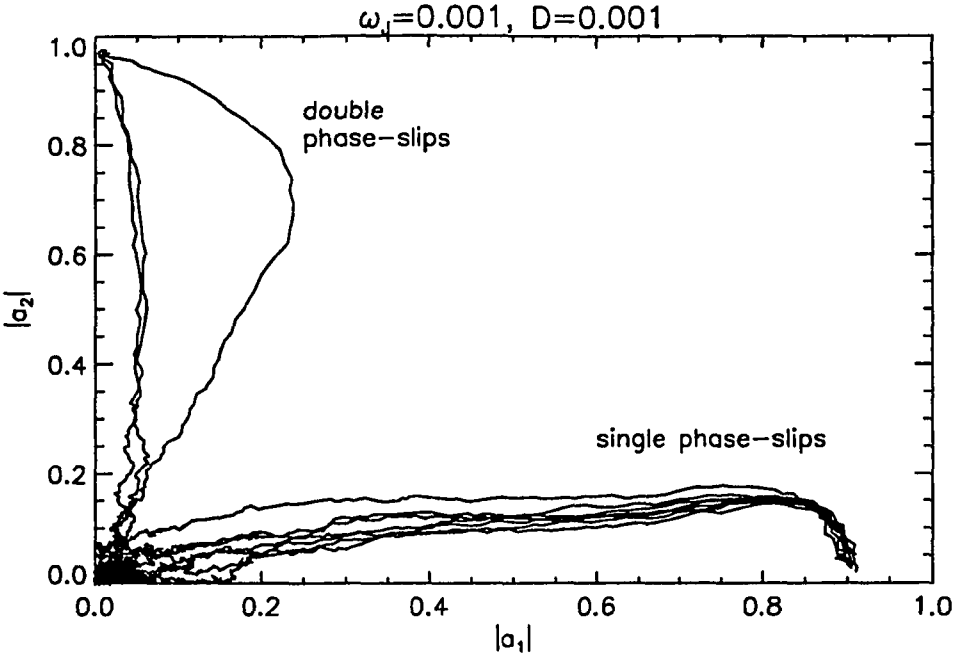

Figure F.1: Ten parametric plots of $|a_1(t)|$ and $|a_2(t)|$. There are 7 single and 3 double phase-slips. Parameter: $h_t = 0.2$.

that $P(a_1, a_2, 0) = \delta(a_1)\delta(a_2)$. (The normalization condition is that, at any time t, $\int da_1 da_2 P(a_1, a_2, t) = 1$.) As the system begins to evolve, the probability distribution will spread out. As long as $\mathbf{a}^{(0)}(t)$ remains stable, i.e., as long as $Q_0(t) < \kappa_1$, the density $P(a_1, a_2, t)$ will remain localized about $\mathbf{a}^{(0)}(t)$. However, once the Eckhaus instability is encountered, $P(a_1, a_2, t)$ will begin to spread out, flowing away from $\mathbf{a}^{(0)}(t)$. For intermediate times, the states lying 'between' $\mathbf{a}^{(0)}(t)$ and $\mathbf{a}^{(\pm n)}(t)$ will be occupied appreciably. However, as time progresses, $P(a_1, a_2, t)$ will begin to accumulate about $\mathbf{a}^{(\pm n)}(t)$. We can estimate, from the characteristic time t_n^* given in eq. (4.39), that this accumulation of the probability will occur for times $> \mathcal{O}(\sqrt{\ell/\omega})$.

The description in the preceding paragraph can be made more concrete if we consider the Fokker-Planck (FP) equation associated with the Langevin equation (F.5), which governs the time-development of the probability density $P(a_1, a_2, t)$. The pur-

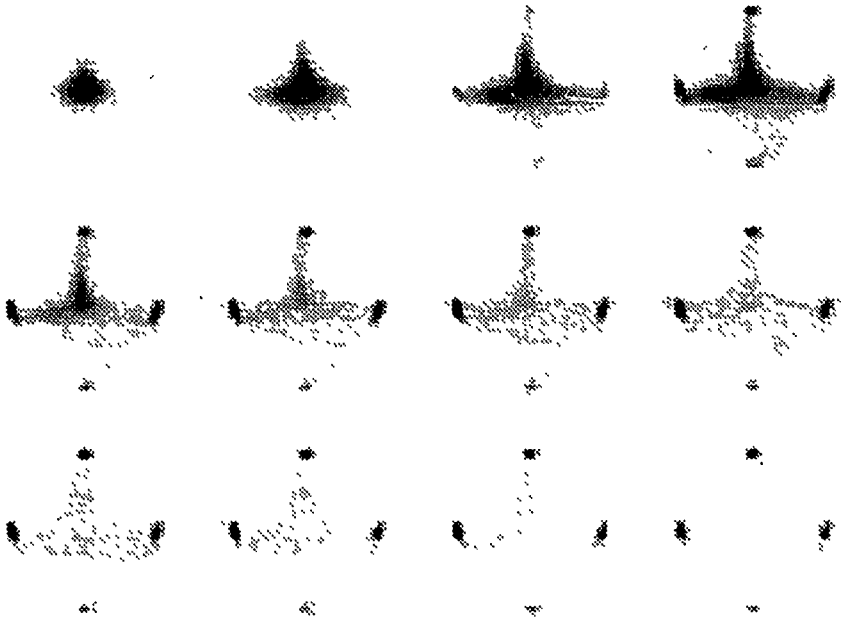

Figure F.2: Temporal sequence of $P(a_1, a_2)$. Dark (light) regions are areas of high (low) probability. The earliest (latest) time is shown in the upper left (bottom right) plot. Parameters: $\omega = 0.001$, $D = 0.1$, $h_t = 0.0005$, $N_a = 32$

pose of studying this equation is to confirm the picture of the dynamics of the probability density that was described in the preceding paragraph. The FP equation for the two-mode DS associated with eq. (F.5) is

$$\frac{\partial P}{\partial t} = -\sum_{n=1}^{2} \frac{\partial}{\partial a_n} \left[g_n P - \frac{D}{2\ell} \frac{\partial P}{\partial a_n} \right], \tag{F.8}$$

and is in the form of a continuity equation. The term in brackets on the right-hand-side of eq. (F.8) is therefore interpreted as the probability current, which we will denote by $\mathcal{J}_n(a_1, a_2, t)$. As discussed in the preceding paragraph, if the probability is initially peaked at $[0, 0]$, we expect it will flow to the four fixed points: $\mathbf{a}^{(\pm 1)}(t)$ and $\mathbf{a}^{(\pm 2)}(t)$. In the numerical simulations of the two-mode DS the transition to a metastable state $\mathbf{a}^{(\pm n)}(t)$ always occurs within a time short enough so that

$A_n(t) = \sqrt{1 - Q_n(t)^2} < 1$. Thus, the domain of P can be taken to be a square, centered at $(0,0)$, and with sides of length $2a$, where $a > 1$. With this restriction to a finite domain, the dynamical equation (F.8) must be supplemented by boundary conditions. These are determined by the requirement that the dynamics preserve the normalization of the probability, i.e, at any time t, $\int da_1 da_2 \, \partial P/\partial t = 0$. As, from eq. (F.8), $\partial P/\partial t = -\sum_n \partial \mathcal{J}_n/\partial a_n$, this condition can be satisfied by requiring that the probability flux out of the square be zero, i.e.,

$$\begin{aligned} \mathcal{J}_1(\pm a, a_2) &= 0 \\ \mathcal{J}_2(a_1, \pm a) &= 0. \end{aligned} \tag{F.9}$$

This condition is sufficient, but not necessary. Equations (F.8) and (F.9), together with an initial condition, completely determine the dynamics of $P(a_1, a_2, t)$ within the square of area $4a^2$ and centered at $(0,0)$.

The numerical integration of the FP equation proceeds as follows. First, we construct a square lattice, centered at $(0,0)$, the points of the lattice being separated by a distance h_a. Time is also discretized in units of size h_t. Then, $P(a_1, a_2, t)$ is approximated by its values $P_{x,y,j} = P(xh_a, yh_a, jh_t) \equiv P_{x,y,j}$ (where x, y and j are integers) on the 'space'-time lattice. The partial derivatives with respect to $\{a_n\}$ are approximated by space-centered finite differences, e.g., $\partial P/\partial a_1 = (P_{x+1,y,j} - P_{x-1,y,j})/2h_a$, and $\partial^2 P/\partial a_1^2 = (P_{x+1,y,j} + P_{x-1,y,j} - 2P_{x,y,j})/2h_a$. The partial time-derivative $\partial P/\partial t$ is approximated by the forward difference $(P_{x,y,j+1} - P_{x,y,j})/h_t$. On the discrete lattice, the boundary conditions are determined by the conservation of probability, i.e.,

$$\sum_{x=-N_a}^{x=N_a} (P_{x,y,j+1} - P_{x,y,j})/h_t = 0, \tag{F.10}$$

$$\sum_{y=-N_a}^{y=N_a} (P_{x,y,j+1} - P_{x,y,j})/h_t = 0, \tag{F.11}$$

where the discrete form of the right-hand-side of eq. (F.8) is used to replace the forward (time) difference, and $N_a \equiv a/h_a$. This requirement determines the discrete form of the boundary condition, i.e., the values of P just outside the domain of P

are determined by the values of P inside the domain, thereby allowing the finite-differences to be computed at the boundaries.

The results of a numerical integration of the FP equation are shown in Fig. F.2. In this case $\omega = 0.001$, and $D = 0.1$. The noise strength was chosen for numerical reasons. The convective derivative $g_n \partial P/\partial a_n$, when computed numerically, causes stability problems. However, these can be obviated by introducing an artificial viscosity [2] or, equivalently we can use a relatively large value of D, such as 0.1. Shown in this figure is a temporal sequence of two-dimensional plots of $P(a_1, a_2)$; the horizontal axis is a_1, and the vertical axis is a_2. Time increases first from left to right, and then from top to bottom. At the earliest time $k(t) = 0.58$, and at the latest time $k(t) = 0.64$. The dark regions represent areas of high probability, and the light regions represent areas of low probability. Thus, we see that the probability that is initially peaked about $(0,0)$, flows away from this point, and accumulates about the four fixed-points $\mathbf{a}^{(\pm n)}(t)$. This result illustrates in concrete terms the dynamics of the probability density for a dynamical system that exhibits the crossover effect, and is consistent with the picture discussed in Sec. 4.6.

We now turn our attention to the time-dependence of the minimum value of the thermodynamic action S. The derivation of S in the preceding section for the STDGL equation can be applied with essentially no modification to the two-mode DS given in eq. (F.5). Thus, the thermodynamic action $S[a_1, a_2]$ for the two-mode DS is given by

$$S[a_1, a_2] = \sum_{n=1}^{2} \int_0^\tau dt[\dot{a}_n - g_n(\mathbf{a}, k(t))]^2. \tag{F.12}$$

In the small D regime, the configurations that dominate the path integral are those that minimize S, subject to the appropriate boundary conditions, which for a type-m process are given by

$$a_n(0) = 0, \tag{F.13}$$

$$a_n(\tau) = \mathrm{sgn}(n)\, \delta_{n,m} A_n(\tau), \tag{F.14}$$

where $\delta_{n,m}$ is the Kronecker delta, and $\mathrm{sgn}(n)$ is $+1$ if $n > 0$, and -1 if $n < 0$.

The first step in the minimization of the thermodynamic action is to regard $S[a_1, a_2]$ as a multivariable function, with a finite number of degrees of freedom. This situation can be achieved if we construct the thermodynamic action $\hat{S}$ for the discrete two-mode DS (F.7):

$$\hat{S}(\{a_{n,j}\}) = \sum_{n=1}^{2} \sum_{j=0}^{N_\tau - 1} h_t \Big(\frac{a_{n,j+1} - a_{n,j}}{h_t} - g_{n,j} \Big)^2, \tag{F.15}$$

where $N_\tau h_t = \tau$ and $g_{n,j} = g_n(a_n(t_j), k_j)$. The variables $a_{n,0}$ and a_{n,N_τ} are not dynamical variables; instead, they are determined by the boundary conditions (F.13). [$\hat{S}$ can also be obtained by performing an Euler discretization of the integrand of $S[a_1, a_2]$ given in (F.12).] Regarding the thermodyanic action as a multivariable function is advantageous because finding the minimum of $\hat{S}$ is an example of an (unconstrained) optimization problem. Such problems arise in many contexts of science and engineering, and so much effort has been devoted to their solution [3]. I have used a relaxational method based on a limited-memory quasi-Newton method, which is advantageous for large-scale problems; the computer code was provided by the Nocedal group at Northwestern University [4]. The essential feauture of the results is that the minimum value of $\hat{S}$ is a monotonically decreasing of τ, achieving very small values in the late-time regime (see Sec. 4.6). To illustrate this, listed in Tables F.2 and F.3 are the minimum values of $\hat{S}$ (denoted by E_n) as a function of τ, for $\omega = 0.001$. The parameter n determines the specific form of the boundary conditions given in (F.13).

The results in Tables F.2 and F.3 support the conjecture made in Sec. 4.6 that in the late-time regime the minimum value of the thermodynamic action is much smaller than D. Thus, according to the results of Tables F.2 and F.3, in the small noise regime, the probabilities are determined entirely by the determinants of the fluctuation operators L_n. In this case, the L_n are 2×2 matrix *ordinary* differential operators, in contrast to those of the previous section, where the fluctuation operators $\tilde{L}_n$ were 2×2 matrix *partial* differential operators. Thus, according to (4.51) and

τ	$k(\tau)$	E_{-1}	E_1
70	0.65	1.3×10^{-3}	1.7×10^{-3}
80	0.66	6.8×10^{-4}	8.7×10^{-4}
90	0.67	3.4×10^{-4}	4.5×10^{-4}
100	0.68	1.7×10^{-4}	2.3×10^{-4}
110	0.69	8.0×10^{-5}	1.2×10^{-4}
120	0.70	3.5×10^{-5}	5.9×10^{-5}
130	0.71	1.5×10^{-5}	3.1×10^{-5}
140	0.72	7.6×10^{-6}	1.8×10^{-5}
150	0.73	5.3×10^{-6}	1.3×10^{-5}

Table F.2: Minimum value of $\hat{S}$ for $n = \pm 1$. Parameters: $\omega = 0.001$, $k_o = 0.58$, and $h_t = 0.4$

τ	$k(\tau)$	E_{-2}	E_2
70	0.65	6.1×10^{-3}	7.4×10^{-3}
80	0.66	2.8×10^{-3}	3.3×10^{-3}
90	0.67	1.1×10^{-3}	1.3×10^{-3}
100	0.68	4.0×10^{-4}	4.1×10^{-4}
110	0.69	1.1×10^{-4}	1.1×10^{-4}
120	0.70	2.8×10^{-5}	2.4×10^{-5}
130	0.71	4.0×10^{-6}	4.6×10^{-6}
140	0.72	4.7×10^{-7}	1.2×10^{-6}

Table F.3: Minimum value of $\hat{S}$ for $n = \pm 2$. Parameters: $\omega = 0.001$, $k_o = 0.58$, and $h_t = 0.4$

(4.52),

$$\frac{P_n(\omega)}{P_m(\omega)} = \sqrt{\frac{\det L_m}{\det L_n}} \; (n, m = \pm 1, \pm 2), \tag{F.16}$$

and

$$\sum_{n=1}^{2} (P_{-n}(\omega) + P_n(\omega)) = 1, \tag{F.17}$$

where P_n is the probability that, in the late-time regime, the metastable state $\mathbf{a}^{(n)}$ (see eq. (F.6)) is occupied. The abscence of the $\mathcal{V}$ factors is a reflection of the lack of zero modes of the L_n, i.e., the integrand of S depends explicitly on time, and there are no internal symmetries in the a_1, a_2 plane.

In principle, eqs. (F.16) and (F.17) provide a closed form expression for the determination of the probability of a single or double phase-slip process. In practice, I have not yet been able to obtain consistent results. My approach has been to compute directly the determinant of $\hat{L}_n$, where $\hat{L}_n$ is the matrix of second order partial derivatives of $\hat{S}$, evaluated at the path of least action.

References

[1] L. Kramer, H. R. Schober and W. Zimmerman, Physica D **31**, 212 (1988).

[2] W. H. Press, B. P. Flannery, S. A. Teukolsky and W. T. Vetterling, *Numerical Recipes* (Cambridge University Press, 1986).

[3] D. A. Pierre, *Optimization Theory with Applications* (Dover, New York, 1986).

[4] C. Zhu, R. H. Byrd, P. Lu and J. Nocedal, Tech. Report, Electrical Engineering and Computer Science Department, Northwestern University (1994).

Vita

Martin Brett Tarlie was born in Port Elizabeth, South Africa on June 23, 1967. At the age of 9, his family and he emigrated to the United States of America. He became a United States citizen at the age of 16. In 1989 he received a B.S. (Honors) degree in Physics, and a B.S. in Mathematics from the University of Michigan (Ann Arbor). In 1991 he received a M.S. in Physics from the University of Illinois at Urbana-Champaign.